Investigating the Effect of Thermal Stresses on the Hollow Glass Microsphere/Polyester Composites Interfacial Strength by Acoustic Emission Method

Investigating the Effect of Thermal Stresses on the Hollow Glass Microsphere/Polyester Composites Interfacial Strength by Acoustic Emission Method

By Zeinab Mousavi, MSc

A Thesis Submitted to the School of Graduate Studies

in Partial Fulfillment of the Requirements for the Degree

Master of Applied Science

Master of Applied Science (2016) **McMaster University**

(Chemical Engineering) **Hamilton, Ontario**

Title: Investigating the Effect of Thermal Stresses on the Hollow Glass Microsphere/Polyester Composites Interfacial Strength by Acoustic Emission Method

Author: Zeinab Mousavi, MSc (McMaster University)

Supervisor: Professor Michael Thompson

Number of Pages: xiii, 95

Lay Abstract

Sheet molded compound (SMC) is a polymer material reinforced by fibers providing a combination of light weight and high mechanical properties and is used in automotive industry. Light weight fillers (hollow glass microspheres) are used to obtain further weight reduction; however, addition of these fillers leads to reduced mechanical properties and further problems during painting process known as ‘paint popping’. The former is due to uncertain interfacial state between polymer and fillers and the latter results from different thermal expansion behavior of the polymer and filler materials while the material is exposed to high temperatures for painting process. This research aims to devise a highly sensitive technique and evaluate its suitability compared to mechanical testing for investigation of the origin of aforementioned problems. Acoustic Emission (AE) is a method with high sensitivity to changes in internal structure of the material which is postulated to provide a better insight on material microstructure compared to more commonly used method i.e. mechanical testing. Use of interfacial controlling agents was examined to reduce the problems as a result of introduction of fillers. The effect of using surface modified fillers and the effect of thermal stresses on material was investigated using AE technique. Application of AE method in this study provided a good insight about the changes in material internal structure; however, it did not demonstrate a significant improvement in detecting the origins of studied problems compared to mechanical testing at least based on the analysis technique used in this study.

Abstract

The effect of coatings on the interfacial strength of a hollow glass microsphere/polyester composite and their capacity to endure thermal stresses were studied by mechanical testing and an active Acoustic Emission (AE) method. AE was postulated to provide more local information at or near the glass/polyester interface due to the sensitivity of elastic waves to the rigidity of polymer chains at the glass sphere/polyester interface compared to mechanical testing.

Three frequency ranges identified by multivariate statistics yet consolidated for the initial analysis into a band of 140-240 kHz, were found to be changing with the different coated glass filler for different glass content and heating state. Considering the acoustic behavior of the composites containing different levels of glass sphere content (1-10 vol%), a lower concentration (aminoethylamino)-propyl-trimethoxy silane coated glass (AS6), demonstrated the lowest attenuation after heating (associated with higher interfacial strength). As anticipated, the highest attenuation after heating was observed for uncoated glass (16K) due to expectedly weaker associations. Mechanical testing results after heating were consistent with the AE response for AS6 and 16K for this frequency range. Trends in amplitude for the three narrower, frequency ranges of 130-160 kHz, 180-220 kHz and 230-260 kHz were compared against that of 140-240 kHz and very small differences were observed. It was found that the frequency range of 130-60 kHz was more descriptive of the changes of interfacial strength in composites (at 10 vol%), being consistent with the mechanical test results. Considering the AE response at 130-160 kHz and mechanical data, higher concentration (aminoethylamino)-propyl-trimethoxy silane (AS12), better endured thermal stresses compared to other coatings. A smaller trial looked at the effect of moisture aging and subsequent thermal cycling on the glass/polymer interface strength as another method to perturb the interface. Attenuation for the band of 180-260 kHz was studied for aged versus non-aged composites. The commercial coating, L21 demonstrated a better moisture resistance before and after thermal cycling compared to uncoated glass spheres.

An improved evaluation of interfacial strength in glass/polyester was expected using AE technique versus mechanical testing due to its higher sensitivity to changes in internal structure, however; no significant improvement compared to mechanical testing was observed, at least based on the analysis technique currently being used.

Acknowledgments

First and foremost I would like to thank my supervisor Dr. Michael Thompson for his invaluable support, guidance and understanding throughout my study.

I would like to acknowledge the Ontario Research Fund and Fraunhofer Project Center in London, Ontario that supported this project, and AOC and 3M Canada for kindly providing resin and hollow glass microspheres.

I would also like to thank Dr. Mhaskar and Kevin Dunn for discussion on statistical analysis and our group members Trevor West and Felipe Gomes for discussion on acoustic results and help with Python code.

I would also like to thank Elizabeth Takacs, Paul Gatt and Dan Wright for their help.

I want to thank my friends at McMaster who supported me during my study and finally I wish to express my appreciation to my parents whose care and encouragement have always been an asset to me.

Table of Contents

List of Figures

List of tables

Abbreviations

16K	iM16K glass spheres
AS6	Glass spheres coated with lower concentration amino-silane
AS12	Glass spheres coated with higher concentration amino-silane
DGSCM	Dynamic generalized self-consistent method
GS6	Glass spheres coated with lower concentration glycidyl-silane
GS12	Glass spheres coated with higher concentration glycidyl-silane
ILSS	Interlaminar shear strength
IFSS	Interfacial shear strength
L21	iM16K-L21 Glass spheres (3M commercial coating)
PLB	Pencil lead break
PL-HT	Pencil lead break at high temperature
PL-RT	Pencil lead break at room temperature
PLS-DA	Partial least square discriminant analysis
SMC	Sheet molding compound
VIP	Variable importance to projection

Introduction

Fiber-reinforced polymer composites demonstrate a combination of high strength & stiffness and light weight, which makes them ideal candidates for applications demanding high specific mechanical properties. The synergistic combination of the constituent phases in these polymer composites results in such properties. The effectiveness of interfacial bonding between the matrix and the reinforcing phase has a major role in determining the mechanical properties of the composites. A well-bonded interface, which is essential for effective stress transfer from the matrix to the reinforcement, is the primary requirement for effective use of constituents properties (Berg & Jones 1998).

Sheet molding compound (SMC) is a composite material comprising of a thermosetting resin (33-42 vol%), fiber reinforcements (33-42 vol%) and fillers (29-40 vol%). Other constituents in a standard SMC formulation are cure initiators, low profile additives for shrinkage control (for class-A applications), thickener (maturating agent), process additives, and mold release agent. SMC is a versatile reinforced plastic used for painted and unpainted automotive components, whether for bumpers, fenders, exterior and interior panels, or structural elements (McConnell 2007). Glass fiber-filled SMC containing unsaturated polyester matrix and calcium carbonate fillers, as used in the automotive industry for exterior body panels, are considered in this study. Weight reduction in glass fiber filled polyester SMC can be obtained by using low density fillers to achieve higher specific mechanical properties, lower fuel consumption and lower emissions. In this work, such lightweighting fillers were hollow glass microspheres.

1.1. Low Density SMC

Hollow glass microspheres are being considered as replacement of some calcium carbonate content in conventional SMC in order to achieve low density SMC with higher specific strength (half of the volume fraction of calcium carbonate can be replaced by glass spheres, for instance for 45% calcium carbonate content, half of that is replaced by 28% glass). The use of hollow glass microspheres has allowed SMC formulations to achieve densities as low as 1.2-1.4 gr/cm^3 (Hamarneh et al. 2013) while standard SMC

density is 1.85 gr/cm^3. However, low density SMC still demonstrates lower specific properties relative to its main competing material, aluminum, due to significantly lower mechanical properties; it also experiences lower strength than standard SMC. The lower-than-expected mechanical properties may be due to the introduction of defects to the microstructure of the composites which may be addressed by choosing the right diameter size for glass spheres. Also, the interfacial strength between glass spheres and polyester is thought to be a critical factor that defines the performance of the composite under stress.

1.1.1. Powder Priming of Low Density SMC

The drop in mechanical properties with low density SMC compared to standard SMC is just one complication for the automotive sector. A problem with powder priming of the low density SMC parts, referred to as "paint popping", is another observed concern. Paint popping is a surface defect on the coated substrates that forms bubbles, pin holes, or craters, that are up to few hundred micrometers in diameter and make the part cosmetically unacceptable for automotive exterior body panels. SMC parts are exposed to elevated temperatures (180℃) during E-coating process. Conductive coating is first applied to SMC surface and cured which dries the SMC; however, moisture absorbed after this stage and before application of the powder primer is crucial in outgassing during paint curing (Basu et al. 2009). It has been shown that outgassing of the entrapped air and the absorbed moisture in the porosity, cracks and other defects in SMC during heating may cause popping (Mason 2003). Changes in the formulation constituents and the type of conductive coating for E-coating process have partially solved the problem by decreasing moisture absorption and outgassing (Kia et al. 2006; Kia 2006a; 2006b; 2009). However, this solution has never fully solved the problem.

In this thesis, another reason for "paint popping" was postulated as being attributed to the considerable differences between the thermal expansion coefficient of the polyester and glass spheres, which results in creating thermal stresses in the composite. Depending on the interfacial strength between glass and polyester this stress might result in detraction of glass from the polyester matrix and the introduction of microdefects along the

glass/polyester interface. These defects deteriorate mechanical performance of the composite and alter the overall thermal expansion coefficient of the part, which in turn could cause buckling (out-of-plane strain relief) of the e-coat/SMC laminates under rapid thermal cycling like a painting operation. Improving the matrix/filler interface with silane coupling agents is postulated as a reasonable approach to reducing these problems.

Higher heating rates during E-coating process are associated with deleterious effects on paint popping in SMC parts attributed to higher rate of outgassing of absorbed moisture (Basu et al. 2009); also this observation is consistent with this hypothesis of relation between formation of paint pops and thermal expansion behavior of the composite.

1.2. Research Objectives

This research aims to investigate the effect of thermal stresses on glass sphere/polyester interface and particularly, its influence on interfacial strength. Realistically, chemistries demonstrating good interfacial properties at room temperature, the norm for mechanical testing, will not necessarily provide these properties at elevated temperatures not endure thermal stresses. A simpler model system compared to SMC, was considered consisting of hollow glass microspheres and polyester to prevent interference by other components on exploring the effect of heat on interfaces. Use of interfacial controlling agents was examined to improve the mechanical properties and lower the overall thermal expansion of the composite.

Comparison of mechanical test results before and after heating was expected to provide insight on the effect of thermal stresses on glass/polyester interface; however, mechanical tests are not sensitive enough to detect changes happening in micro- and meso-scale and provide bulk properties of the material (Hamarneh et al. 2013). On the other hand, acoustic (AE) techniques can be very sensitive in detecting damages formed in material, at early stages long before they affect bulk properties and thus are considered preferential methods in the characterization of microstructural changes. AE techniques were hypothesized in this thesis project to provide more local information as to whether the glass spheres detracted from the polyester due to thermal stresses, due to sensitivity to the

state of polymer chain mobility at or near the interface of the rigid surface with matrix. And so, in this study a non-destructive active AE technique was used to investigate the microstructure of the composites, particularly those changes in structure arising from residual thermal stresses in glass/polyester composites. Correlation of attenuation behavior of the acoustic wave with the polymer chain mobility at or near the glass/polyester interface was expected to provide information on interfacial strength and the effects of heat.

1.3. Outline

This thesis consists of 6 chapters including this chapter. In chapter 2, literature is reviewed on interfacial strength in fibrous and particulate composites containing solid/hollow glass spheres. Then use of passive and active AE techniques for characterization of microstructural changes in composites is reviewed. In chapter 3 materials and methods are described. Then curing of polyester and characterization of composite and the effect of glass spheres coating type and loading on its flexural stiffness are presented in chapter 4. In chapter 5, experimental results from mechanical and acoustic studies on the effect of thermal stresses on glass/polyester and its effect on interfacial strength are presented and compared. Also the effect of thermal stresses on attenuation behavior of acoustic waves in aged composites is investigated. Concluding remarks is presented in chapter 6.

Chapter 2: Literature Review

2.1. SMC Production Process

SMC production process involves mixing the ingredients i.e. resin, initiator, processing aids and fillers to form a paste. This paste is cast onto a carrier film where the amount of paste is evenly distributed by a doctor blade. Next, chopped glass fibers are immersed onto the resin paste. A second layer of the resin paste is laid on top to form a sandwich. This sandwich containing paste and fiber mixture is lightly pressed by passing through a set of compaction rollers for better wetting out of the fibers by resin as well as to squeeze out trapped air and other volatiles. Finally the compound is gathered into rolls and stored (3-5 days) for maturation (i.e. the increase in viscosity of the resin is allowed to reach a leather-like consistency) for easier handling. Matured SMC is molded into parts by a compression molding process (Kia 1993; Amos & Yalcin 2015).

A new SMC production method has been developed in which the compound is inline manufactured and subsequently directly molded. This technology, called “Direct SMC”, provides a fully automated processing method from raw material supply to the molded parts in which a better consistency of material treatment and a short processing time is achieved. The process stages include the combination of a batch-to-continuous dosing unit for the liquid raw materials; compounds the resin filler paste in a twin screw extruder; compounds the fibers into the paste on a sheet machine with subsequent fast maturation; and direct compression molding of the part occurs. Fig.2.1 demonstrates the process set up of a direct SMC production line (Potyra et al. 2011).

Preparation of Direct-Low density SMC has been reported (Keckl et al). It was found that the kneading elements of the mixing extruder had to be removed to retain intact a higher fraction of glass spheres thus achieving a lower density. The mechanical test results confirmed that low-density formulation can be successfully prepared through D-SMC process.

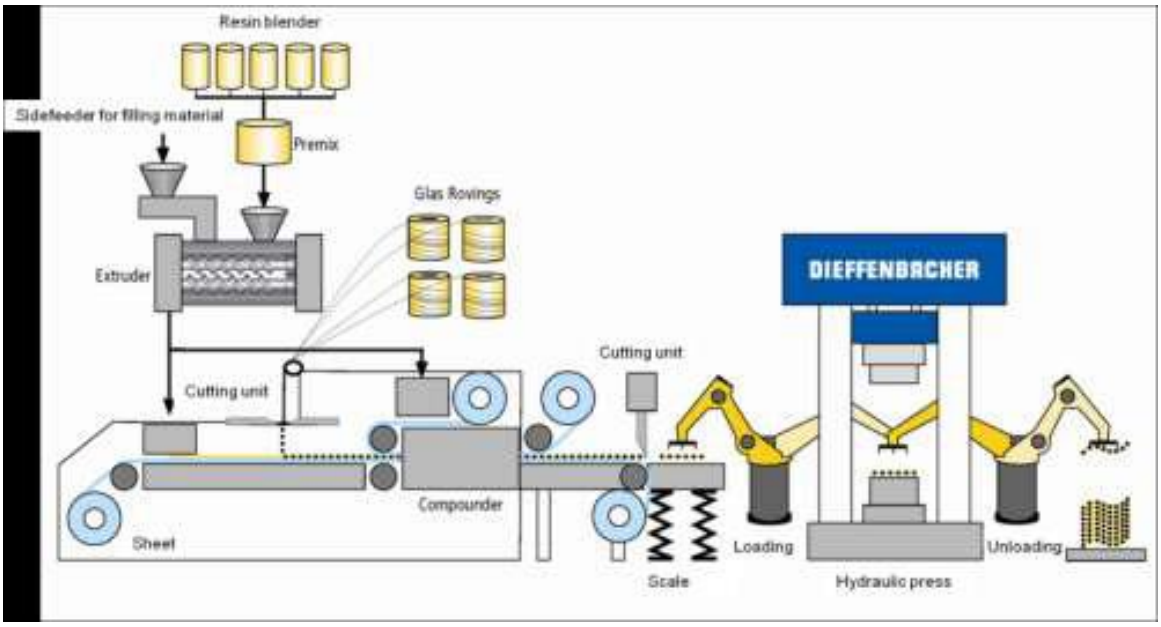

Fig.2.1. Process sequence of direct-SMC (Adopted from Potyra et al. 2011)

Low density SMC has been reported in the literature using surface modified glass spheres treated with different types of silane coupling agents to improve mechanical properties. Methacryl silane, glycidyl silane and amino silane were used. Flexural strength and modulus of the low density SMC prepared with surface modified glass spheres demonstrated an improvement compared to SMC containing unmodified glass spheres however the flexural properties were relatively insensitive to the silane type (Hamarneh et al. 2013).

As previously mentioned in the introduction chapter, the main aim of this study was to investigate the interfacial strength between glass spheres and polyester matrix and more specifically the effect of thermal stress on interface between glass sphere fillers and polyester which was assumed to cause the problems concerning the drop in mechanical properties and "paint popping" effect. Thus a system containing glass sphere/polyester was considered for our investigations to prevent interactions from other components in the material on studied properties. Due to the simpler system, the literature survey carried out focused primarily on the interfacial strength of glass fiber/polyester or glass sphere/polyester, which both provide valuable insights into the materials used.

2.2. Interfacial Strength in Glass Fiber Reinforced Polyester

The interphase between fiber and matrix has a major role in determining the mechanical interfacial properties of composites. Efficiency of stress transfer between fibers and matrix depends on both molecular interaction at interface as well as the properties of the formed interphase, such as thickness and strength (Madrer & Pisanova 2000). Treating the fiber surface with coupling agents is an effective way of creating an interphase thus improving mechanical properties of the composite (Park et al. 2000).

Silane coupling agents have been reported to improve the interfacial adhesion between glass fibers and polyester. The mechanism of adhesion by silane onto glass fiber surface involves association of the hydroxyl groups within the silane coupling agent to those on the glass fiber surface through siloxane bonding or hydrogen bonding, as demonstrated in Fig.2.2 (Park & Jin 2001).

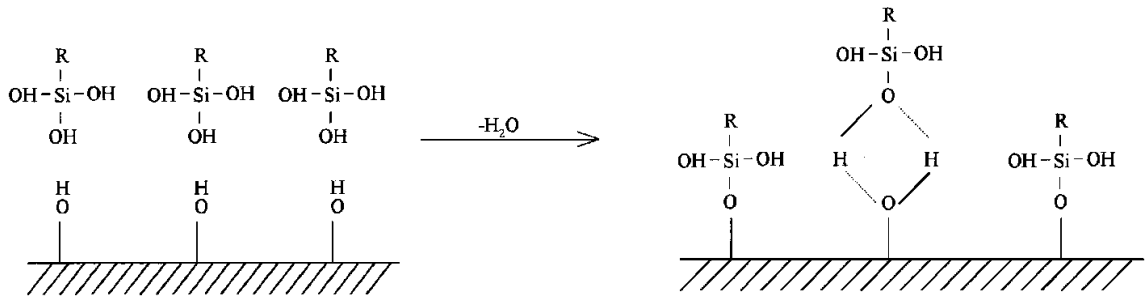

Fig.2.2. Structure of silane treated glass fibers (adopted from Park 2001)

The effectiveness of silane coupling agents in improving the interfacial adhesion depends on parameters such as type and thickness of the silane layer and its application method. A monomolecular reactive surface layer that form strong chemical bond with both constituent is expected to provide the optimum adhesion (Dibenedetto 2001). A detailed study on the efficacy of adhesion promotion by silane coupling agents has been performed by Jenkins et al.(2004) considering the effects of organofunctional groups and surface coverage. Park and Jin (2002) studied the effect of silane coupling agent on properties of glass fiber/polyester composites. Different concentrations of methacryl silane solution were applied on the glass fiber surface and their effects on improving the

adhesion were compared. In another study, methacryl silane (90 wt%) containing aminosilane (10 wt%) in cosolvent of methanol and water was applied to the surface treatment of the fibers at different concentrations. The silane coupling agent containing amino silane coupling agent improved the mechanical interfacial properties of composites, compared with those where a single coupling agent had been used (Yue & Quek 1994; Park 2001).

There are different tests for estimating the interfacial shear strength between fiber and matrix, and investigating the effect of glass fiber treatments on improving the glass/matrix interfacial adhesion. Single fiber composite tests such as *single fiber fragmentation*, *single fiber pull out* and *micro-indentation* have been widely used for this purpose. A comprehensive review on these methods can be found in a study by Herrera and Drzal (1992). Among these tests, the first one is the most popular method. This test is used to relate the mean fragment length to interfacial shear strength based on a force balance of the system consisting of a polymer matrix with an embedded elastic fiber. In this test a single fiber embedded in a matrix is broken under tensile load. Load is increased up to a point that no more fiber fragmentation occurs. Fragmentation saturates when all the fragment lengths are smaller than a critical length. This length is the minimum length which permits the tensile stress induced by interfacial shear stress to reach the tensile strength of the fiber. Interfacial shear strength (IFSS) is calculated based on the fiber tensile strength and the critical fragment length measured from a distribution of fragment lengths. Failure of the interface is the event that limits the ability to transfer of more load to fiber (Shioya & Takaku 1995).

Measuring the interfacial mechanical properties of the composite is another way to investigate the adhesion improvement at the interface indirectly. Properties based on interlaminar shear strength (ILSS) (determined by short beam shear test) and the critical stress intensity factor demonstrate improvement with silane treatment. Also an improvement in other mechanical properties of the composite such as tensile and flexural properties is obtained by surface treatment of reinforcing phase by silane coupling agents. An increase in ILSS and the critical stress intensity factor of the silane treated glass fibers

was reported by the author for a 0.2 wt% concentration of a combination of methacryl silane and an aminosilane in cosolvent of methanol (95 wt%) and water (5 wt%) (Park & Jin 2001). In another study treating fibers with 0.4 wt% of methacryl silane in cosolvent of methanol and water demonstrated the highest interfacial mechanical properties (Park & Jin 2002). Varga et al. (2010) reported the effectiveness of amide and ester-amide types of coupling agents for improving fiber/matrix interfacial strength by demonstrating an increase in tensile and flexural properties of the composite due to improved adhesion between treated glass fabric and polyester matrix. Park et al. (2000) have compared the ILSS and stress intensity factor of glass fiber/polyester composites in which fibers were treated with three types of silane coupling agents, namely aminosilane (AS), methacryl silane (MS) and glycidyl silane (GS) in a polyester matrix. MS demonstrated higher surface energies and better performance (in terms of improving mechanical properties) compared to the other two silanes followed by AS and GS. Effectiveness of silane coupling agents on improving the wet strength of glass/polyester and epoxy composites is attributed to factors such as chemical reactivity of the organofunctional group of the coupling agent to form covalent bond with matrix, the primary or secondary chemical bond formation at the glass interface and the ability of polymer to diffuse into siloxane interphase to form a network between bulk matrix and glass reinforcement (Plueddemann 1992; Dibenedetto 2001). It is reported that for the dry state strength, compatibility of the coupling agent tail group with the matrix is more important than its chemisorption on glass surface. However, for wet durability, chemisorption is essential. Decreases in composite flexural properties with wet aging are due to degradation of interphase (Wu et al. 1997).

Moisture aging studies on polymer composites indicate the deterioration of mechanical properties due to absorbed water. Water aging affects the matrix and degrades it through plasticization and chemical hydrolysis. It also attacks the reinforcement/matrix interface. The effect of hygrothermal history on moisture sorption and on degradation of ILSS was studied in glass/polyester composites. Glass fibers were treated differently to create different levels of adhesion with the matrix. It was concluded that strong interfaces led to

matrix dominant water sorption while weaker interfaces offered an easy path for water penetration in the composite (Pavlidou & Papaspyrides 2003).

2.3. Mechanical Properties of Particulate Composites and the Effect of Interfacial Strength on their Mechanical Properties

Mechanical properties of particulate composites depend on parameters such as particle loading, particle size and interfacial strength between the particulate filler and matrix. A survey of tensile and flexural properties of particulate composites and syntactic foams (composites containing hollow particles) is presented. Morphology of fractured surface under tensile and flexural loads is also considered.

Inclusion of inorganic micro-particles in polymer matrices results in increased stiffness of the polymer. On the other hand, strength of a particulate polymer composite depends on the interfacial strength between the particle and matrix and the effectiveness of stress transfer from matrix to particles. For a strong interface, strength increases while for a poor interface, there is a drop in strength observed (Fu et al. 2008).

Theoretically, an improved stiffness is predicted for polymer matrices containing rigid particles based on Einstein's equation; however it should be considered that this equation is only valid for low particle loading (due to an assumption of no particle interaction), for perfect adhesion at particle/matrix interface and for perfect dispersion of fillers in the matrix. The dependence of the stiffness of particulate composites on particle size, particle loading and matrix/filler interfacial strength has been investigated experimentally. Kenyon and Duffey (1967) reported an increase in stiffness for glass sphere/epoxy composites with an increase in particle loading from 0 to 50 vol%, which was attributed to replacing a portion of the matrix with semirigid particles. Dependence of modulus (slight decrease) on particle size (10-60 μm) was observed at high inclusion volume fractions (30-46 v%) while no dependency was observed at lower loadings (8-10 vol%) for a glass sphere/epoxy composite. In another study on glass sphere/epoxy composites (DiBenedetto & Wambach 1972), an increase in modulus was observed with increased glass loading but surface treatment of glass spheres did not affect modulus. The effect of

interfacial strength on flexural modulus of a glass sphere (30 μm) filled epoxy and polyester was investigated and yet no clear effect was observed. Since modulus is measured at low deformations there is not enough dilation to cause interface separation. (Fu et al. 2008).

Variation in strength of polymers by the introduction of inorganic particles and its dependency on particle loading and interfacial strength has been reported. For particles in the micron range of size, strength decreases with an increase in glass loading, which is attributed to increased stress concentration. Kenyon and Duffey (1967) reported a decrease in strength in glass sphere/epoxy composites with an increase in particle loading. The changes in strength resulted from the influence of particles on the stress field in the composite under load. For the silane treated glass spheres a slight increase in strength compared to the base resin was observed. The tensile strengths of glass sphere/polystyrene composites (glass spheres in 10-53 μm diameter range) having different levels of interfacial adhesion were studied (Dekkers & Heikens 1983). A reduction in composite strength was observed with increasing glass content while better interfacial adhesion resulted in higher composite strength.

As previously mentioned the adhesion strength at the interface determines the stress transfer between filler and matrix. In the case of poor sphere/matrix adhesion, debonding between particle and matrix under load results in the introduction of a small cap shaped cavity at the top of the sphere which produces in increased stress concentration and microcrack formation at the edge of that cavity at a lower applied stress compared to strongly bonded particles in which no debonding occurs (Fu et al. 2008).

The effects of thermal residual stresses on particle/matrix adhesion in a single particle composite (glass sphere/poly(vinyl butyral)) were investigated by Harding et al. (1998). The thermal residual stress state was varied by changing the processing conditions of the composite thus changing the stress state at the interface then interfacial strength was calculated and reported as a function of residual stress state. Surface modified glass spheres were used to create poor and strong adhesion between the particle and matrix. An

increase in the thermal residual stress level demonstrated a worsening effect on the interfacial strength for both composites especially for the one with interface with poor adhesion. To the best knowledge of author literature has sparsely covered the studies on the effect of thermal stresses on the interfacial adhesion in particulate composites especially on quantitative investigation of the effect of thermal residual stresses on interfacial strength such as the study by Harding et al.(1998). Thus research conducted in this thesis, examined the effect of thermal stresses on inclusion/matrix interface in hollow glass sphere/polyester composites using AE technique which is expected to provide high resolution for investigation of changes at interface on a meso-scale.

The introduction of hollow microparticles into polymer matrices at high loadings (well above 20 vol% normally) forms a class of materials known as syntactic foams. Addition of hollow spheres to polymers gives the advantage of weight reduction; however, they are not as effective as solid particles in improving the mechanical properties of the base resin due to their lower imparted strength. Wouterson et al. (2005) studied the tensile and flexural properties of an epoxy matrix containing different types of hollow spheres i.e. glass spheres having different wall thickness and strength (3M glass spheres; K15 and K46) as well as a polymeric hollow particle. Changes in tensile and flexural stiffness were dependent on the type of microspheres. Stiffness increased with the use of K46 and was almost constant for the other two. Specific stiffness increased with increased microsphere loading for K46 while was almost constant for K15. For K15, a proportionate decrease of density and modulus resulted in the constant trend. Increased density and larger thickness to radius ratio in K46 compared to K15 and the polymeric hollow sphere resulted in increased specific stiffness. Gupta and Nagorny (2006) also studied the tensile properties of glass sphere/epoxy syntactic foams. Glass spheres had different wall thickness thus different strength and densities. Modulus decreased with increasing glass loading when using the lowest wall thickness (0.52 μm) as a result of its lower strength, while no significant changes were observed in modulus with increasing glass loading for other glass spheres with thicker walls and higher strength. Also, the modulus for the lowest strength glass decreased compared to neat resin while increasing

slightly for the stronger glass spheres. Inclusion of weak particles relative to the same volume of load bearing matrix led to a decrease in strength and modulus. Huang and Gibson (1993) also reported a decrease in modulus with increasing glass loading; however they used a weaker glass microsphere in a stronger matrix compared to Gupta's study. The fracturing of these weaker glass spheres while under tension may be leading to sensitivity of the composites with a lower glass strength relative to its loading while stronger glass spheres which do not fracture significantly show an insensitivity to their added volume fraction. Results from a theoretical study on tensile properties of syntactic foams (Bardella & Genna 2001) showed the possibility of obtaining increased modulus of syntactic foams in case that glass spheres are strong enough.

Tensile and flexural strength of hollow glass sphere/epoxy composites decreased with an increase in particle loading from 0 to 50 vol%. There is an increase in specific tensile strength for composites with increasing filler content up to 10 vol%; however, beyond this content there is a decreasing trend since the reduction in strength becomes larger as density is further reduced. This nonlinearity in specific tensile strength was attributed to the reduction of the matrix volume fraction as the load bearing phase while glass microspheres only provided light weighting with minimal strengthening effect; the reduction of matrix volume fraction outweighs the stiffening effect of microsphere shells as a significant response to microsphere addition (Wouterson et al. 2005). According to Gupta and Nagorny (2006), a decrease in tensile strength of the glass sphere/epoxy composites compared to neat resin was observed for all glass sphere types (different wall thickness). With changing glass loading in the range of 30 to 60 v%, a 25-60% decrease in strength was observed. This was due to a decrease in the matrix volume fraction and consistent with results from Wouterson et al. (2005).

Maharsia and Jerro (2007) studied the effect of adding nanoclay to a hollow glass sphere/epoxy syntactic foams in order to improve its strength characteristics without compromising its damage tolerance properties. Composite contained 60-63 vol% glass spheres and 2-5 vol% nanoclay. An increased tensile strength was observed in the presence of intercalated nanoclay particles. A reduction in stiffness demonstrated the

increased fracture strain and toughness. Composites containing lower density glass spheres (0.22 gr/cm^3, 2.7 MPa) with thinner wall and lower strength failed under tension load due to glass sphere fracture and crack propagation while for stronger glass spheres (0.46 gr/cm^3, 41 MPa) glass matrix debonding and crack growth around the glass spheres was the observed fracture mode.

Kishore et al. (2005a;2005b) studied the shear properties of the glass sphere/epoxy syntactic foams under short beam shear tests. They observed a decrease in shear strength of glass sphere/epoxy syntactic foams from 5.8 MPa to 3.9 MPa with an increase in glass loading from 38 to 57 vol%. They reported a dependency of strength characteristics on the inter-particle distances. An effect of surface treatment of the glass spheres with paraffin was reported on shear properties of the syntactic foams. A decrease in shear strength was observed compared to foams containing untreated glass spheres due to the weakening of the interface and hence lowering the efficiency of load transfer. An improvement in flexural strength of censosphere/polystyrene foams with surface treatment by silane coupling agents was observed (Cardoso & Shukla 2002). Zhang et al. (2014) investigated the effect of surface treatment of hollow carbon microspheres with coupling agents on improving the flexural strength and modulus of composite. They also reported improved flexural properties in syntactic foams containing dopamine coated hollow carbon microspheres.

Investigation of failure modes for syntactic foams under three point bending by Kishore et al. (2005a) revealed the presence of similar features in its tension and compression regions with specimens fractured under pure tension and compression loads respectively. Glass sphere/matrix debonding, partial glass sphere cracking and river-like markings in the matrix were all observed as failure modes on the tension-dominated face of the foam while for the compression-dominated face, crushing and collapsing of the glass spheres and glass debris were observed. This was also reported by Wouterson et al. (2005) for the fractured surface under three point bending. Different loading modes at the upper and lower parts of the cross sectional areas of the specimen were observed. Similar features in the part loaded in tension with specimen tested under pure tension were observed.

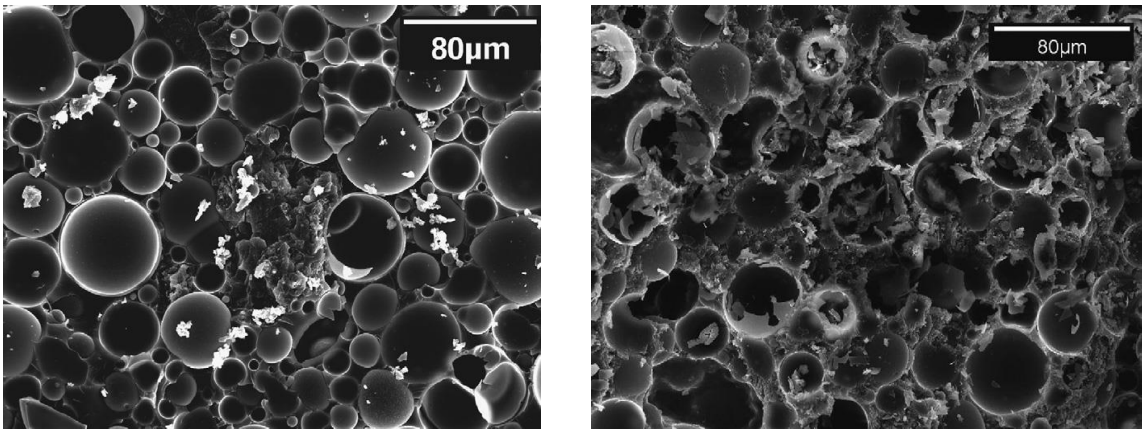

(a) (b)

Fig.2.3. Tensile fractured surafce of epoxy matrix containing (a) high density, (b) low density glass spheres (Maharsia and Jerro 2007)

Wouterson et al. (2005) examined the morphology of tensile-fractured surfaces and observed the presence of step-like structures, indicative of the plastic yielding of the epoxy matrix under tension. Intact microspheres were observed. Crack growth over the interface indicated the presence of debonding caused by the complex stress state around the particle/matrix interface. Similarities were observed as failure mode of specimens under tensile load and three-point bending explains the similarity in tensile and flexural behavior of the composites.

Fig.2.3 compares the fractured surface of syntactic foams under tension for high and low density microsphere. In the foam containing stronger glass sphere (thicker wall, higher density), debonding of the glass from matrix was observed without significant amount of glass debris while for the glass sphere with thinner wall, fractured microspheres were observed (Maharsia & Jerro 2007).

2.4. Acoustic Emission (AE) Technique

As demonstrated in the previous sections, mechanical property characterization of composites provide information about the material at the macro-scale but does not have enough resolution to detect microdefects such as matrix microcracks or matrix/reinforcement debonding at their early stages of formation. AE techniques are

capable of damage detection at early stages of damage formation, much before reaching a critical stage that affects bulk properties. Formation of microfailure events in a material under load is associated with a redistribution of the strain energy around the damaged area, generating elastic waves in the process. Passive AE technique deals with the detection of these elastic waves upon reaching the surface of a part with a transducer. Hence, AE techniques are preferential methods to investigate the microstructure changes in materials. In active AE techniques, the propagation behavior of a generated elastic wave in material is investigated. Ultrasonic characterization of materials is a type of active AE technique in which high frequency sound waves in the range of 1 to 10 MHz are generated and their velocity and attenuation in material is studied. This thesis research has been performed on evaluating the interfacial adhesion strength of composites using active AE methods. Our method was to introduce an AE signal using the "pencil lead break" method (more commonly used to calibrate AE sensors) and examine its propagation behavior in the material before and after experiencing thermal stresses in order to investigate changes in microstructure due to heating and specifically its influence on interfacial strength. Literature on both passive and active AE in examining composites is reviewed below.

2.4.1. Passive AE in Fiber and Particle Reinforced Composites

Passive AE is a useful method to detect and locate the active damage in fiber/particle reinforced polymers and also to characterize the damage mode. Different damage modes observed in fiber reinforced polymer composites include matrix cracking, fiber/matrix debonding, fiber breakage and delamination. Many studies have examined the possibility of damage source identification with AE technique through changes in the acoustic signature for each damage source. Conventional AE methods use time domain features such as amplitude distribution, counts, duration, energy, rise time, first hit, etc. to identify different damage modes in material. The relationship between amplitudes of emitted waves during fracture and damage mode has been reported by different researchers. Fracture behavior of glass/polypropylene was investigated by Wang et al. (2008) and different amplitude ranges were assigned to different damage sources; 40 to 70 dB was

related to matrix deformations and interfacial debonding, 70-85 dB to fiber pull-out and 85-90 dB to fiber breakage. Kotsikos et al (2000) used AE to investigate damage sources in glass/polyester composites. They assigned low amplitudes, 40-55 dB, to matrix cracking, 55-75 dB to delamination and debonding, and high amplitudes (higher than 80 dB) to fiber fractures.

AE can be used for detection of partial processes like interphase debonding which release elastic energy at the moment of failure. Bohse (2000) has correlated the number of AE events in polymer blends under tensile load with specific interphase area. A linear correlation between energy of the emitted wave under tensile loading with the energy of the microfracture process (interphase debonding and break of fibrils) has also been demonstrated for polymer blends. Single fiber pull-out test have demonstrated the relation between signal energy and energy of microfailure processes such as fiber/matrix debonding and fiber break.

Investigation of interfacial strength by means of passive AE technique has been reported. In single fiber fragmentation test in conjunction with AE, acoustic emissions are generated by each fiber break (Petitcorps et al. 1989; Netravali et al. 1991). This technique has been used to measure the number of fiber fragments. Also Netravaldi et al. (1991) has used this technique to locate the fiber fracture source and measure the fiber fragment length, thus calculating the IFSS from the fragment lengths. This method is especially useful in cases of non-transparent matrices where optical methods do not work for monitoring the fiber breakage. Park et al.(2004) correlated the number of AE events with the number of fiber fractures where again the fragment length was used to calculate IFSS for carbon/epoxy composites. Treated fibers showed increased number of fragments versus non-treated fibers.

Minko et al. (1998; 2000) used AE to study the interfacial strength and local debonding stress in glass sphere/polystyrene particulate composites under tension. The average debonding stress was obtained from the maximum of the number of AE events per stress unit which was fitted with a Weibull function. The number of AE events was in the same

range as the number of inclusions. The ratio of the numbers was treated as a function of the interfacial adhesion present. AE amplitudes were fitted with the same distribution function to obtain the released AE energy under tensile load from the maximum of the function. An increase in the average debonding stress was observed with an increase in interfacial strength for the modified glass surface. AE amplitude usually needed to be fitted with two Weibull functions with two large and small values for a maxima, A-I and A-II. An increase in adhesion resulted in a decrease in A-I and A-II. A-I was associated with the microdefects at the interface formed during the material preparation stage. A-II was related with the dewetting of the glass spheres. A small amplitude (i.e. A-I) was observed in the case of a weak or a strong interface. Small amplitude for the strong interface was suggested to be a result of propagation of the cracks from the interface to the matrix.

Frequency features of the AE waveform from different damage modes are believed to be highly effective in characterizing the microstructural changes during fracture (Wang et al. 2011; Sause & Horn 2013; Gomes et al. 2014). Calabro et al. (1997) highlighted the relevance of frequency content analysis of AE signals in order to reconstruct the whole damage process. Different viscoelastic relaxation processes near each damage source (i.e. matrix cracking, fiber/matrix debonding and fiber breakage) enables damage mode identification based on frequency content of the emitted wave. Different intrinsic frequencies and elastic acoustic velocities result from different elastic moduli and densities, thus different relaxation processes in fiber and matrix are detectable (Bohse 2000).

Giordano has used the frequency content of AE data emitted from tensile testing of a single fiber composites (carbon/polyester) to study the acoustic fingerprint of fiber breakage in terms of frequency content (1998; 1999). Generation and acquisition of acoustic events due to a specific failure mode (i.e. fiber fracture) enabled a basic characterization of the signal. Acquisition of different events during different tensile tests which were then compared showed that a clear acoustic finger print could be

characterized in terms of frequency content. Yu et al. (2006) associated the frequencies of 100 and 230 kHz to matrix and fiber failure, respectively in carbon/epoxy composites. Ramirez et al. (2004) performed tensile testing on glass/polypropylene composites and associated the 100 KHz to fiber/matrix debonding, 200-300 kHz to fiber slippage and pull-out, and 400-450 KHz to fiber breakage. De Groot et al. (1995) associated frequencies between 240 KHz and 310 to fiber/matrix debonding, and 180-240 KHz to fiber pull out in a carbon/epoxy composite.

Kotsikos et al. (2000) studied the effect of hydrolytic aging on AE characteristics of glass fiber reinforced polyester composites. Hydrolytic aging in glass fiber/polyester composites cause matrix plasticization, and weakening of the interfacial strength between fiber and matrix. An increase in the number of AE events under four point bending was observed for the aged composites. The number of events in the amplitude ranges associated with matrix cracking, fiber/matrix debonding and delamination was influenced by pre-exposure to water while not for fiber breakage. On the contrary, Godin et al. (2006) has reported a decrease in AE activity with aging for 45° and 90° off-axis unidirectional samples under tensile load, mainly concerned with the events in the amplitude range of 50-70 dB and a relative increase in the number of events in the amplitude range of 70-90 dB which demonstrated dominance of an interfacial debonding damage mechanism occurred in aged composites compared to the non-age composites. Gomes et al. (2014) studied the effect of aging fluids on acoustic signature of polyethylene under tensile load. They reported a correlation between signal envelope energy and aging time.

Discriminating the AE signals resulting from different types of damage in a composite enables damage mode identification. Conventionally, single parameter descriptors such as amplitude or duration of a signal were correlated to a specific damage mechanism; however it has been proven that single parameter analysis can hardly result in a proper discrimination among signals while complex damage modes are involved due to the overlap of the range of the parameters describing the damage mode. Pattern recognition

techniques in which multiple AE descriptors are used lead to a better discrimination among signals emitted from different damage sources and a more reliable classification of signals based on AE source (Yang et al. 2009). Classification is performed based on the similarities and differences among these descriptors. Also, the use of multivariate statistical analysis has proven effective for the classification of AE signals. Johnson et al. reported classification of AE characteristics to matrix cracking, local delamination and fiber breakage in glass reinforced epoxy composites using principal component analysis (PCA) (Johnson & Gudmundson 2000; Johnson 2002). Manson (Manson et al. 2002) used PCA and cluster analysis for classification of AE data. Huguet et al.(2002) and Godin et al.(2004)(2005) used Kohonen's self organizing neural network, k-mean cluster analysis and k-nearest neighbor method for classification of AE signals from different damage modes in glass/polyester composites. Sause and Horn (2013) used pattern recognition technique to classify signals based on a number of frequency domain features for damage mode characterization in carbon fiber reinforced polymers.

In our study, acquisition of passive AE from thermally stressed material was not successful so an AE source was used instead produced through pencil lead breaks against a part and monitoring the propagation of the wave to investigate changes in the microstructure before and after heating. Changes in the acoustic signature (frequency-amplitude) due to thermal stress for different interfacial strengths were investigated. A supervised classification method was used to recognize the frequencies that were more important in distinguishing the acoustic signatures. The following section reviews the research work conducted on the use of active AE methods for characterization of the microstructure in particulate polymer composites.

2.4.2. Active AE in Particulate Composites (Propagation of Elastic Waves in Material)

Propagation of elastic waves in materials is characterized by velocity and attenuation of sound wave travelling through a certain medium. Acoustic characteristics (velocity and attenuation) of sound waves in materials can be used for characterization of their elastic properties and microstructure (Lionetto & Mafezzoli 2008). Velocity is directly related to

density and stiffness of a material. Attenuation is a decrease in energy (notably the amplitude of a signal) upon transmission from one point to another, resulting from scattering, absorption or reflection of the propagating wave (Drury 2005). Scattering is due to inhomogeneity of the material and an acoustic impedance mismatch between two interfaces having different sound velocities or densities. Absorption is due to conversion of sound energy to heat and reflection is due to discontinuities in material. In this section theories on elastic wave propagation behavior in particulate composites are briefly reviewed. Studies considering the effects of viscoelasticity of matrix polymer and imperfect interfacial state on wave propagation are included to realize the expected wave behavior in a system similar to the one examined in this thesis. Research conducted on measurement of wave attenuation in glass sphere containing polymers is included.

Theories have been developed to investigate wave propagation in an inhomogeneous medium such as particulate composites. Waves undergo multiple scattering while travelling through such a medium, which leads to frequency-dependent dispersion and attenuation. Multiple scattering of elastic wave by spherical inclusions in an elastic medium have been studied by Waterman and Truell (WT) (1961) to estimate phase velocity and attenuation of waves in terms of microstructure and properties of the matrix and inclusions. Deviations between predicted values from WT and experimental results at high inclusion concentrations are observed (Kim 2010). Theories based on self-consistent methods were introduced to overcome the limitation of the WT method at high concentrations. In these theories, the behavior of an inclusion embedded in a homogeneous medium with the effective properties of the composite is considered (Sabina and Willis 1988). Dynamic generalized self-consistent methods (DGSCM) for studying the wave behavior in composites were reported by Yang and Mal (1994), (Kim et al. 1995), Yang (2003; 2004) and Wu et al. (2006). Differential approaches such as a model by Beltzer and Brauner (1987) considered an incremental realization of the effective medium which implements the homogenization process numerically (Biwa et al. 2004). Kim (2010) has done a comparative study on different models predicting the

elastic wave propagation in random particulate composites to investigate the disagreements between predicted and measured values for wave velocity and attenuation.

Effects of viscoelasticity of matrix on wave propagation in particulate composites were studied by Beltzer et al. (1983) and Biwa (2001) in which absorption loss due to matrix viscoelasticity was introduced to the models. Biwa et al (2002) explained the attenuation of elastic waves in particulate composites based on independent scattering/absorption theory in which the absorption loss by the viscoelastic matrix was explicitly accounted and is only valid for dilute particle concentrations. Frequency and particle size dependence of attenuation behavior of particulate composites was demonstrated. Biwa et al. (2004) proposed another model based on differential scheme with improved predictability at higher particle concentration compared to independent scattering/absorption approach for predicting the wave propagation in particulate composites with viscoelastic matrix. Numerical results from Biwa et al. model (2002) predicting the attenuation coefficient versus particle size at 20% particle concentration for 2 and 5 MHz showed an increase with particle radius; however, for particles with radius lower than 10 μm, attenuation appeared to be independent of particle size and governed by absorption loss in matrix. Comparison with experimental results from Kinra et al. (1980) for 8.6%, demonstrated good agreement due to dilute concentration. For higher concentration, 45.1%, predicted values from Biaw.et al. (2004) model based on differential scheme demonstrated improved predictability compared to the values from independent scattering model (Biwa 2002).

Effect of imperfect interface between matrix and inclusion on wave propagation behavior in a random particulate composite was studied by Wei and Huang (2004). They studied the dynamic effective properties of particle reinforced composites with a viscoelastic interphase. Numerical simulation for SiC-Al case showed the influence of viscosity of the interphase on the effective wave velocity, elastic moduli and attenuation. Viscous effects of the interphase can reduce the effective phase velocities and effective elastic moduli and increase the effective attenuation. Attenuation of the effective wave was related to

multiple scattering effects and the material dissipation of the viscoelastic interphase. The dissipation effect of the interphase dominated in a range of relatively low frequencies. After sufficient relaxation of the interphase, the composite behaved as a porous material. A theoretical study by Liu and Wei (2008) considered the wave interaction with particulate composites with imperfect interfaces in which the function of the interphase was modeled by a spring. Imperfect interface exhibited different scattering characteristics compared to perfectly bonded interface. The influence of interface strength on the propagation constants (velocity and attenuation) of the wave was confirmed especially in the case of weak interface. Velocity of the effective waves showed sensitivity to weak interface damage while less sensitivity was observed for stronger interface.

Wu et al. (2006) have considered spherical inclusions in an amorphous matrix to model spherulitic polymers. Measurements of acoustic characteristics were implemented on glass sphere/epoxy matrix composites and agreement of the result with the WT model and a dynamic generalized self-consistent method was investigated. Attenuation of longitudinal waves as a function of frequency were measured for three concentrations; 5.6%, 10% and 41.3%. Attenuation demonstrated a monotonic increase with increasing frequency for all three concentrations. Acoustic characteristics at 1.5 MHz and 7 MHz were measured as a function of particle concentration. At 1.5 MHz a decrease in measured values for attenuation from 6 to 4 dB/cm was observed between 5% and 10% concentration followed by an increase to 12 dB/cm for 15%. Attenuation was stable around 6 dB/cm for higher glass concentrations up to 40%. Predicted values from DGSCM model demonstrated a slight decrease in attenuation with increased particle concentration. Measured values for attenuation at 7 MHz versus glass concentration demonstrated an increase from 55 to 95 dB/cm for an increase in glass content from 5 to 15% then gradually decreased to 75 dB/cm with a further increase in concentration to 40%. A good agreement with the DGSCM model was demonstrated while WT demonstrated a good agreement only at low concentrations. DGSCM prediction of attenuation results was closer to experimental data than WT at both frequencies for concentrations higher than 15 vol%. This was also observed by Kim et al. (1995).

Dependence of attenuation on wavelength to radius ratio (λ/r) and particle concentration was investigated for glass/polyester particulate composites having radius of 22.5 μm over 3-6 MHz (Biwa et al., 2004) for 21% and 33% particle concentrations. A lower attenuation in composite versus attenuation in viscoelastic matrix was observed at certain frequency range. It was shown both theoretically and experimentally that the attenuation of the composites decrease with particle concentration when the particle size was sufficiently smaller than the wavelength. For 3 MHz, attenuation decreased with increased particle concentration while for higher frequencies, non-monotonic particle-fraction dependence was seen. It was attributed to the dominance of viscoelastic loss in overall composite attenuation when the particle size is small compared to wavelength.

Experimental works on elastic wave propagation in particulate polymer matrix composites has been performed by Datta and Pethrick (1980). An increased attenuation in composite compared to neat polymer was attributed to the scattering effects due to introduction of solid glass spheres (197, 368 and 690 μm) to polyethylene and polymethylmethacrylate. Kinra et al. (1980) investigated the wave behavior in an epoxy matrix containing glass spheres (150 μm). Longitudinal and shear wave velocities as well as attenuation of the longitudinal waves as functions of frequency and volume fraction of glass inclusions were studied. Attenuation as functions of frequency for 8.6% and 45.1% concentrations, demonstrated an increase with an increase in frequency from 0.5 to 3 MHz. In another study by Kinra et al. (1998) transmission of longitudinal plane waves in a layer of spherical lead inclusion in polyester matrix was investigated. Excitation of the rigid body translational resonance was the dominant feature of the transmission spectrum. Influence of resonance effects on wave propagation in a lead sphere/epoxy composite was reported (Kinra et al. 1982).

Mylavarapu and Woldesenbet (2008) measured the velocity and attenuation coefficient in hollow/solid glass sphere in an epoxy matrix. A lower attenuation was expected for solid glass containing composite compared to hollow glass/epoxy composite due to the porosity of hollow spheres; however, a reverse trend was observed. This difference was

attributed to the presence of resonance effects in solid glass particulate composites not seen with hollow particles. Absorption of the acoustic signal in the hollow glass particles was considered to be responsible for the attenuation not attributable to scattering effects. Comparison of attenuation in composites containing hollow glass particles with different wall thickness (same outer radius) thus different radius ratio (r_{in}/r_{out}), demonstrated increased attenuation with a decrease in wall thickness and thus an increase in cavity size inside the hollow particle. Attenuation within the composites was measured with an increase in glass particle concentration from 10% to 60% at 1 MHz frequency. An increase was observed from 10% to 30% followed by a decrease. Increased attenuation at lower concentration was attributed to an increase in scattering effects. Replacing a fraction of matrix with glass particle was expected to reduce the attenuation due to reduced absorption however according to Mylavarapu and Woldesenbet (2008) the scattering effects were dominant at that particle concentration range. Decreased attenuation from 30% to 60% was attributed to scattering from a cluster of particles (λ/D=65-100) due to decreased spacing between particles and also due to reduction of highly attenuating matrix. A decrease in velocity with an increase in particle concentration was observed due to decreased density in hollow glass containing composites. It should be mentioned that results from Mylavarapu and Woldesenbet (2008) contradicts our findings.

Chapter 3: Experimental

3.1. Materials

Unsaturated Polyester Resin, Grade T320-70, was provided by AOC (Guelph, Ontario). This is a high reactivity and un-promoted pultrusion resin. Specific gravity and viscosity are 1.06 and 2.35 Pa-s, respectively.

Hollow Glass Microspheres, iM16K (uncoated) and iM16K-L21342A (coated) high strength glass bubbles with a crush strength of 110 MPa were provided by 3MCanada (London, Ontario). Both are the same low density fine powder containing 97wt% soda lime borosilicate glass. Average diameter and specific gravity of glass spheres were 20 μm and 0.46. The proprietary coating L2-1342A was specified by 3M for the polyester resin and is known to be different from the coatings applied in this work.

Methylethylketone Peroxide (Luperox DDM9; Arkema Inc, King of Prussia, PA) was purchased from Sigma Aldrich. 35 wt% peroxide diluted in 2,2,4-trimethyl-1,3-pentanediol diisobutyrate (9% active oxygen). Society of Plastics Industry (SPI) Activity at 25^{o}C, minimum cure time = 33.1 min (1% in isophthalic polyester resin).

[3-(2-aminoethylamino)propyl]-trimethoxy silane and **(3-Glycidyloxypropyl) trimethoxy silane** were purchased from Sigma Aldrich (Fig.3.1(a-b)).

Sodium montmorillonite clay (Cloisite Na+; Southern Clay Products) was purchased from BYK Additives, whereas technical grades of methanol and glacial acetic acid were purchased.

(a) (b)

Fig.3.1. Chemical structure of (a) [3-(2-aminoethylamino)propyl]-trimethoxysilane and (b) (3-Glycidyloxypropyl) trimethoxy silane

3.2. Preparation of Coated Glass Spheres with Silane Coupling Agents

Two different types of silane coupling agents were used to coat the iM16K glass microspheres, namely [3-(2-aminoethylamino)propyl]-trimethoxy silane, and (3-Glycidyl)oxypropyl)-trimethoxy silane. To treat the glass spheres surface with different silane concentrations, 0.008-0.001 wt% and 0.004-0.005 wt% of silane (based on total solvent) was added to a solution containing methanol (95 wt%) and distilled water (5 wt%). After hydrolyzing the silane solution for 1 hr at a pH: 4 (adjusted with acetic acid), glass microspheres were added and kept in solution for 1 hr. Then the solution was decanted and coated glass spheres were left over night to dry in ambient air. Finally the coated glass spheres were dried in an oven for 1 hr at 105℃ and particles smaller than 125 μm were collected with a fine mesh sieve for specimen preparation. Coated glass spheres were stored in a desiccator before use. Burn off tests in a muffle furnace at 600℃ for 1 hr were performed on dried glass spheres to determine the weight fraction of organic coating on the glass sphere surface. The concentrations of the silane solution were chosen based on the burn off test results of iM16K-L21342 glass spheres which were coated by 3M Canada. 3M coated glass spheres showed a 0.6-1.1% weight loss after burn off test and the concentration of silane solution (0.008-0.01 wt%) was adjusted to obtain a similar weight loss in burn off test (obtained 1.1-2.4% weight loss). A lower silane concentration (0.004-0.005 wt%) was also chosen for comparison (obtained 0.35-0.7% weight loss).

Hollow glass microspheres having different coatings are represented by 16K, L21, AS6, AS12, GS6 and GS12 Table.3.1 shows the coating types used for modification of glass spheres used in this study. These alphanumeric codes will be used to refer to respective glass spheres or coatings.

3.3. Preparation of Hollow Glass Microsphere/ Polyester Composites

Hollow glass microsphere/polyester composites containing 0.5%, 1% and 5% (w/w) glass spheres (based on resin weight) were prepared (1, 2 and 10 vol% respectively). All specimens contained 1% (w/w) clay, Cloisite Na+, to obtain uniform heat distribution in

specimens for further testing (thermal cycling) and also to improve ductility of the composite specimens for mechanical testing. Specimens with no clay and low glass sphere concentrations were too brittle for mechanical testing, fracturing in the grips of the instrument. First, clay was mixed in with resin then glass spheres were added. The mixture was mixed with an impeller for 1 hr at 225 RPM and 25℃. Afterwards, the mixture was de-foamed under vacuum in a vacuum oven at 60℃ for 15 min to facilitate removal of entrapped air. After cooling at ambient temperature for 5-10 min, 1 wt% of peroxide, DDM9, (based on resin weight) was mixed in for 5-10 min and finally the mixture was cast into dog bone or rectangular shaped molds and cured in oven for 3 hrs at 120 ℃. Neat polyester was used for control specimens.

Table.3. 1. Coating type on hollow glass microspheres

Glass spheres	**Coating type**
16K	No coating
L21	Commercial 3M coating
AS6	Lower concentration (aminoethylamino)-propyl-trimethoxy silane, 0.008-0.01 wt% (in 95% methanol, 5% distilled water solvent)
AS12	Higher concentration (aminoethylamino)-propyl-trimethoxy silane, 0.004-0.005 wt% (in 95% methanol, 5% distilled water solvent)
GS6	Lower concentration (glycidyloxypropyl)-trimethoxy silane, 0.008-0.01 wt% (in 95% methanol, 5% distilled water solvent)
GS12	Higher concentration (glycidyl-oxypropyl)-trimethoxy silane, 0.004-0.005 wt% (in 95% methanol, 5% distilled water solvent)

3.4. Methods

3.4.1. Flexural Test

A bench-top universal mechanical testing system, Model 3366 (Instron Corporation; Norwood, MA) with a 5 KN load cell was used for mechanical testing. Three point

bending tests were conducted in accordance with ASTM D-790 to characterize the flexural properties of rectangular specimens of average 3 mm thickness, 118 mm length and 25 mm width. This test method was used for neat polyester samples. Cross head speed and span length were 1.668 mm/min and 48 mm, respectively. Five specimens were tested for each condition.

3.4.2. Modified Flexural Test

This modified flexural test was conducted on composites containing 0-10 vol% 16K and L21 glass microspheres to optimize the curing reaction for the subsequent thermal cycling tests. No clay was used in these tests and since the pure polyester was extremely brittle, such that it could be fractured when using the standard tensile grips, a flexural test was the decided approach. Non-standard dog bone specimens (Fig.3.2) were used in which the narrow section was off-center (with respect to the mid-length of the specimen) since this molded shape would be subsequently necessary to allow attaching AE sensors in the thermal cycling studies; no acoustics were reported during the flexural tests. The width and length of narrow section are 12 mm and 18 mm respectively. Average thickness was 3 mm. Total length of sample is 118 mm and width of sample is 25 mm. At least four specimens were tested for each condition. A cross head speed of 5 mm/min was used in the tests and a support span length of 77 mm was chosen.

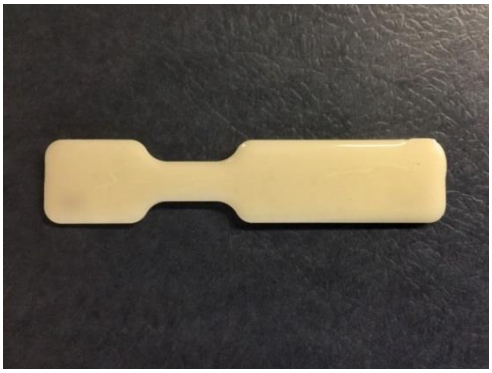

Fig.3.2. Modified dog bone specimens used in all trials, flexural and tensile for this project.

3.4.3. Tensile Test

Tensile tests were conducted on composites containing glass spheres with different coatings to investigate the effects of glass loading and interfacial strength on tensile modulus. Tensile properties of composite before and after thermal cycling experiment (described in Section 3.4.7) were compared to investigate the effect of thermal stresses on their stiffness. Non-standard dog bone specimens (described in section 3.4.2) were used. All composites contained 1% (w/w) clay (based on resin weight) in addition to the glass microspheres, in order to minimize brittle fracture in the grips. A cross head speed of 5 mm/min was used for testing. Four specimens were tested for each condition.

3.4.4. Light Microscopy

Axioplan 2 imaging universal Microscope in transmission mode was used to investigate the glass microsphere dispersion state in polyester matrix. The microscope is located in the Canadian Centre for Electron Microscopy (CCEM).

3.4.5. Scanning Electron Microscopy

Scanning electron microscope (JEOL 7000, USA) at 3 and 10 KV (a few images at 10 KV), was used to study the fractured surface and interfacial strength of hollow glass microsphere/polyester composites after tensile loading. Specimens were platinum sputtered. Both secondary and backscattered mode images were obtained. The microscope is located in the Canadian Centre for Electron Microscopy (CCEM).

3.4.6. Acoustic Emission (AE) Monitoring System

AE testing was used for characterizing the effect of thermal stresses on glass sphere/polyester composites with different interfacial strength and glass sphere loading through both passive and active AE testing. During testing, two flat response wideband AE sensors (F-30α, Mistras Group Inc.) demonstrated in Fig.3.3 were mounted on both faces of the sample 58 mm away from the center of the narrow section. F-30 α sensor has a very high sensitivity and flat response in the bandwidth of operation; 150-700 kHz. The signals from one sensor were pre-amplified by 20 dB prior to acquisition and were

sampled at a rate of 2.00 MHz with a 10 MHz 12-bit-4-channel simultaneously-poling data acquisition card (National Instruments Corporation) attached to a computer running custom code written in LabVIEW™ (National Instruments Corporation). The code was created by other researchers in the lab and essentially operates to collect high speed signals and record to files the burst signals related to AE events. Hit detection for recognition of an AE event used a threshold value of 6 mV based on the amplified sensor signal.

In addition to passive AE recording, active AE recording was also conducted at different stages of the experiment. In active AE, an elastic wave was created externally on the samples by breaking a pencil lead on the surface of the sample (according to ASTM E976) and the propagation of the elastic wave was investigated.

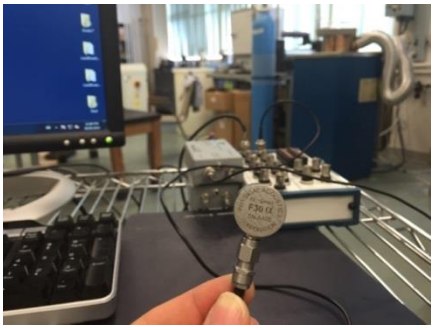

Fig.3.3. F-30α AE sensors which have high sensitivity and flat response at band width of 150-700 kHz

3.4.7. Thermal Cycling-AE

The method of passive acoustics analysis relied upon thermal stresses rather than mechanical stresses to affect the glass sphere /polymer interface and hopefully elicit an elastic wave due to debonding. An 50x60x70 cm environmental chamber was used in order to perform a heat-cool cycle on the specimens, isolated from conditions in the room. A hot air gun (Milwukee, 537^{o}C) and a cold air gun (Vortec) were attached to the chamber to provide heating/cooling sources (Fig. 3.5). The hot air gun was used to convectively heat the samples from room temperature to 110-130℃ at a rate of approximately (4-8℃/min) then chilled air was used to cool the samples back to room temperature. This heat-cool cycle was repeated two times and monitored by a K-type

thermocouple affixed to the top-side of the sample where the hot air was applied (60-70 mm away from the point where air was directly blown at). The distance between heat gun and sample was 65 mm. The AE sensor was protected from the hot air by an insulated metal barrier. Passive AE were recorded during first and second heating cycle in order to capture events related to micro-cracking or particle-matrix de-bonding caused by thermal expansion coefficient mismatch of glass spheres and matrix.

3.4.7.1. Thermal Cycling-Active AE test (Pencil Lead Break Test)

Active acoustic emission testing was conducted by breaking a pencil lead (PL) on surface of samples at different stages of the test and the resulting propagation of an elastic wave in the specimen was investigated. The effect of thermal stresses was investigated by comparing the pencil lead break AE signatures before applying any thermal stresses on composites and after thermal cycling, also changes with changing interfacial strength and glass loading was investigated.

For the pencil lead break (PLB) tests a distance of 75-90 mm was kept between the point for lead break and the sensors. In order to ensure reproducibility in the pencil break test, the procedure outline in ASTM E976 was followed, where a Nielsen Shoe, as seen in Fig.3.6 was used to maintain a consistent break angle.

Pencil lead break tests at room temperature (PL-RT) were conducted before (PL-RT1) and after (PL-RT2) first heating cycle and before (PL-RT2) and after (PL-RT3) second heating cycles. Pencil lead break tests were also done at the peak temperature of each cycle i.e. PL-HT1 and PL-HT2. Five consecutive lead breaks were performed using a Pentel Hi-Polymer 0.5 mm HB pencil lead at each condition for each specimen. Four specimens were tested for each condition, i.e. 20 pencil lead break test were performed per each condition. A Python code developed by other researchers in the lab was used to analyze the recorded AE signals. Fig.3.4 and Fig.3.5 show a schematic of thermal cycling-AE recording experiment and the experimental set up for thermal cycling, respectively.

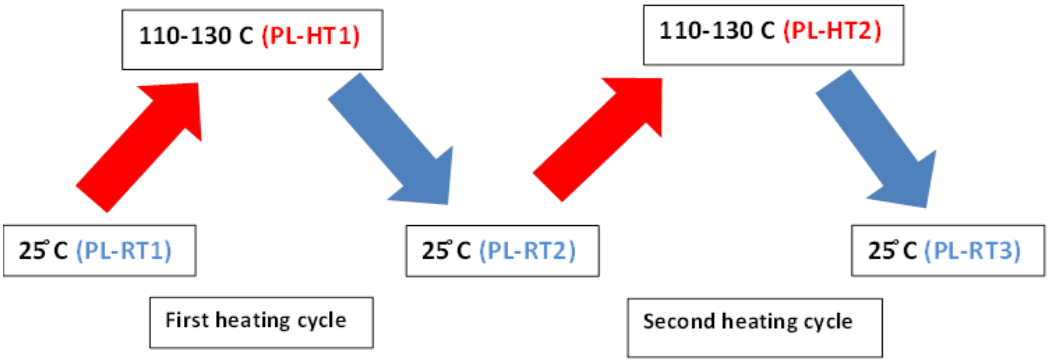

Fig.3.4. Diagram illustrating data acquisition stages and temperatures during the thermal cycling experiment

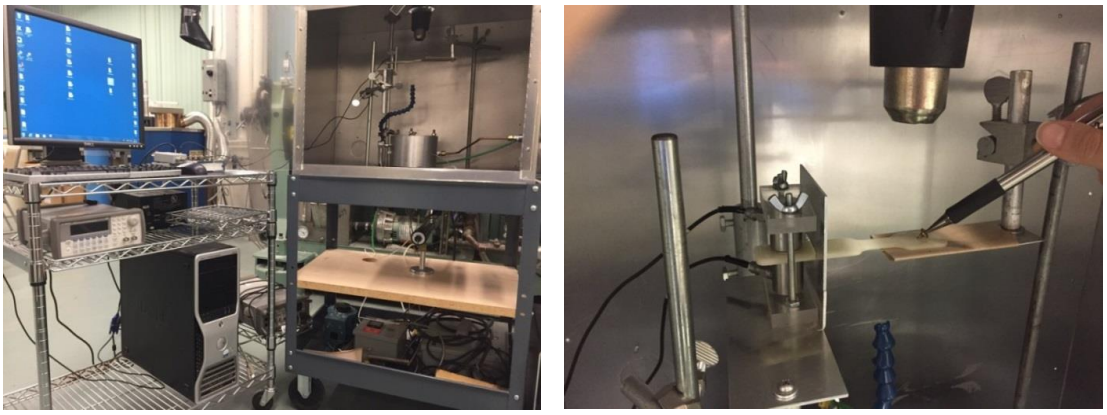

Fig.3.5. Photos of the thermal cycling-AE experimental set up

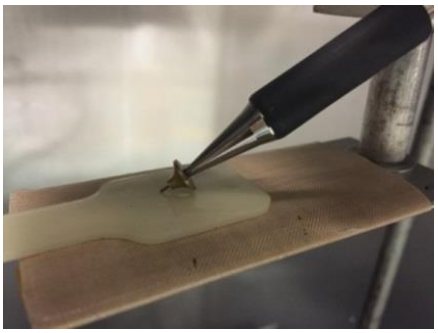

Fig.3.6. Nielsen shoe used for pencil lead break test

3.4.7.2. Thermal Cycling-AE of Aged Specimens

Specimens were immersed in water for two weeks in a room with controlled temperature and humidity, 23 ℃, 50% RH, then the same passive and active AE recordings were made, following the procedure described in the previous section (Section 3.4.7.1).

3.5. Method of AE Analysis

AE testing methods were used for characterizing the effect of thermal stresses on the glass sphere/polyester composites with different interfacial strength and glass sphere loading, through both passive and active AE recording methods.

The acoustics monitoring system used was as previously described, with a computer running LabVIEW™ responsible for the recording and writing of the acoustic data to a TDMS file format. Each separate acoustic event was housed within its own TDMS file. The TDMS files produced by the LabVIEW™ programs were then analyzed by code written in the Python programming language by other researchers in the lab. Hit detection for recognition of an AE event used a threshold value of 6 mV based on the amplified sensor signal.

Fig.3.7 demonstrates several characteristics related to the time domain of the signal such as rise time, duration, maximum amplitude, etc. These measures are routinely used within the published literature to quantify physical material features with AE signals. However power spectra of the emitted acoustic waves were chosen for further analysis of thermally cycled specimens due to providing unique and more precise information about the material. The Python code was used to extract the power spectra of each acoustic event after having filtered the data through the Haar Wavelet Transform (HWT) for noise reduction without harm to the time-frequency information. Furthermore, a Butterworth band-pass filter was applied to negate frequencies below 45 kHz, which were attributed to noise, and frequencies above 450 kHz out of concerns for aliasing of sub-harmonics based on the 2.0 MHz sampling and application of the HWT.

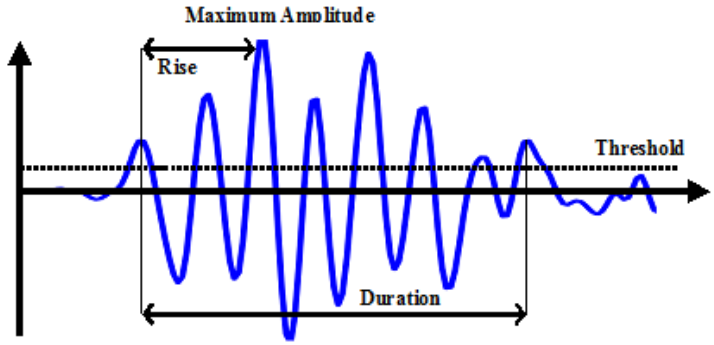

Fig.3.7. Parametric properties of an acoustic wave

For the tests examining the effect of thermal stresses on composites with different interfacial strength and glass loading, a multivariate parameter approach was used in place of a single parameter approach. Therefore, the power spectra of the active AE test, i.e. pencil lead break test performed prior to thermal cycling and after thermal cycling were compared for composites containing different coated glass filler. Since the temperature of the material can introduce an artifact into the signal not related to the damage being analyzed at the polymer/glass interface, it was decided to only compare datasets at the same temperature. Properly quantifying the differences between the power spectra of different composites with different interfacial strength and glass loading was difficult based on direct observation of the frequency domain information. Visually identifying important frequencies was quite limited and a rather slow tactic, and so it was decided to use multivariate statistics, offered by the program Prosensus MultiVariate (ProMV). In order to use ProMV, a second Python program was used, developed by other researchers in the lab, which divided the power spectrum of acoustic events into frequency bins of desired size (10 kHz) and wrote the results to a convenient text file for import into ProMV. Within ProMV, Partial Least Squares Discriminant Analysis (PLS-DA) was used to find specific frequencies which differentiated between different coatings and glass loadings before and after thermal cycling and correlated frequencies with interfacial strength and glass loading.

Chapter 4: Curing Optimization and Characterization of the Hollow Glass Microsphere/Polyester Composites

Prior to a detailed study of interfacial properties for a hollow glass microsphere/polyester composite and the effects of thermal stresses on said material, it was necessary to carry out a lengthy study to optimize its mechanical properties. This chapter describes the examination of how mixture preparation and different curing conditions affected the stiffness of the polyester thermoset. Mechanical properties in a thermoset resin are dependent upon its degree of cure (Zhang 1997); in this study, temperature and duration of the reaction were focused on to control the curing behavior. The goal was to minimize porosity and maximize the flexural modulus of prepared test specimens; flexural testing was used in place of tensile since the polymer was often too brittle to mount the test specimens in the grips of the testing apparatus.

4.1. Curing Conditions of the Pure Polyester

A Design of Experiments (DOE) was performed to find the optimum curing time and temperature for obtaining the highest possible flexural modulus. Cure temperature was changed from 80℃ to 140℃ and curing time was changed from 1 to 5 hrs. Table 4.1 depicts the curing conditions. Final curing conditions were set at 120℃ and 3 hrs. Fig.4.1 and Fig.4.2 show the flexural modulus of neat polyesters versus curing temperature and curing time, respectively. As can be seen, increasing curing temperature resulted in a significant increase in stiffness while increasing curing time saw a notable increase in stiffness but only for certain temperatures. For instance, at 110℃, an increase in curing time from 1 to 5 hrs resulted in an increase in stiffness from 3 to 3.7 GPa while an increase in temperature from 80℃ to 140℃ increased stiffness from 2.3 GPa to 3.8 GPa. This is attributed to higher rate of curing reaction at elevated temperatures which yields a higher degree of cure.

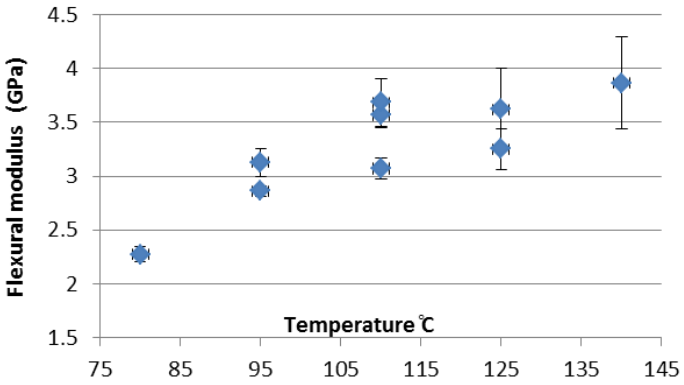

Fig.4.1. Flexural modulus versus curing temperature (for different durations)

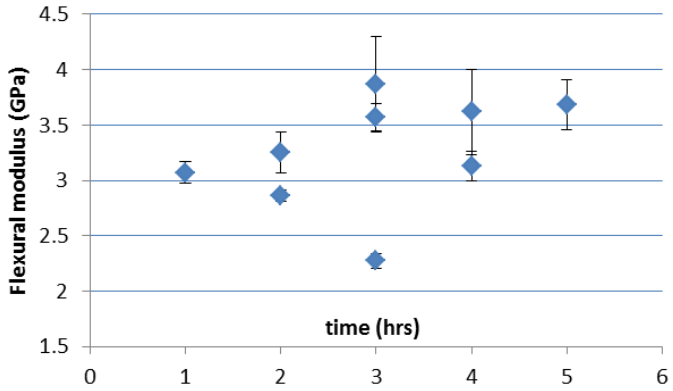

Fig.4.2. Flexural modulus versus curing time (for different temperatures)

Table.4.1. Curing time and temperatures

Cure Temperature ℃	Cure time (hrs)
80	3
95	2,4
110	1,3,5
125	2,4
140	3

4.2. Composite Fabrication

Composites containing either 16K or L21 at 0.2, 0.5, 1, 2, 6 and 10 vol% glass loading were prepared. Initially, mixing of the glass sphere and resin was done manually. Extreme care was taken to create the least amount of entrapped air during mixing. However, agglomeration of the glass particles at 2 vol% was occurring and a more vigorous mixing for a longer time was necessary. Consequently, resin and glass sphere were mixed for an hour with different mixing speeds using an impeller mixer. Fig.4.3 shows the changes in flexural modulus with changing the mixing speed from 100 RPM to 225 RPM and compares to a case using a very high speed homogenizer instead. An increase in modulus was observed with increasing the mixing speed from 100 RPM to 225 RPM but using the homogenizer did not improve the stiffness. On the other hand, mixing at higher speeds and longer duration produced a large amount of air bubbles which were visible in the produced test specimens. To remove the entrapped air, a vacuum oven was found to be beneficial. Elevated temperature assists the bubble removal by lowering the viscosity of the mixture; the mixture had not been poured into the casting mold at this stage. However, this temperature was carefully selected to not initiate curing of the sample even though the samples did not contain the MEK peroxide at that stage. Fig4.4 compares the modulus of composites that were de-foamed in vacuum oven at 25℃ and 65℃. As can be seen, except at 1 vol% and 10 vol% glass, de-foaming at higher temperature corresponded to an improved stiffness in the final test specimen, which can be attributed to better air bubble removal while under vacuum.

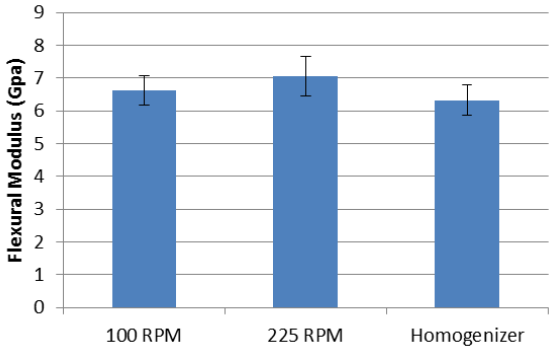

Fig.4.3. Flexural modulus versus mixing speed level at 2 vol% glass loading

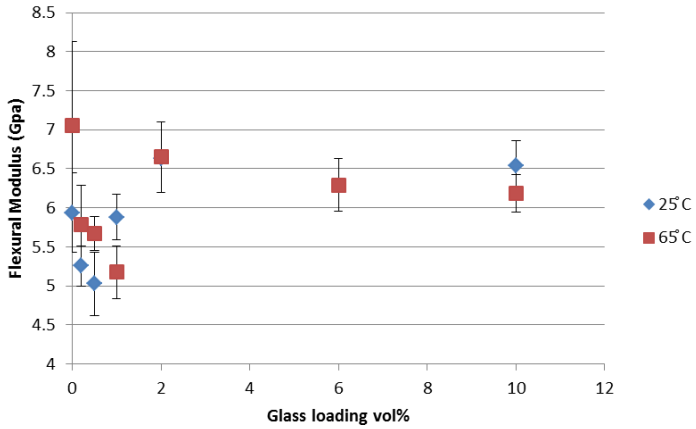

Fig.4.4. Flexural modulus versus glass loading of 16K containing composites de-foamed at 65℃ and 25℃

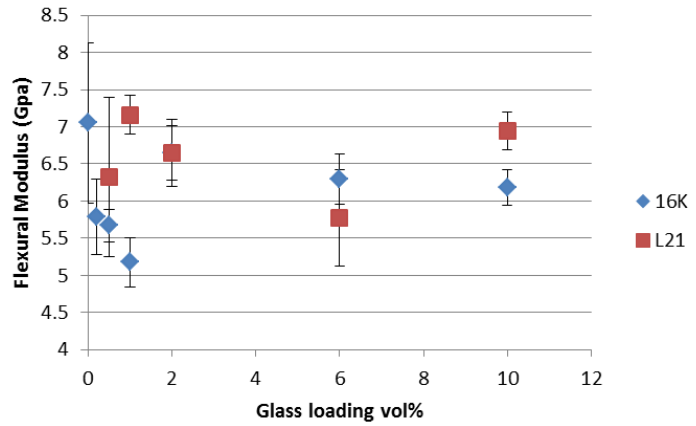

Fig.4.5. Flexural modulus versus glass loading of 16K and L21 containing composites de-foamed at 65℃

Fig.4.5 shows the flexural moduli of composites containing different loadings of 16K (uncoated) and L21 (coated) glass spheres. It was expected to observe an increase in flexural modulus with increased glass loading (Wouterson et al. 2005); however, 16K glass spheres demonstrated decreased stiffness compared to the neat polyester with introduction of 0.2 vol% glass spheres. Decreasing trend was observed with further increase in glass content to 1 vol%. Higher glass loadings demonstrated an increased stiffness but still lower than the neat polyester stiffness. The presence of agglomerates might be the reason for the decrease in stiffness with increased glass loading from 0.2 to

1 vol% which act as defects in material. For higher glass loadings, increased viscosity of the mixture would improve mixing and reduces agglomeration. Introduction of coated glass spheres which improve the interfacial strength with the matrix polymer was expected to demonstrate improved mixing and a more definitive increasing trend in flexural stiffness versus glass loading but increased content of L21 did not demonstrate an increasing trend. Stiffness was higher compared to 16K containing composites except at 6 vol%.

Overall, flexural modulus was not found to be sensitive enough to discriminate composites containing very low glass loadings. Also, it did not show a clear difference in trend between composites containing coated and uncoated glass sphere. Strength might be a better indicator of interfacial strength; however, problems due to presence of voids in composites hindered using strength for comparisons. This emphasizes the need for a more sensitive technique for investigation of the interfacial strength in composites and its influence on the changes in the microstructure under different stresses.

As mentioned in introduction, the main aim of this thesis was to investigate the effect of thermal stresses on microstructure of the composite specifically glass/polyester interface and its influence on interfacial strength. Mechanical testing was not showing notable differences with changes in interfacial strength in composite. We needed a very high sensitivity to recognize minute changes in microstructure. Also, mechanical tests were not capable of detecting defects in material at early stages while acoustic emission techniques are very sensitive in detecting local changes in microstructure long before they cause a major failure in material and so an AE technique was decided for this study to investigate interfacial strength, effect of thermal stresses on glass/polyester interface and its influence on interfacial strength.

4.3. Morphology of Composites with Different Interfacial Strength

The dispersion state of particles in a polymer matrix was observed using a light microscope. A proper mixing level is required to achieve reliable results from mechanical and AE tests. Presence of agglomerates in composite will result in a drop in mechanical properties and affects the elastic wave propagation in the composite. Composites with different coatings were observed, showing an acceptable level of mixing and the presence of few agglomerations in specimens. This was sufficient for further acoustic investigations.

Fig.4.6-4.7 and Fig.4.8-4.9 show the morphology and dispersion state in composites containing 1 and 10 vol% glass sphere respectively with different coatings at two magnifications. A minor degree of agglomeration was observed in composites containing AS6 and AS12 at both glass loading levels. No agglomeration was observed in the other composites. Glass spheres with higher interfacial strength with matrix were expected to mix better in matrix and form fewer agglomerations as seen in most of these composites.

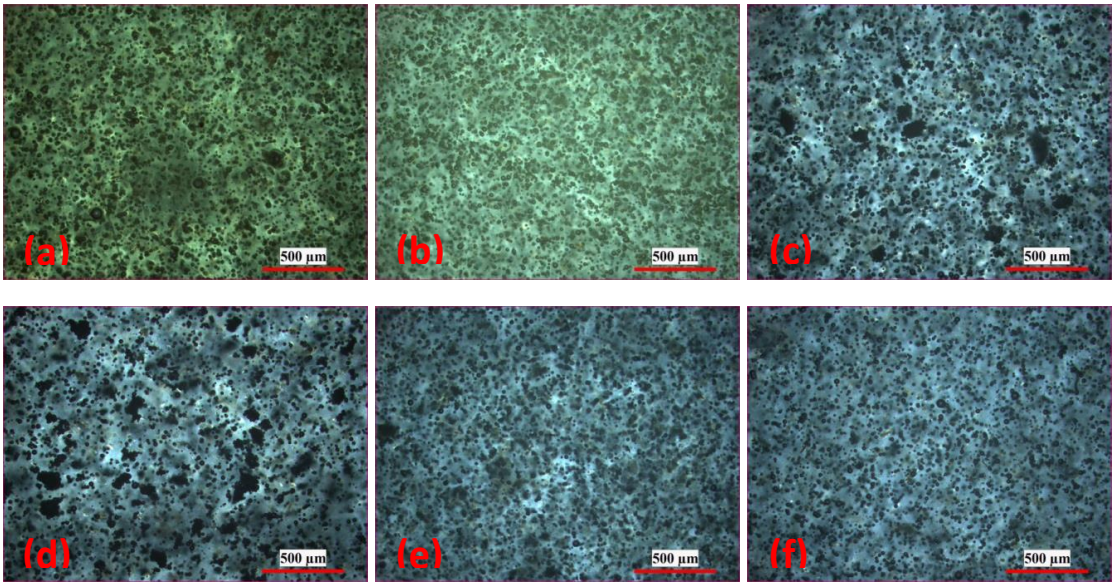

Fig.4.6. Optical microgarphs demonstrating state of glass dispersion in composites containing 1 vol% (a) 16K, (b) L21, (c) AS6, (d) AS12, (e) GS6 and (f) GS12 glass sphere.

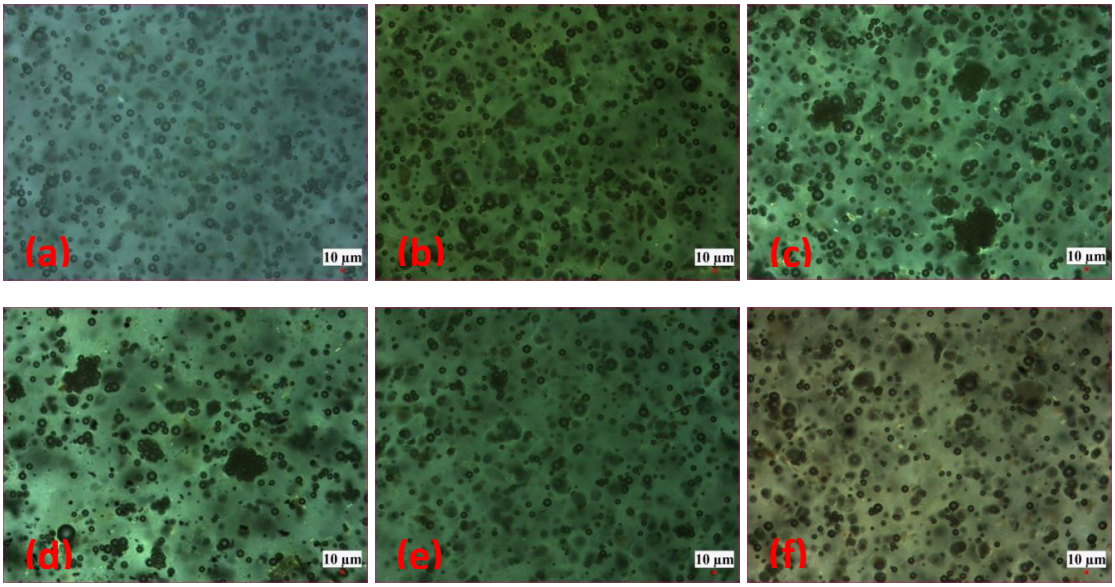

Fig.4.7. Optical microgarphs demonstrating state of glass dispersion in composites containing 1 vol% (a) 16K, (b) L21, (c) AS6, (d) AS12, (e) GS6 and (f) GS12 glass sphere. (higher magnification)

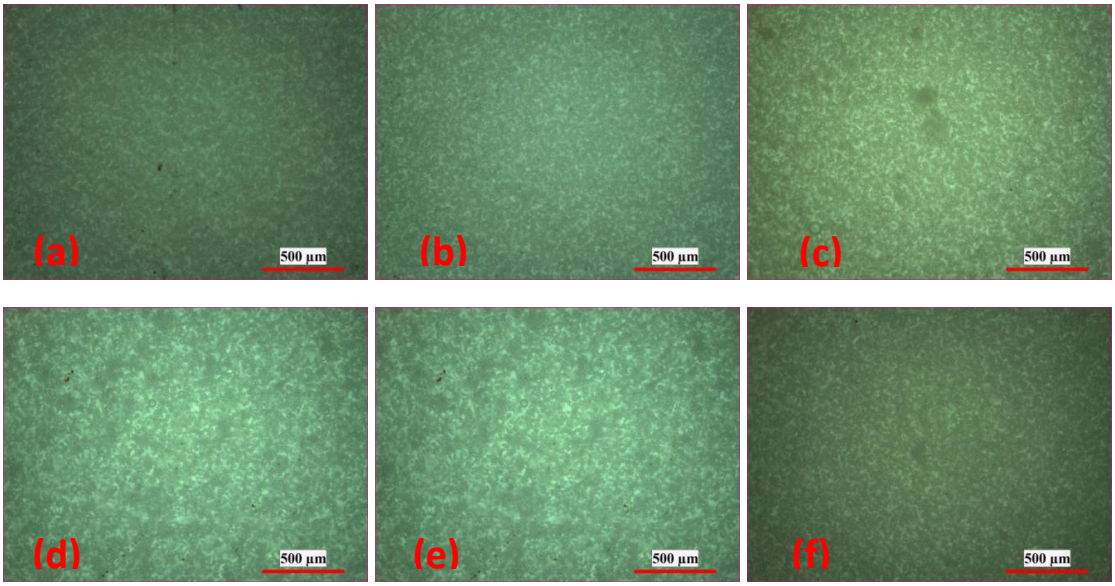

Fig.4.8. Optical microgarphs demonstrating state of glass dispersion in composites containing 10 vol% (a) 16K, (b) L21, (c) AS6, (d) AS12, (e) GS6 and (f) GS12 glass sphere.

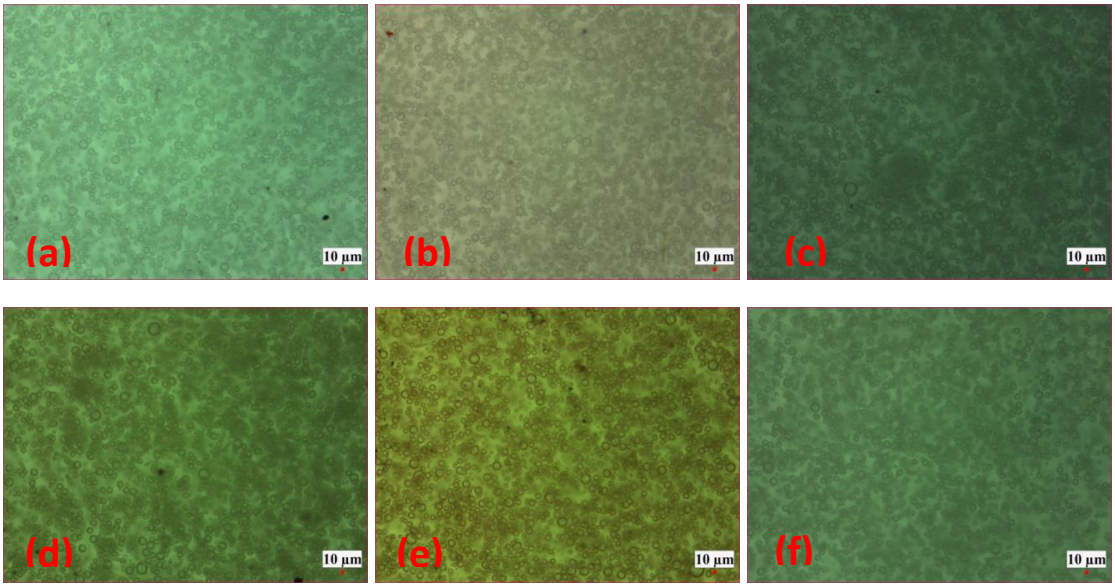

Fig.4.9. Optical microgarphs demonstrating state of glass dispersion in composites containing 10 vol% (a) 16K, (b) L21, (c) AS6, (d) AS12, (e) GS6 and (f) GS12 glass sphere. (higher magnification)

Chapter 5: Results and Discussion

Particulate composites were prepared with differing glass loading levels and interfacial strength. Mechanical testing and active AE studies were used separately to investigate the effects of interfacial strength and thermal stresses on macro- and meso-scale properties of the composites. Composites with 1, 2 and 10 vol% hollow glass microspheres were prepared. Preparation of composites with higher glass loadings would have encountered mixing problems, produced undesirable agglomeration, and introduced excessive voids to the specimens due to increased viscosity.

5.1. Effect of Interfacial Strength and Heat Treatment on Tensile Modulus of the Particulate Hollow Glass Microsphere/Polyester Composites

Tensile moduli of composites containing 1, 2 and 10 vol% hollow glass microspheres with different coatings, were compared in Fig 5.1 before heating (RT1) and after a second heating cycle (RT3). It was expected that increased stiffness would result from increasing the volume fraction of hollow microspheres, just as seen by Wouterson et al. (2005) for an epoxy composite containing hollow glass spheres. Bardella and Genna (2001) have stated that the increase in stiffness should correspond to the strength of the hollow spheres, which in this work were higher than those used by Wouterson et al. (2005); the 16K base glass spheres in this work had a crush strength of 110 MPa versus the 41 MPa for K46 used by Wouterson and hence increased stiffness was reasonably expected. The top graph of the figure for the condition before heating presents the tensile moduli of composites containing 1 and 2 vol% glass spheres as being close in value between 660 to 750 MPa, while some composites containing 10 vol% glass spheres showed more significant variations in modulus with the changes in glass sphere/polyester interfacial strength; a definitive increase in modulus with increased glass loading for a specific class of composite was taken as the most significant evidence of a stronger interface than simply having a higher modulus at any specific glass loading, which meant that AS12, GS6 and GS12 were considered to be showing better bonding than L21 or AS6.

Comparing the trend in modulus versus glass loading level provides more generalized information about the effect of the addition of glass spheres on stiffness of the composite and the expected behavior from their addition while considering its effect on modulus at only one specific glass loading level is less reliable and more prone to error. For example, comparing the actual values of modulus at 2 vol% instead of considering the trends with an increase in glass loading level, L21 coating would be mistaken as the best coating while considering the trends provides more accurate information about the changes in modulus with addition of glass spheres of different adhesion levels to polyester. The addition of 1 vol% 16K glass particles with no coating to the neat polyester (654 MPa) slightly increased the stiffness to 694 MPa. Higher loadings of 16K resulted in a decrease in modulus since the interface was not strong enough and the particles did not mix very well with the resin. By 10 vol% glass loading, the composites containing AS12, GS6 and GS12 coatings showed a slightly improved modulus compared to the neat polyester or the composites containing 16K glass spheres or L21 (commercial coating) at similar loading contents. Composites containing AS6 glass spheres showed moduli close to L21 containing composites; samples with both coatings showed improved mechanical properties over 16K or the neat polyester. Despite the minor differences noted in the figure, overall no coating appeared to stand out as superior before heating. Considering the effect of coating thickness, higher concentrations of AS and GS coatings demonstrated better performance than the lower concentrations. This was expected since higher concentration was closer to the coating thickness in the commercial coating and that coating should be a monolayer on glass surface as it provides the best coating performance.

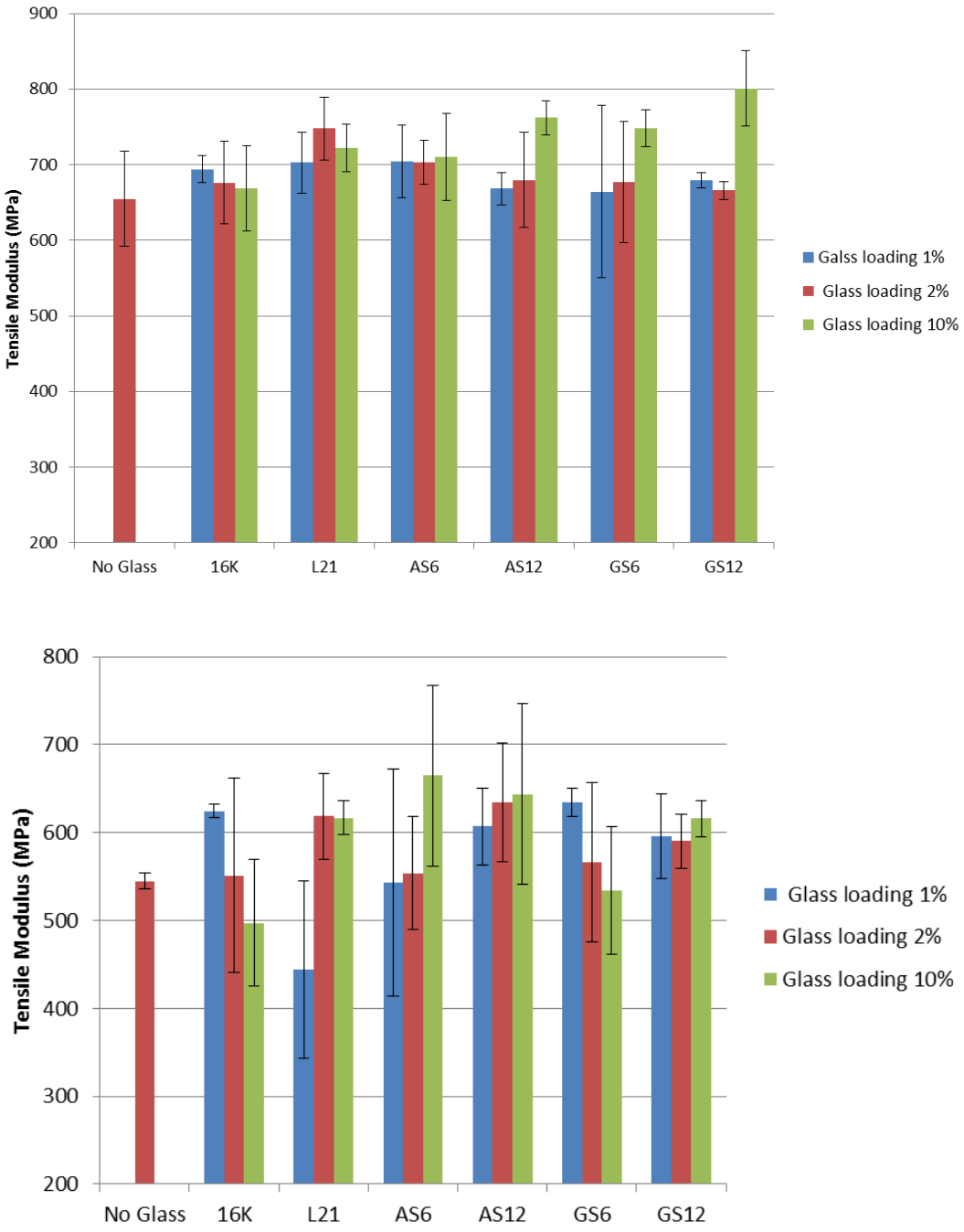

Fig.5.1. Tensile modulus of composites with different hollow glass microsphere/polyester interface strength before (top) and after heating (bottom).

Heating and cooling the composites twice for the RT3 condition caused the stiffness of the composites to drop significantly but also the matrix resin, possibly as a result of hydrolytic degradation. The bottom graph of Fig 5.1 shows results from the RT3 condition where the modulus of the neat polyester had dropped by 17% from 654 MPa to 544 MPa after two heating-cooling cycles. Comparatively, the modulus of all composites had nominally dropped by 5%-36% for instance for GS6 (1 vol%) and L21 (1 vol%) respectively after heating. Before heating it was difficult to see major differences between the coatings but after heating, more differences were apparent. Compared to the stiffness of samples for the RT1 condition, the decreases in moduli after heating for 16K/polyester, L21/polyester and AS6/polyester composites at 1 vol% glass loading were more significant compared to AS12, GS6 and GS12 containing composites. For 16K/polyester, the modulus deteriorated with increased glass loading. This was reasonably expected since there is no coating on glass spheres in this composite and its interface with matrix should be the weakest among the glass types; the higher modulus at 1 vol% 16K than most other composites was surprising but it did not change our belief that overall the uncoated glass microspheres exhibited the worst interfacial bonding especially considering the fact that its modulus decreased progressively below neat polyester with higher glass content, which was taken as evidence that their inclusion was being treated as voids mechanically.

Considering 16K as the worst case in terms of damage caused by heating, the rest of the composites are compared against the 16K results. At all other glass levels besides 1 vol%, L21 and AS6 performed better in building stiffness in the composite. The other composites at 1 vol% showed similar moduli as 16K/polyester and better at higher loadings.

AS12 and GS12 showed higher stiffness compared to 16K at comparable contents of 2 and 10 vol%. AS6 containing composites showed the highest stiffness among all at 10 vol% while GS6 at 10 v% produced the lowest stiffness, being close to 16K. The AS coating at both coating thickness levels showed an increasing trend in modulus with glass

loading though the slope was higher for the lower AS coating thickness which was inferred as better performance of AS6 compared to AS12. Thicker GS coating i.e. GS12 performed better than thinner i.e. GS6 coating. The large uncertainty on account of the brittle nature of these samples made it difficult to determine preferred coatings but across all glass content levels, the AS coating appeared consistently better. The composites with AS coating showed a consistent increase in modulus with glass loading whereas composites with the GS interface showed no evidence of significant increasing stiffness and with GS6 actually decreased. The commercial L21 coating showed adequate bond strength but that its modulus did not increase at 10 vol% leaves concerns whether poor mixing was the cause or that the interface could not bear the higher stresses.

We conclude that modulus is not a sensitive enough parameter to see changes in the interfacial strength because it is measured at relatively low deformation and there is not enough dilation to cause interface separation. Tensile strength is more sensitive to interfacial adhesion; however, due to presence of voids from the curing of the polyester, and the overall sensitivity of this parameter to any weak point in a test specimen it is not used for comparing interfacial strength either.

Insensitivity of mechanical properties to silane type has also been reported by other researchers (Hamarneh et al. 2013). Thus, AE was chosen as a more sensitive method in comparing interfacial strength and will be the focus of the remaining discussion.

5.2. Acoustic Studies on the Interfacial Strength of the Hollow Glass Microsphere/Polyester Composite

Mechanical testing is suitable for uncovering the bulk properties of a material and is capable of detecting defects on the macro-scale. On the other hand, AE is a much more sensitive technique in detecting changes present in materials on the meso-scale, noting damage long before major failures are evident at the macro-scale. An AE technique was hoped to provide more local information as the glass microspheres detracted from the polyester as a result of the thermal stresses, being sensitivity to the state of polymer chain mobility near the interface of the rigid surface. Resonant vibrations in the polymer at

specific frequencies will be sensitive to the altered chain mobility as the polymer/glass sphere interface is affected by heat.

Our initial aim was to use passive AE to acquire data related to any changes in the microstructure due to heating and its dependence on interfacial strength. Composites were thermally cycled to create heat-induced microdefects in the composites while trying to capture and analyze the elastic waves generated by microdefects forming in the material. However, the recorded signals did not seem to contain useful data for further investigations, probably caused by deficiencies of the sensors at elevated temperature and the high attenuation of elastic waves at those temperatures.

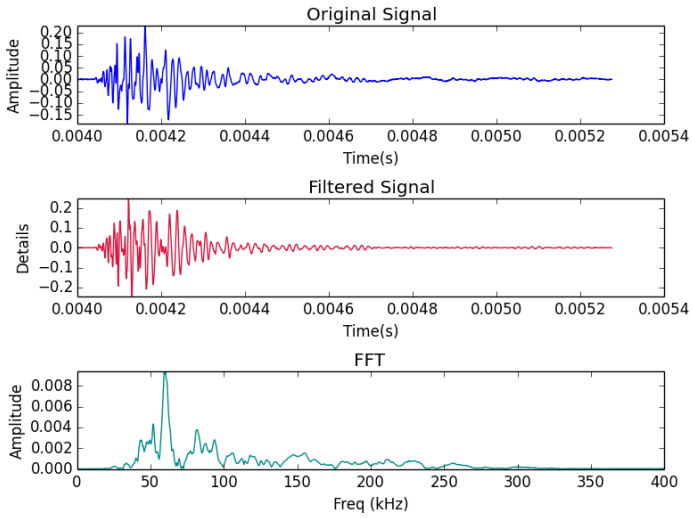

Fig.5.2. Analysis of a pencil lead break AE event showing the time domain signal (top), Haar wavelet filtered signal (middle) in the time domain and power spectrum of the signal (bottom) showing the frequency domain data for a PLB on 10 vol% AS12/polyester composite before heating.

Active AE became the preferred method in this work for studying the changes in microstructure of the composites after the passive method proved to be inadequate. Pencil lead break (PLB) tests were performed on our composites and elastic wave propagation was investigated. Fig.5.2 demonstrates a typical detected signal from a PLB test with one of the specimens. The time domain of the original signal is shown in the top chart, which was then cleaned up using a Haar wavelet filter to avoid inducing a

frequency shift (typical of band pass filtering) and then converted into the frequency domain by using the fast Fourier transform (FFT) method in the lower chart; the lower chart is known as a power spectrum.

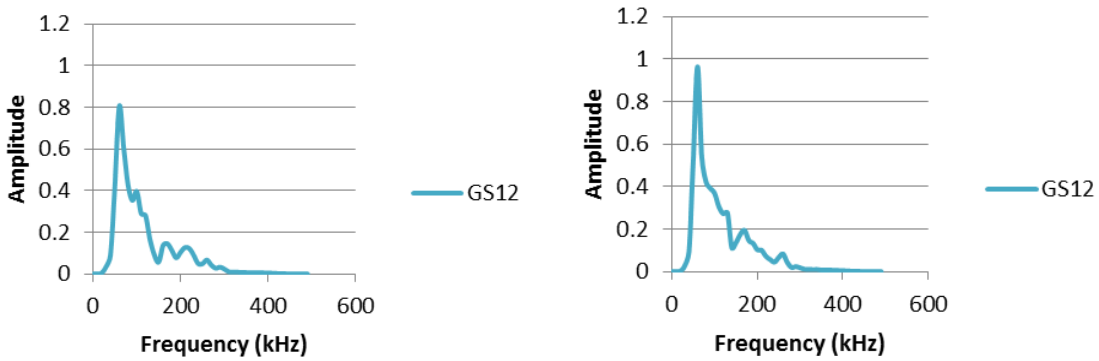

Fig.5.3. Power spectrum of an AE event from PLB test on 10 vol% GS12/polyester composite before (left) and after heating (right).

Fig.5.3 shows the averaged power spectra of a PLB test performed on four (4) samples of 10 v% GS12/polyester composites, before (RT1) and after (RT3) a second heating cycle. Signals were normalized relative to the max peak amplitude for each spectrum and then were averaged in each 10 kHz frequency band for all samples. Changes in the acoustic signature (i.e. frequency-amplitude distribution) of the material with heating can be observed. Frequency features of the AE waveform from different damage modes is believed to be highly effective in characterizing the microstructural changes during fracture using passive AE method (Wang et al. 2011; Sause & Horn 2013; Gomes et al. 2014). Different viscoelastic relaxation processes near each damage source (i.e. matrix cracking, fiber/matrix debonding and fiber breakage) enables damage mode identification based on frequency content of the emitted wave. Different intrinsic frequencies and elastic acoustic velocities will result from different elastic moduli and densities (Bohse 2000).

The large peak seen at lower frequencies around 50-60 kHz in Fig 5.3 relates to interactions of the elastic wave with the softer, amorphous matrix forming the majority of the volume fraction of the composite. Gomes et al. (2014) have also reported the

frequency range of 50-60 kHz as being related to matrix interactions with elastic wave in high density polyethylene. Yu et al. (2006) associated 100 kHz to matrix failure in carbon/epoxy composites. However, we were more interested in investigating the behavior of the polymer at, or near, the glass/matrix interface and thus considered higher frequencies related to stiffer materials compared to matrix i.e. glass spheres and/or the glass/polymer interface. The interphase contains polymer chain segments with reduced mobility and higher rigidity compared to polymer chains in amorphous matrix due to bonding to the glass particles. For surface modified glass spheres, the mobility of chains near the interface depends on the effectiveness of the coating, i.e. stronger interface means that a higher fraction of chains should experience limited mobility and hence display higher stiffness. As can be seen in the figure above, amplitudes at higher frequencies are much lower compared to the largest peak due to the lower volume fraction of glass relative to the matrix. Changes at the interface were expected to cause very minute changes in the power spectrum due to their very low volume fraction in composites (interface layer volume versus matrix and glass spheres volume) unless all interfaces were damaged simultaneously.

5.2.1. Effect of Glass Coating and Heat on the Acoustic Signature

To study the effects of glass coatings and heat on the resonant meso-structure of our composite, PLB tests were performed at different heat states and the power spectra were compared. To make comparisons within this large multivariate data set, a statistical package called Prosensus MultiVariate (ProMV) was used. The spectral data was broken down into 10 kHz frequency "bins" for ProMV. Each spectrum from a PLB tests was treated as an observation that had 50 variables, i.e. frequency "bins" for a scanned acoustic region of 0 to 500 kHz, that were compared against other observations. Within ProMV, Partial Least Square Discriminant Analysis (PLS-DA) models were built for the supervised classification of these power spectra of the different composites. The models were intended to recognize the specific X-space variables (frequencies) which were responsible for discriminating between the different classes (Y-space categorical variables). Use of classification methods for damage mode characterization has been

reported in literature (Sause & Horn 2013; Wang et al. 2011). A supervised classification method (PLS-DA) was used in this work in which labels of different classes (i.e. coating type and heat state) were know and intention was to find variables which were responsible for difference among different classes.

5.2.1.1. Collected Acoustic Signatures before Heating

The first PLS-DA model was built for comparison of the first two composites, 16K/polyester and L21/polyester. Then another coating was added to the model in each step to see how the classification changed with adding a new class. It should be mentioned that the accuracy of the PLS-DA model was highest when comparing two classes and R^2 (which is an evaluating measure of accuracy of the model) started to drop quickly with adding more classes to the model. Fig.5.4(a) shows a visual representation of a model (i.e. a loading bi-plot) that compared the frequency-amplitude plots for the four composites containing either 16K, L21, AS12 and GS12 coated hollow glass microspheres (10 vol%). Fig 5.4(b) is the same plot but now includes the X-variables (frequencies) as labels in the plot, which make it much more difficult to read. A loading bi-plot such as these in Figure 5.4, demonstrates the scores for each observation and allows the user to make interpretations of the relation between observations and the X or Y variables easier. Variable importance plots (VIP) demonstrate the significance of each variable in the built model. Variables showing quantities higher than 1 are considered significant in discriminating between classes.

Fig.5.5 shows the VIP plot for the model corresponding to frequencies in the 16K, L21, AS12 and GS12 hollow glass microsphere composites (10 vol%) before heating; significant frequencies that differed between the coated samples were: 110, 130, 140, 150, 170, 180, and 260 kHz. Lower frequencies below 100 kHz were thought to be related to a matrix response and were not considered since as mentioned previously, we were interested in exploring the glass/polyester interface in more detail.

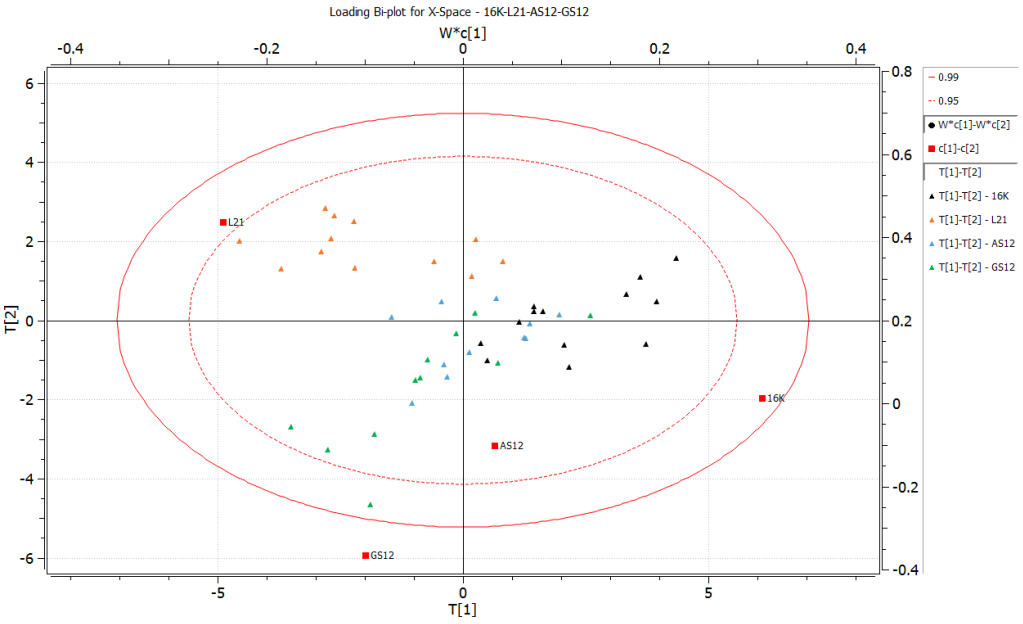

(a)

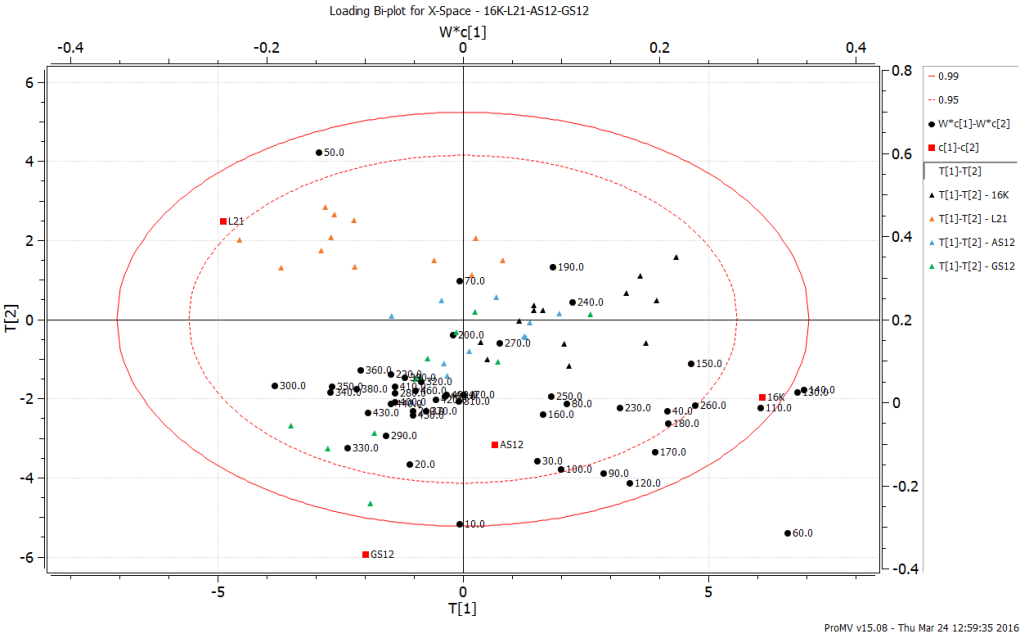

(b)

Fig.5.4. A bi-plot showing the scores from first and second component on primary axes and loadings for each variable on secondary axes. Variables closer to red squares are important variables in discriminating different classes of composites (higher correlation with y variables).

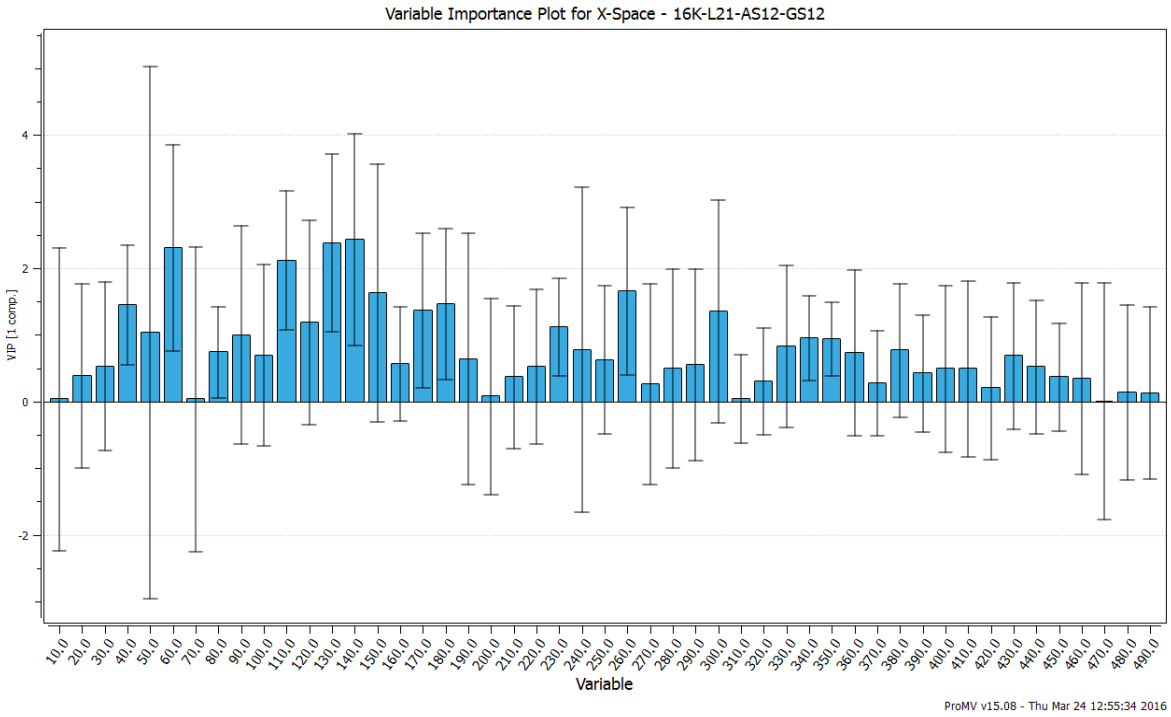

Fig.5.5. VIP plot showing important variables in discrimination of classes. Variables that have a value higher than one are usually considered significant which in this specific model are 110, 130, 140, 150, 170, 180, 260 kHz.

Fig.5.6(a-c) show the model beta coefficients corresponding to each class of composites, indicating the variables (frequencies), which were most responsible for discriminating between different classes of composites. Variables that have higher absolute beta coefficient values are more important in building the model. As previously mentioned the first model compared 16K /polyester vs L21/polyester and then one more class was added in each subsequent model; however, for brevity only the beta coefficients plots from three models are presented to highlight how sensitivity was lost with each new class added. Different researchers have reported frequencies associated with fiber/matrix debonding and fiber pull out in passive AE characterization of damage mode in fiber composites. Ramirez et al. (2004) associated 100 kHz to fiber/matrix debonding, 200-300 kHz to fiber slippage and pull-out, and 400-450 kHz to fiber breakage in glass/polypropylene composites. Frequencies between 240 kHz and 310 kHz were associated with fiber/matrix debonding, and 180-240 kHz to fiber pull out (de Groot et al. 1995) in

carbon/epoxy composites. Yu et al. (2006) associated 230 kHz to fiber failure in carbon/epoxy composites. Based on the VIP plot and all beta coefficients, it was decided to narrow the frequencies to be examined as descriptors of interfacial adhesion down to 140-240 kHz.

Fig.5.7 shows the averaged amplitudes over the 140-240 kHz range recorded from the PLB tests for samples before heating versus the coating type applied to the glass for composites with 1, 2 and 10 v% glass loading. The average amplitude was calculated for each observation. A clearer trend was observed for 10 vol% glass loadings compared to lower content and thus it was mainly considered for interpretation of the results; the error bars shown correspond to the standard deviation in average amplitude among all repeats in each class.

The increase in amplitude observed for the 16K/polyester compared to neat polyester shows the effect of introducing rigid inclusions into the neat polyester and that affect on wave propagation and attenuation, though the extent of the increase (nominally) is inexplicitly large compared to all other composites in this study before and after heating. In general, wave attenuation in particulate composites with viscoelastic matrix occurs due to scattering effects by inclusions and absorption in viscoelastic matrix. It has been theoretically demonstrated by Biwa et al. (2004) that attenuation in viscoelastic matrix particulate composites decrease with increasing particle volume fraction when the inclusion size is sufficiently small compared to wavelength and inclusions are much stiffer than the matrix. They attributed their finding to the dominance of absorption losses in viscoelastic soft matter as well as to minor scattering effects by the particles; however, at dilute concentrations (<15 vol%), rigid inclusions produce less scattering. Thus, the increase in amplitude for 16K/polyester can be attributed to decreased volume fraction of its matrix polymer replaced by rigid inclusions which in turn reduced the capacity of the composite to attenuate the elastic wave energy through absorption. Attenuation of the poorly bonded 16K was not higher than the matrix since increased attenuation resulting from increased void content (due to weak interface and cavity in glass spheres) was offset

by replacing a part of matrix with stiff inclusion which increased the stiffness of polyester and lowered the attenuation.

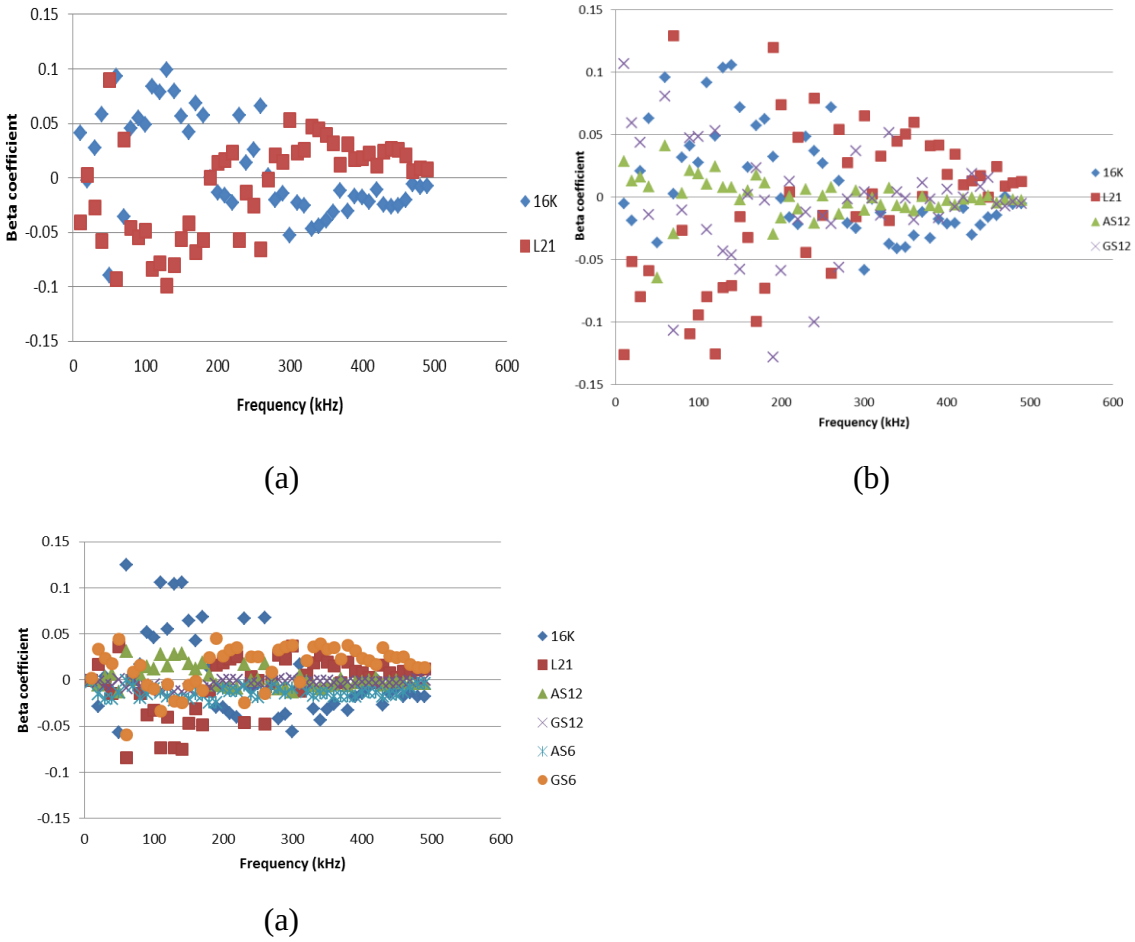

Fig.5.6. Beta coefficient plots from PLS-DA model built on FFTs from PLB tests before heating of composites containing 16K, L21, AS6, AS12, GS6 and GS12. Beta coefficients from second component for comparison of composites containing 10 vol% (a) 16K and L21, (b) 16K, L21, AS12 and GS12, (c) all coatings.

Our results with 16K differed from those of Mylavarapu and Woldesenbet (2008) who measured the attenuation in syntactic foams containing hollow glass spheres with different wall thicknesses. Like our glass spheres, their particles were hollow and the void content they argued should increase wave attenuation. They found that at 10 vol% glass loading, attenuation in the neat matrix was lower than in the composites regardless of the wall thickness. A model was developed by the same authors (2010) to predict

attenuation of elastic waves in glass/epoxy syntactic foams. A term was introduced to account for an additional attenuating mechanism in syntactic foam i.e. absorption in the cavity of the glass spheres. That model predicted an increasing trend for attenuation with increasing glass loading from 10 to 30 vol%. Considering all the effects of i) a volume fraction reduction in viscoelastic resin, ii) increased rigidity by a stiff inclusion, iii) introduction of higher volume fraction of voids and iv) potentially weak interface, we are more inclined to accept the 'after heating' result where 16K and the neat polyester had comparable attenuation.

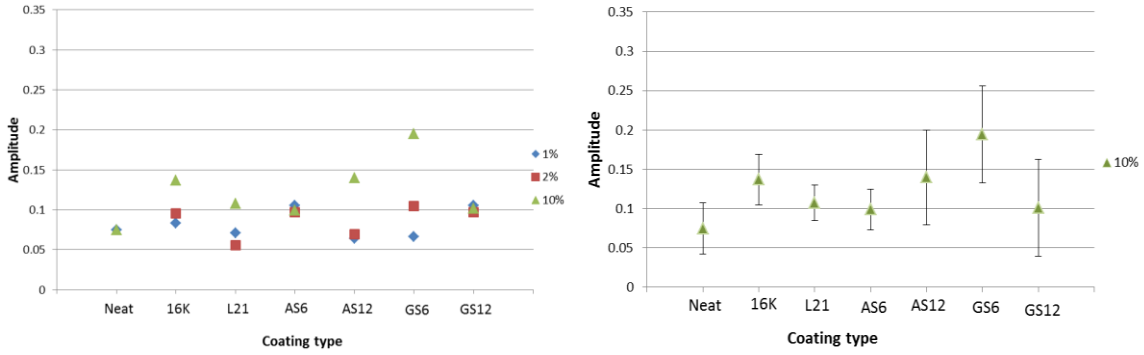

Fig.5.7. Average amplitude versus coating type from PLB before heating for composites with 1, 2 and 10 vol% glass loading. Right graph shows only the 10 vol% glass loading for clarity of discussion.

The 10 vol% composites with coatings L21, AS6, AS12 and GS12 before heating showed nominal amplitudes similar in value to that of 16K/polyester. The GS6/polyester composite reportedly produced the highest amplitude compared to 16K/polyester. Since these different composites shared similar glass loading level and particle size, the wave attenuation should now only vary depending on glass/polymer interface strength – hence the comparison to 16K/polyester and not neat polyester. A stronger interfacial association means that a high fraction of polymer chains are now retarded in their mobility at the glass/polymer interface as well as better transfer of wave energy from matrix to glass inclusions. By this hypothesis, the GS6 coating was superior. The thinner GS coating performed better than the thicker one, which was not consistent with the results from

mechanical testing i.e. poorer performance of GS6 versus GS12. AS coating performance at both thickness levels were the same. The effect of an imperfect interface between particle and matrix on the wave propagation behavior was theoretically studied by Wei and Huang (2004). The authors claimed that viscose effects of the interphase can increase the attenuation. Another study on wave propagation within particulate composites by Liu and Wei (2008) studied the function of the interphase by mechanically modeling it as a spring and found the influence of interface strength on attenuation, especially in the case of weak interfaces.

Based on mechanical testing results before heating (Sec 5.1), GS12, AS12 and GS6 showed the highest stiffnesses but were indistinguishable from one another, particularly at 10 vol%. GS6 exhibited an acoustic response indicative of a higher interface strength followed by AS12, but no result by acoustics could explain all three coatings. It is safe to say that determining whether acoustics is an improved discriminator of interfacial strength, the materials must be perturbed in a manner that the interface is affected. The subsequent section focused on the changes created by heat, which according to the tensile modulus data damaged the interface partially in almost all cases.

5.2.1.2 Collected Acoustic Signatures after Heating

The composites were heated to 110-130℃ then evaluated by PLB testing after they had reached room temperature; the samples were actually evaluated at the elevated temperature by PLB testing as well but concerns about the altered attenuation behavior of the polymer at such temperatures led us to believe that the data could not be interpreted properly. Fig.5.8 compares the typical power spectrum for two classes of composites at their 10 vol% glass loading over the frequency range of 0-500 kHz before heating (RT1) and after a second heating cycle (RT3). A clear difference between amplitudes before and after heating is observed, but more so for the composite containing 16K hollow glass microspheres. Comparison of the power spectrum of composites containing 10 vol% glass sphere with different coatings after heating was once again performed using ProMV

and its PLS-DA model. VIP plot variables (frequencies) showing values higher than 1 were 110, 120, 140,150, 160, 230, 240 kHz. (Fig.5.9).

Fig.5.10 shows the beta coefficients for the models built with the composites of different coatings. Frequencies with high absolute values of beta coefficient were considered more important in discriminating between the different classes within the built model. Similar to previous sections, the same frequency range (140-240 kHz) was chosen from the coefficient plots and VIP plots for further exploring the attenuation of amplitude versus coating type.

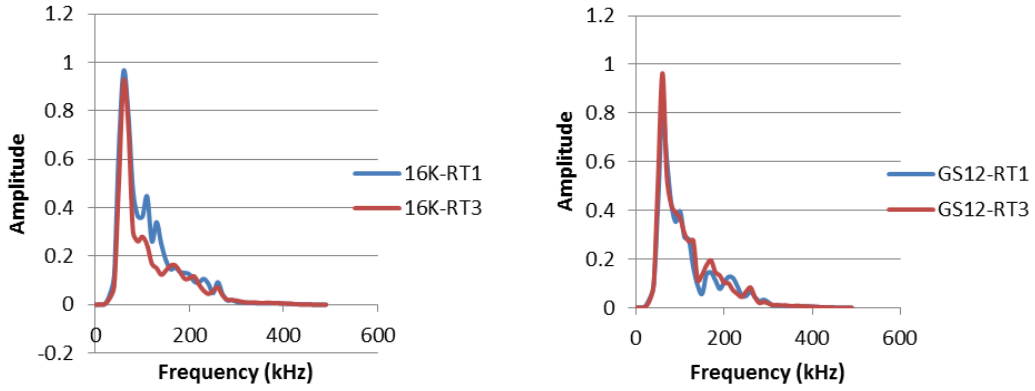

(a) (b)

Fig.5.8. Comparison of acoustic power spectra recorded by the PLB test, before and after heating for composites containing hollow glass microspheres with (a) no coating or (b) GS12 coating.

Fig.5.11 shows a comparison of the averaged amplitudes recorded after heating over the 140-240 kHz range versus coating type. The amplitudes were higher after heating suggesting a lower attenuation coefficient due to drying since plasticizers like water have been found to result in increased attenuation in polyester (Jayet et al. 1999) and dampening of the signal (Pérez-Pacheco et al. 2013); more evidence of the effects of moisture on attenuation are given in Section 5.4. A clearer trend was once again seen for 10 vol% glass loading as was found before heating but now that trend was much more consistent with lower glass loadings. The trend appeared only slightly different from the results before heating. For 10 vol% glass loading, 16K/polyester and neat polyester

showed the same amplitude, differing slightly from before heatings where the neat polyester sample had a lower amplitude compared to all of the composites. Composites containing GS12 showed the same amplitude as 16K while L21/polyester and AS12/polyester had slightly higher amplitudes compared to 16K/polyester. AS6/polyester may have had a higher amplitude than L21 and AS12 containing composites but there was so much variability in the results that the uncertainty was large in this case. However, looking at the 1 vol% and 2 vol% results in addition, it seemed reasonable to consider the higher amplitude as a real outcome for AS6/polyester.

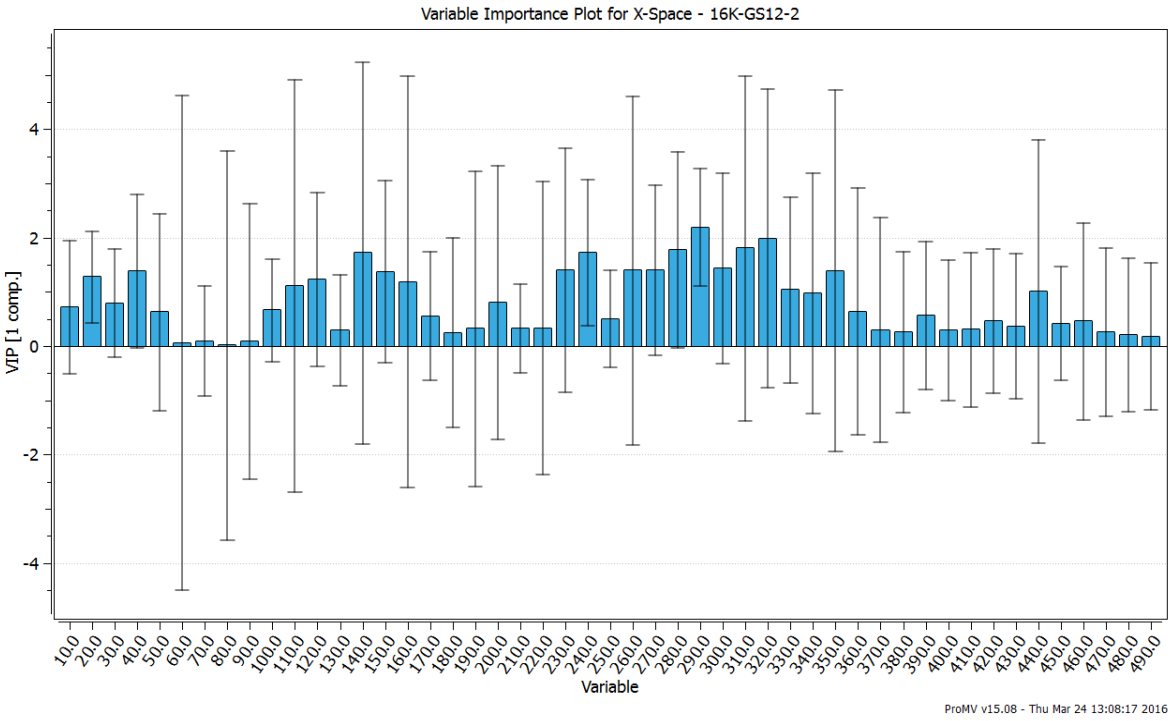

Fig.5.9. VIP plot showing important variables in discrimination of classes. Variables that have a value higher than one are usually considered significant which in this specific model are 110, 120, 140,150, 160, 230, 240 kHz.

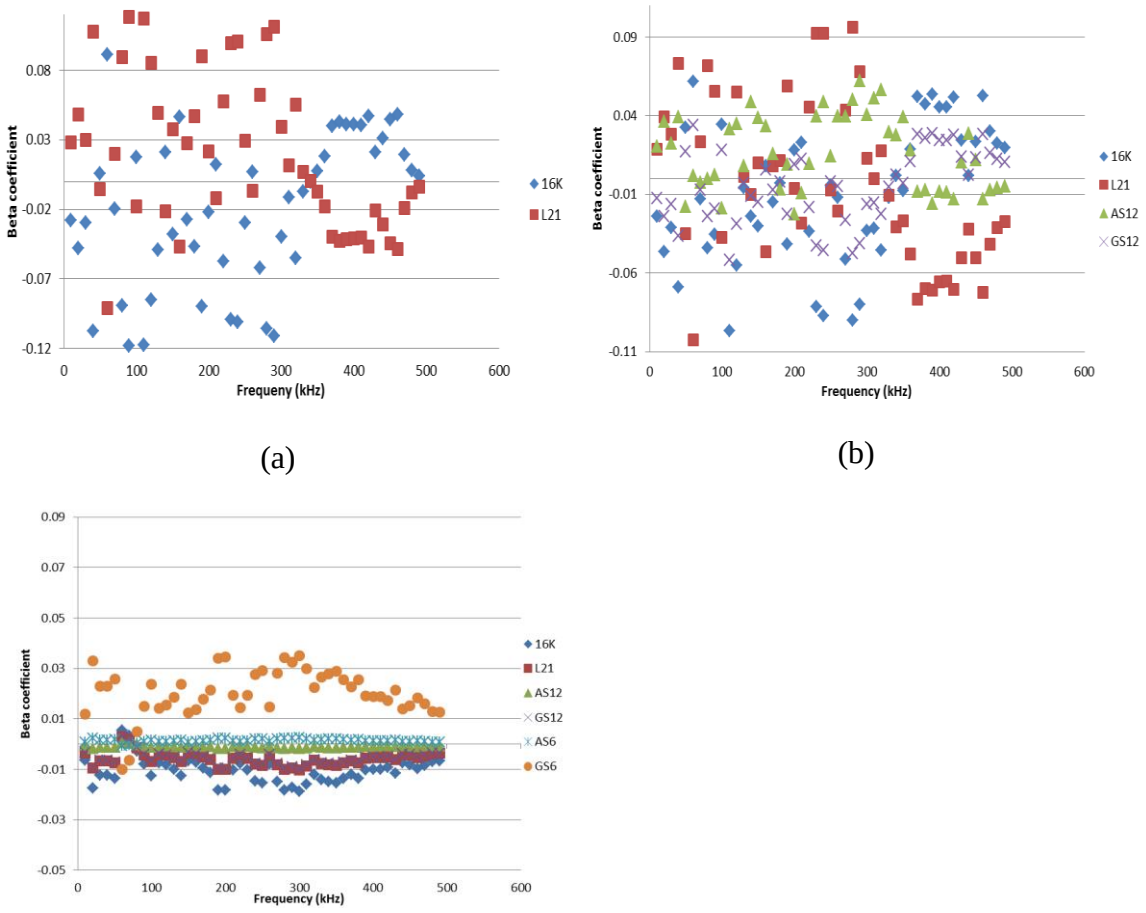

Fig.5.10. Beta coefficient plots from PLS-DA model built on FFTs from PLB tests after heating of composites containing 16K, L21, AS6, AS12, GS6 and GS12. Beta coefficients from first component for comparison of composites containing 10 vol% (a) 16K and L21, (b) 16K, L21, AS12 and GS12, (c) all coatings.

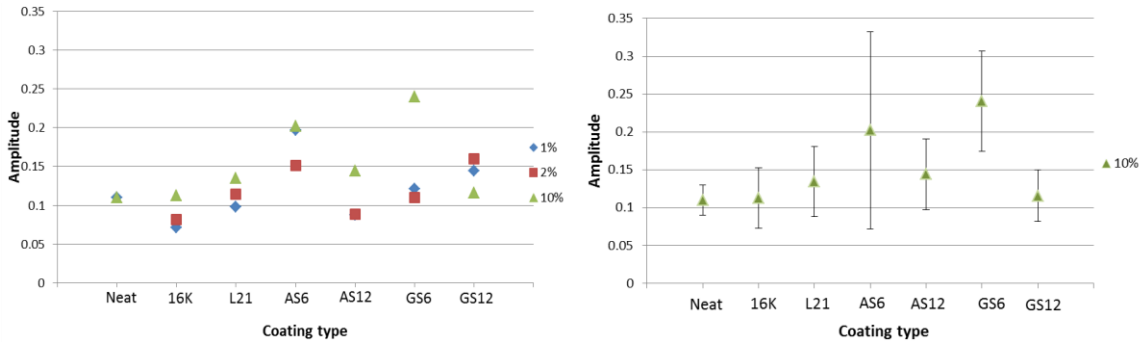

Fig.5.11. Averaged amplitude versus coating type from PLB after heating for composites with 1, 2 and 10 v% glass loading. Right graph shows only the 10 vol% glass loading for clarity of discussion.

The GS6/polyester exhibited the maximum amplitude once again similar to before heating and it was the only composite to be significantly different from the others at the 10 vol% content level. Assuming that stronger interfaces result in better transfer of wave energy from the matrix to glass spheres, giving lower attenuation, and now looking at all of the nominal data points in Fig 5.11 (1-10 vol%) for consistent trends, it seemed that 16K had the weakest interface compared to other coated glass/polyester composites. L21 and AS12, had slighty higher interface strength followed by GS6 and GS12. AS6 had the lowest amplitude attenuation thus the highest interface strength. Once again, coatings with lower thickness i.e. AS6 nad GS6 demonstrated better performance than thire counterparts at higher coating concentrations, which was not consistnet with results from mechanical tests in case of GS coating showing better performance for thicker ones.

Changes observed in acoustic signature of composites after heating demonstrate the changes in microstructure with thermal stresses. These changes can be associated with changes in stiffness of interphase due to thermal stresses resulting from degradation of coating at elevated temperature and possibly debonding at interface. Highest attenuation observed for 16K comapred with coated spheres after heating confirms that surface treatments of glass spheres provide an improved resistnace against thermal stresses.

The mechanical test results after heating (Sec 5.1) found that L21, AS6, AS12 coating showed stronger bonding between the polyester and glass, whereas GS6 performed poorer yet still slightly improved over 16K. The AE results confirm strong interfacial bonds with AS6, L21 and AS12. The AE results for 16K after heating were also consistent with mechanical test results. GS6 results could not be explained. Presence of void in some samples which significantly attenuate the sound waves might be a reason for the observed unexpected behaviours in acoustics results. High noise to signal ratio and high sensitivity of AE test to changes in microstructure of composites might explain some of the discrepancies in results. No conclusions regarding coatings is being made at this point since more analysis was required.

5.2.2. Effect of Using More Discrete Frequency Bands in the PLB Analysis

The analysis above was based on an averaged amplitude across the entire 140-240 kHz frequency range; however, the VIP plots suggested three smaller frequency ranges within that region where the changes in meso-structure were being detected acoustically, which are: 130-160 kHz, 180-220 kHz and 230-260 kHz. These more discrete frequency ranges were observed in the power spectrums before and after heating for different coatings as important frequencies for discrimination of classes. Averaged amplitude versus coating type for the 10 vol% composite at these three frequency ranges were investigated to see whether they provide more information on microstructure of the composites and wave propagation behavior; perhaps averaging all amplitudes between 140-240 kHz was actually dampening some of the more important changes.

Fig.5.12 shows the changes in amplitude versus coating type for the three frequency ranges in comparison to the full range between 140-240 kHz for composites containg 10 vol% glass sphere. For 130-160 kHz, the trend of amplitude (plot(a)) at the RT1 condition were similar to those observed at 140-240 kHz except for 16K/polyester which had a higher amplitude at this narrower range. Now AS12/polyester exhibited a higher amplitude closer to GS6/polyester. In fact, 16K and AS12 containing composites all

showed higher nominal amplitudes for 130-160 kHz over 140-240 kHz, now being comparable to GS6/polyester which consistently showed the highest amplitude. Thicker AS coating demonstrated better performance than thinner AS while the opposite was observed for GS coating. For the RT3 condition, amplitude increased for all coatings but relative amplitudes did not change in regards to amplitudes observed at 140-240 kHz, except AS12 and GS12 showed an increase. AS coatings at both levels demonstrated similar behavior while GS6 performed better than GS12.

Changes in amplitude versus coating type over the band of 180-220 kHz, before and after heating, is demonstrated in Fig.5.12(b). The trend in RT1 amplitudes was very similar to what was observed over 140-240 kHz, except for a decraese for 16K and AS12. AS coatings demonstrated similar behavior at both thickness levels while GS6 performed better than GS12. For RT3, AS12 showed decreased amplitude and GS6 showed increased amplitude compared to the results at 140-240 kHz. Both AS and GS coatings performed better at lower concentrations. GS12, AS12 and 16K showed the lowest interface strength which was inconsistent with results from mechanical tests for AS12. Mechanical tests demonstrated high stiffnesses associated with improved interfacial strength for L21, AS6, AS12.

Amplitued versus coating type over 230-260 kHz before and after heating is demonstrated in Fig.5.12(c). No significant changes in amplitude was observed for different coatings except for GS6 being a little higher. Trend in amplitude for RT3 was very similar to that of 140-240 kHz. However, at 230-260 kHz all amplitudes were much lower compared to amplitudes at 140-240 kHz. Difference in coating performances as a function of coating thickness was very small for both before and after heating.

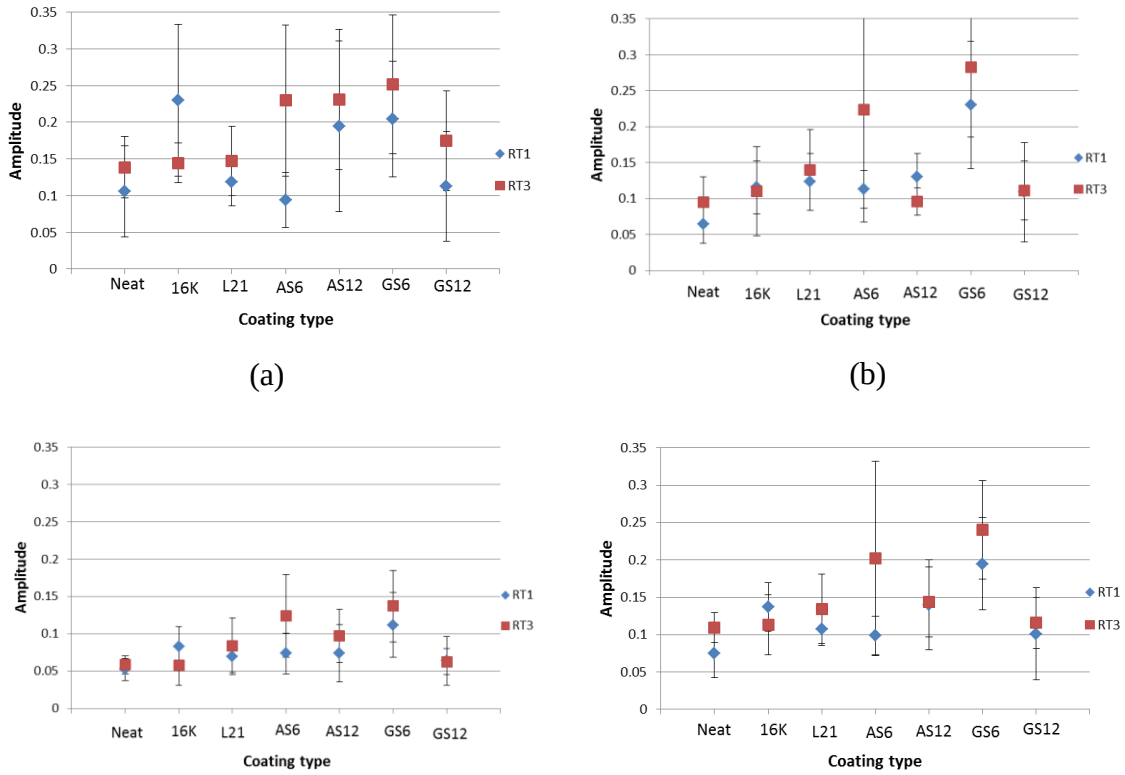

Fig. 5.12. Averaged amplitude versus coating type based on results from the PLB test, before and after heating, for frequency ranges of (a) 130-160 kHz, (b) 180-220 kHz, and (c) 230-260 kHz compared to earlier results looking at the entire frequency range of (d) 140-240 kHz for 10 vol% composites.

Changes in amplitudes over these frequency ranges were observed. Trends and relative amplitudes were almost similar to the trends observed over the broader range of 140-240 kHz except for some few differences. The 130-160 kHz frequency range demonstrated a more significant change regarding AS12, i.e. increased amplitued which provides more consistency between acoustic and mechanical test result (i.e. increasing modulus with an increasing glass content) but also some unusual behavior for 16K, thus is considered a better frequency range to represent changes in meso-structure and interfacial strength in particulate composites.

5.2.3 Considering the Influence of Glass Loading on Acoustic Behavior

Till this section, the majority of the analysis has focused on composites at the 10 vol% loading due to improved clarity of trends as we sought to relate averaged amplitudes for specific frequency ranges with the stiffness of a composite and by association, the strength of the interfacial bond between glass and polyester. The beta coefficients from PLS-DA model comparing power spectra of the composites with different glass loading (separately for each coating) before and after heating showed that the 140-240 kHz frequency range was still suitable, as used previously with the 10 vol% composites exclusively.

Fig.5.13 shows a comparison of average amplitudes for composites with different glass loadings. An increase in amplitude with increasing glass loading was considered a necessity to actually conclude that interfacial strength was improved by a coat, similar to the discussion regarding modulus in Sec 5.1.2. Such a trend was observed for most of the coatings, both before and after heating, though a few did not show a clear increasing behavior. Increased amplitude with glass loading for RT1 were seen more clearly for 16K, AS12 and GS6, while it was less clear for L21. The amplitude for AS6 and GS12 was quite constant with changing glass loading demonstrating the effects of decreased attenuation due to replacing a part of matrix with stiff glass spheres while offset by increased attenuation due to increased porosity (weak interface or agglomeration). After heating, a trend of increased amplitude with glass loading was obserevd clearly for 16K, GS6 and AS12 while only slightly for L21. Looking between 1% and 10%, changes were least obvious based on loading for AS6. A decrease was observed for GS12. Higher AS coating thickness demonstrated better performance compared to lower thickness while the opposite was observed for GS coating both before and after heating.

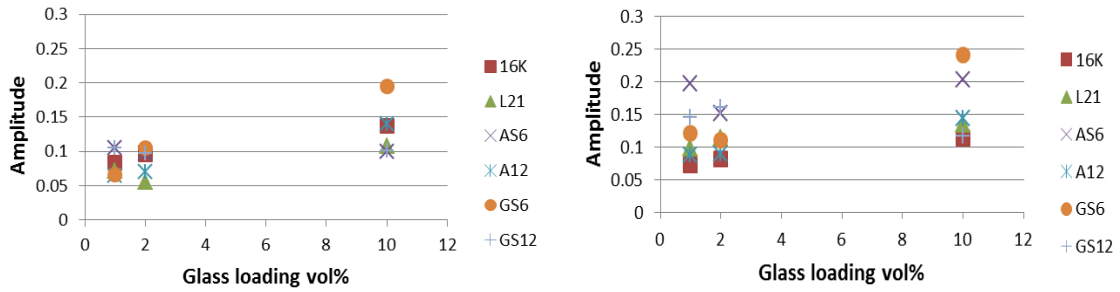

(a) (b)

Fig.5.13. Average amplitude versus glass loading for all composites with 1-10 vol% glass loading (a) before and (b) after heating at 140-240 kHz.

Increased amplitude was observed due to a reduction of viscoelastic matrix volume fraction and its replacement by rigid inclusions which led to reduced absorption losses (increased stiffness at/near interface as well as no absorption loss in glass sphere shell). Similar decreasing trend in attenuation was reported by other researchers (Biwa et al. 2004; Wu et al. 2006). Absorption loss is the main contributor to attenuation in particulate composites with viscoelastic matrix when the particle size is sufficiently small compared to wavelength (Biwa et al. 2004). Increased void content (due to 'weak interfaces' and cavity in glass sphere) by increased glass content also negatively affects the amplitude.

Based on the acoustic results for 140-240 kHz, it appeared that interfacial strength in 16K, AS12 and GS6 are higher than L21, AS6 and GS12 based on the trend sought. However, not all of these are consistent with results from the mechanical test. Especially in case of 16K (before and after heating) and GS6 (after heating). Earlier it was suggested that the 130-160 kHz frequency range showed better correspondence with mechanical observation. And so, changes in amplitude with glass loading over 130-160 kHz, 180-220 kHz and 230-260 kHz were investigated and compared with changes over 140-240 kHz to see the difference in trend of amplitudes compared to 140-240 kHz (Fig.5.14-5.16).

Over 130-160 kHz (Fig. 5.14), changes under the RT1 condition became more significant for 16K and AS12. Increasing trend for 16K after heating demonstrated a lower slope

compared to before heating which might be indicative of debonded particles after heating. In RT3, L21 demonstrated a decreasing trend with glass loading. A clearer increasing trend for AS12 was also observed for this range of frequencies. Trend for other coatings were similar to the analysis using 140-240 kHz though with slightly higher amplitudes. Over 180-220 kHz (Fig. 5.15), RT1 amplitude demonstrated a slight increasing trend for 16K with lower slope compared to 140-240 kHz. A very slight increasing trend for L21 was observed too. No other differences were observed between trends over this frequency range and 140-240 kHz. For RT3, changes with glass content becomes less clear for AS12 but it remained the same for the rest of the coatings. Changes for the RT1 and RT3 conditions over 230-260 kHz (Fig.5.16) were similar to the 140-240 kHz range, while a reduction in amplitude was observed for all coatings presenting a less clear increasing trends with glass loading.

Comparison of the changes in amplitude versus glass loading for the three narrower frequency range versus 140-240 kHz band demostrated few differences, especially at 130-160 and 180-220. The analysis range of 130-160 kHz demonstrated a clearer increasing trend for 16K, GS6 and AS12 before heating. After heating, the increase with GS6 and AS12 in terms of amplitude was more clearly obeserved, indicating higher interfacial strength compared to other coatings while for 16K increasing trend demonstarated a lower slope which indicated a weaker interface compared to GS6 and AS12 and possibly debonded particles. The clearer trend observed with AS12 is more consistent with mechanical properties that demonstrated an increasing trend with increased glass loading; however, not in the case of 16K which demonstrated a decreasing trend with increased glass laoding. 130-160 kHz was considered a band more descriptive of the changes in meso-structure even though differences between trends in amplitude in this range and 140-240 kHz is not very significant.

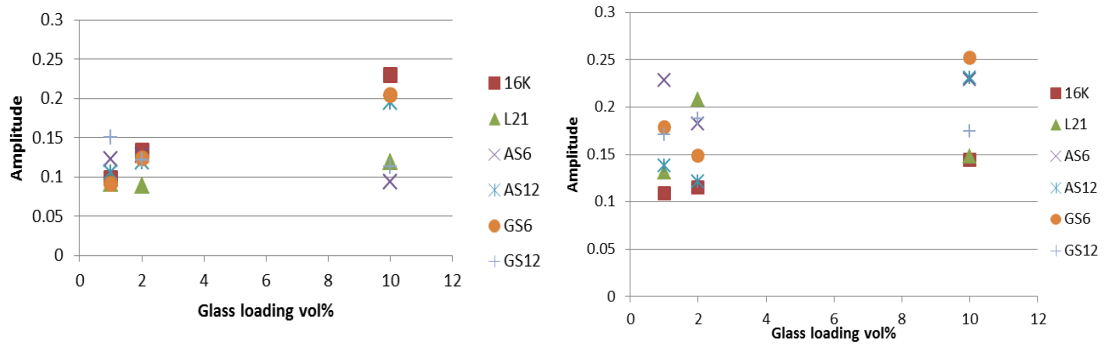

(a) (a)

Fig.5.14. Average amplitude versus glass loading for all composites with 1-10 vol% glass loading before (a) and after heating (b) at 130-160 kHz.

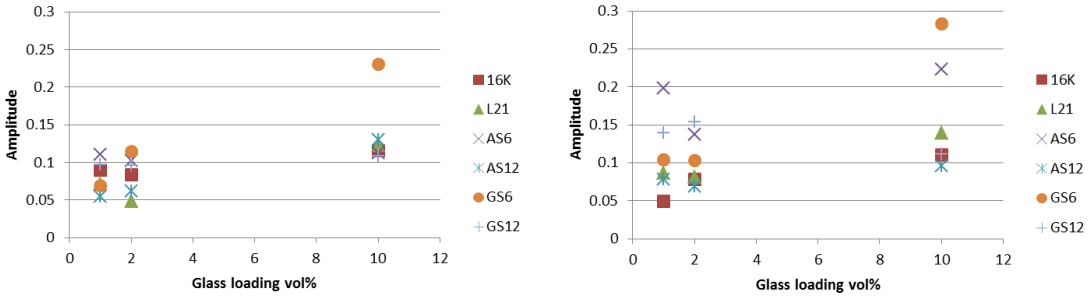

(a) (b)

Fig.5.15. Average amplitude versus glass loading for all composites with 1-10 vol% glass loading before (a) and after heating (b) at 180-220 kHz.

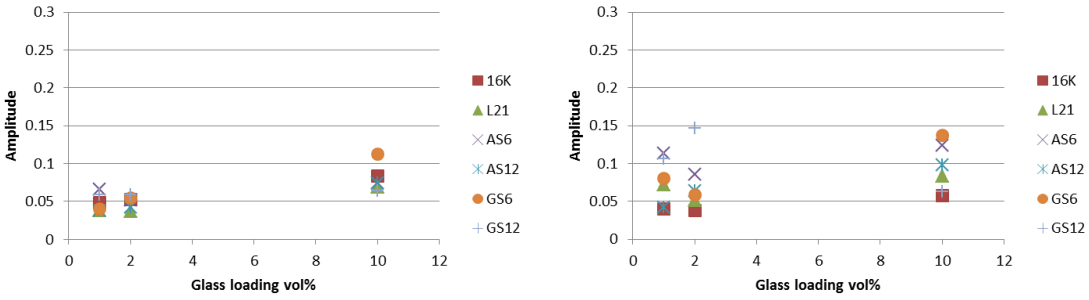

(a) (b)

Fig.5.16. Average amplitude versus glass loading for all composites with 1-10 vol% glass loading before (a) and after heating (b) at 230-260 kHz.

5.3. Differences between Mechanical and Acoustic Results

Fig.5.17 shows the averaged amplitudes of the PLB tests over 130-160 kHz versus the moduli of composites for each coating at 10 vol% glass loading. As stated earlier, an increase in AE amplitude is expected with increased stiffness of that material; however some of our results were not completely following this trend and admittedly, acoustics were not expected to fully follow the behavior of mechanical properties else the analysis would have no merit. In general, the plots in Fig 5.17 confirm that there is a trend of increased amplitude with stiffness, both before and after heating, though on an individual basis this accertion was not always true. A higher slope of amplitude versus modulus was expected for the RT1 condition compared to RT3 due to less damage to the glass/polymer interface and higher general stiffness thus higher amplitudes compared to RT3, though not much difference was actually observed between slopes which was taken as a very positive indicator that there was truly a relationship between these two test methods. Based on mechanical results in RT1, composites with AS12, GS6 and G12 glass microspheres had the highest stiffnesses yet GS12 did not correspondingly exhibit a higher amplitude. And the acoustic results of 16K demonstrated higher than expected amplitudes in spite of its non-treated surface. After heating, a good agreement between mechanical and acoustic results was observed except for GS6 which demonstrated less attenuation than its modulus would have predicted.

Overall, GS6 and AS12 coatings before heating and AS6 and AS12 after heating demonstrated consistency between mechanical and AE results. GS6 and AS12 performed better than other coatings before heating while AS12 demonstrated better performance after heating. The almost constant trend observed in amplitude versus glass loading for AS6 implied that it might not be as strong as AS12 in spite of their similar behavior observed in Fig. 5.17 (b). Considering the effect of coating thickness on effectiveness of AS and GS coatings, a better performance was observed for the higher AS coating thickness before and after heating. In the case of GS coating, lower coating concentration resulted in higher adhesion both before and after heating but the result after heating was

not consistent with the results from mechanical tests i.e. poor performance of GS6 compared to GS12.

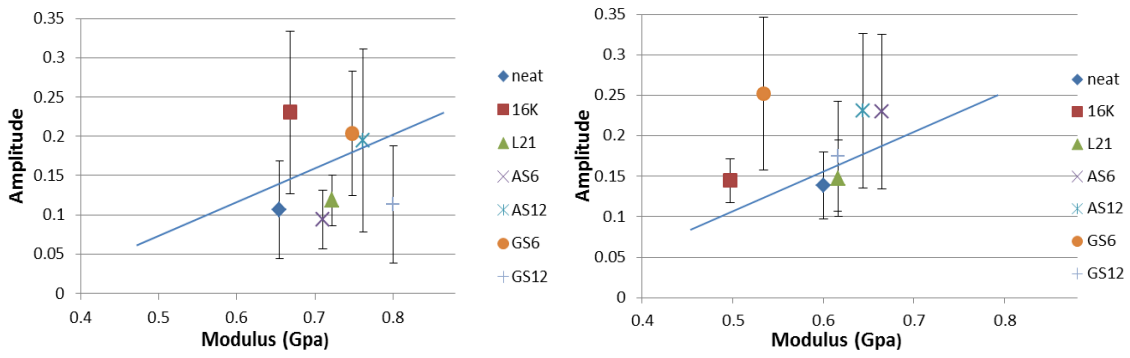

Fig. 5.17. Averaged amplitudes at 130-160 kHz from the PLB test versus tensile modulus for 10 vol% composites with different interface strength (a) before and (b) after heating.

5.4. Effect of Hydrolytic Aging on Microstructure of the Composites and Wave Propagation Behavior

Samples of the different glass/polyester composites were immersed in water for 14 days at 23℃ and 50% RH to investigate the effect of moisture on the matrix, glass/polyester interface and on the wave propagation behavior in these composites. Subsequently, heating these aged composites where more hydrolytic degradation should be induced and comparing to the results of the non-aged composites should assist in understanding the change in acoustics noted in Section 5.2.1.2. Fig.5.18 shows bi-plots demonstrating the clustering of aged versus non-aged composites containing 10 vol% 16K and L21 glass spheres, (a) before and (b) after heating. As can be seen, a clear discrimination based on aging was seen between these two glass sphere types, as opposed to previous models. Fig.5.19 shows VIP plots for the same composites, (a) before and (b) after heating. Considering the beta coefficients and VIP plots produced by the model, two frequency ranges of 180-220 kHz and 230-260 kHz were considered to be most significantly responding to differences between the samples.

Fig.5.20 shows a plot of the averaged amplitudes from the PLB tests over the 180-260 kHz frequency range for aged versus non-aged neat polyester, 16K/polyester and L21/polyester composites containing 1 and 10 vol% glass, both before and after heating. A clear decrease in amplitude with aging was observed for all glass content levels and coatings, both before and after heating. For neat polyester, the amplitude decreased from 0.06 to 0.045 (before heating) after aging whereas after heating, the non-aged amplitude increased to 0.08 while the aged amplitude was below 0.04. The decrease in amplitude before heating was due to a decrease in stiffness and increased attenuation coefficient for the plasticized matrix and possibly a weakening interface. Assarar et al. (2011) have reported a decrease in passive AE amplitude for signals that were associated with interfacial debonding in glass/epoxy composites whereas Gomes et al. (2014) found a decreased AE amplitude with plasticized high density polyethylene by toluene. After heating, the non-aged samples had been simply dried and hence attenuation decreased just as found in Section 5.2, but with excessive water bound after aging, hydrolytic chain damage dominated and attenuation increased as a result.

The composites showed much higher sensitivity to aging compared to neat matrix based on the relative change in amplitude (aged versus non-aged) and that relative change was more significant for composites with higher glass loadings. This is consistent with results reported by Jayet et al.(1999) using ultrasonic spectroscopy to examine moisture-aged versus non-aged glass fiber/epoxy matrix composites. An increase in attenuation was observed after aging, which they reported was higher for higher glass loaded composites (i.e. appearing as materials containing simply more voids once the interface was weakened). Those authors claimed that the increased attenuation was evidence of interface-dominant damage, producing increased scattering at the glass/epoxy interface. Higher glass loaded composites should be more prone to aging damage by having a higher interfacial area.

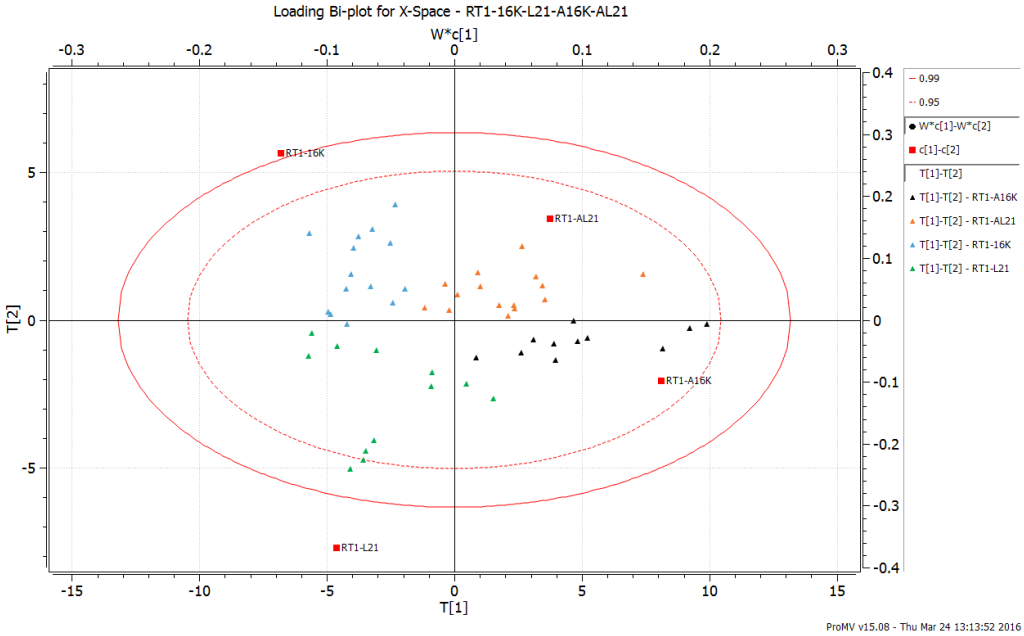

(a)

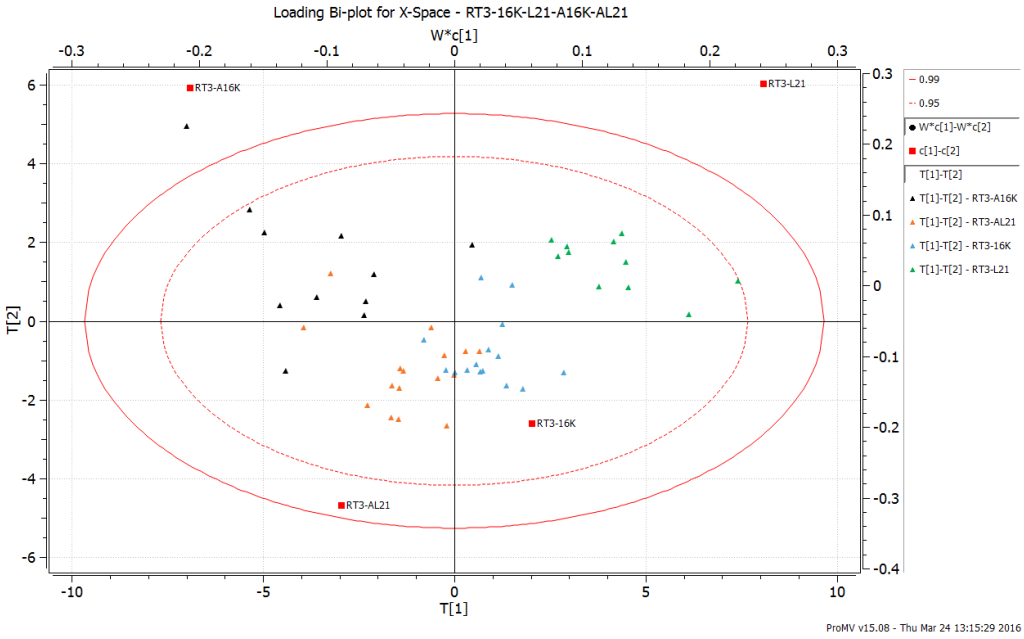

(b)

Fig. 5.18. Loading bi-plot from PLS-DA models built on the PLB tests for aged versus non-aged 10 vol% 16K/polyester and L21/polyester (a) before and (b) after heating.

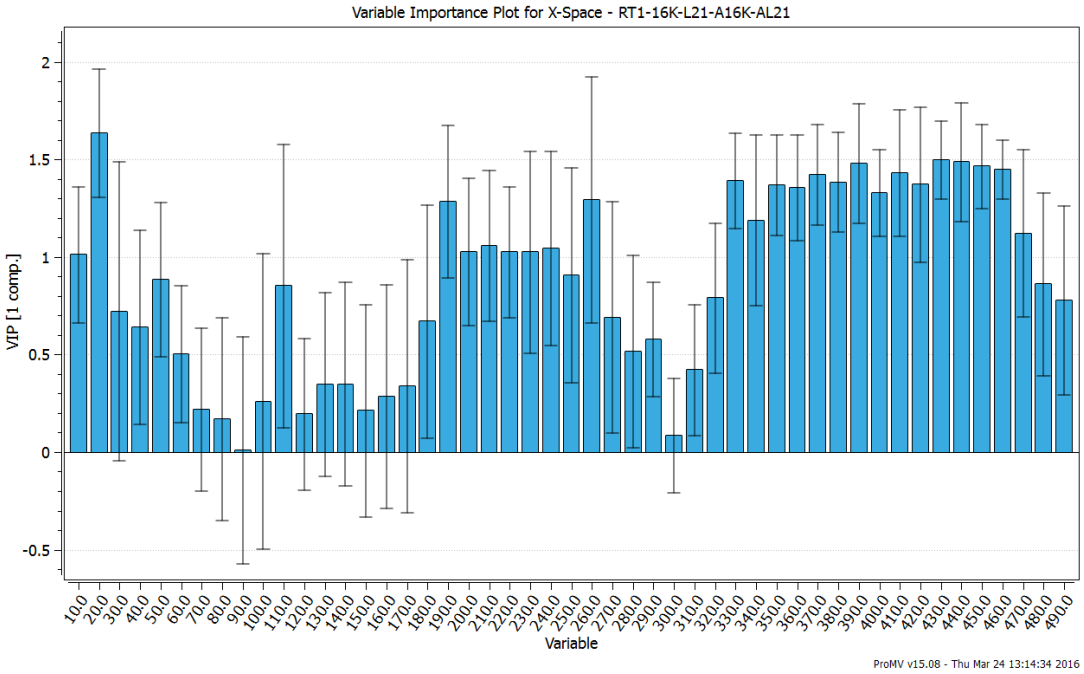

(a)

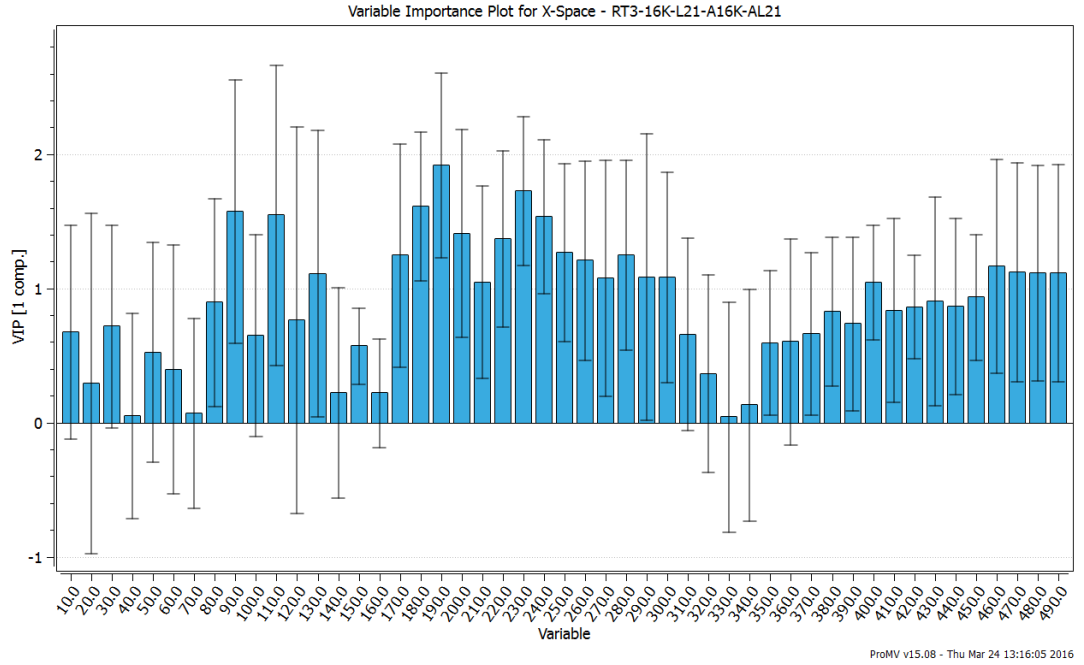

(b)

Fig. 5.19. VIP plots from PLS-DA models built on the PLB tests for aged versus non-aged 10 vol% 16K/polyester and L21/polyester (a) before and (b) after heating.

A decreased dependency of mechanical properties on moisture aging was observed in a treated carbon/epoxy composites having higher fiber/matrix interfacial strength compared to non-treated carbon fibers (Pérez-Pacheco et al. 2013). AE studies demonstrated the change in failure mode from fiber/matrix debonding to fiber failure for improved interfacial adhesion between fibers and matrix.

In the case of the 16K/polyester composite, aging always reduced the amplitude to a comparable level as the neat polyester, seemingly negating the influence of the weakly bonded glass spheres in the matrix and the voids they introduced into the matrix. This was observed at both glass loadings, and before and after heating.

The effects of moisture-aging were much more varied for the L21/polyester. This variance was expectedly due to the absorbed water disrupting the coating bonded at the glass/matrix interface. At lower glass loading, aged L21/polyester showed a lower amplitude compared to 16K and neat polyester. Non-aged L21/polyester also showed lower amplitudes compared to 16K/polyester for this loading. After heating, an increase in amplitude was observed showing improved performance of aged L21/polyester compared to 16K/polyester after heating. Similar behavior was observed for the non-aged L21. At 10 vol% glass loading, aged L21 demonstrated higher amplitude compared to 16K/polyester before heating while the non-aged L21/polyester still showed a low amplitude comparable to 16K. Heating resulted in a slight decrease in amplitudes for aged L21/polyester composite; however, it still showed better performance than 16K/polyester after heating. Non-aged L21/polyester also showed higher amplitude compared to 16K after heating. This coating showed what appeared to be good moisture resistance in these tests.

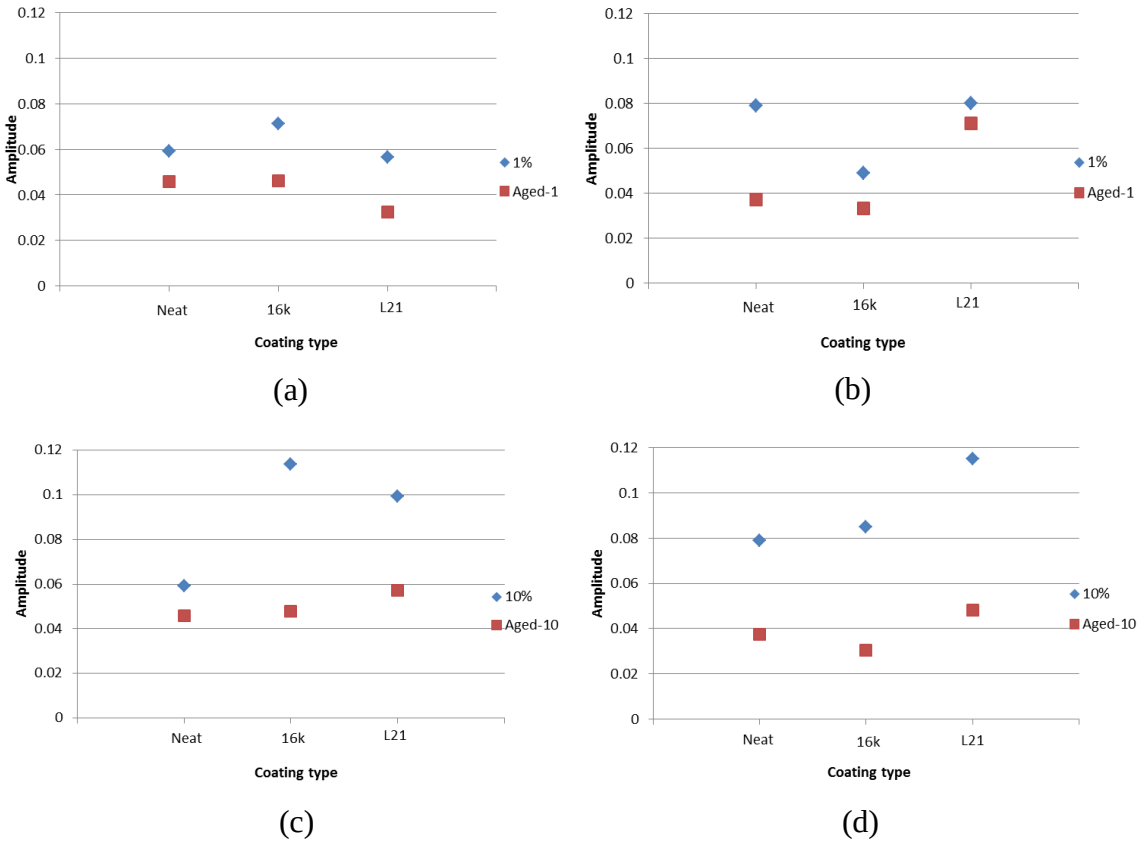

Fig. 5.20. Average amplitudes from the PLB tests on aged and non-aged composites over the frequency range of 180-260 kHz (a) before and (b) after heating for 1 vol% glass loading and (c) before and (d) after heating for 10 vol% glass loading.

The analysis in Fig 5.20 were based on the averaged amplitudes spanning the full range of frequencies between 180-260 kHz, though the VIP plots indicated two smaller frequency bands within this range. It was interesting to compare the results above to analyses looking at the two smaller ranges separately, as was similarly done in earlier sections. Fig. 5.21 (a-d) demonstrates plots of the averaged amplitudes from the PLB tests over the 180-220 kHz and 230-260 kHz frequency ranges for aged versus non-aged neat polyester, 16K/polyester and L21/polyester composites containing 1 and 10 vol% glass, both before and after heating.

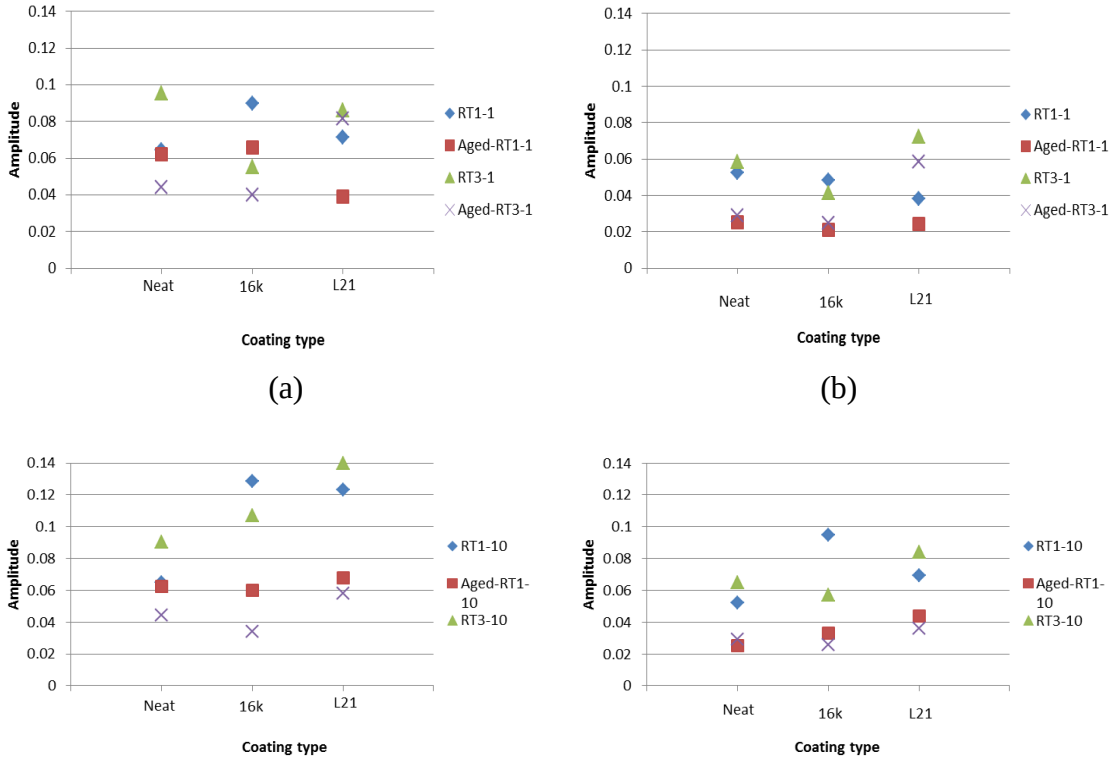

Fig. 5.21. Average amplitudes from the PLB tests on aged and non-aged composites before and after heating over the frequency range of (a) 180-260kHz and (b) 230-260kHz for composites with 1 vol% glass loading and before and after heating over the frequency range of (c) 180-260kHz and (d) 230-260kHz for composities with 10 vol% glass loading.

The trends in amplitudes for aged and non-aged composites containing 1 vol% glass over 180-220 kHz (Fig. 5.21(a)) were similar to 180-260 kHz while amplitudes were slightly higher. For aged composites, the amplitude over 230-260 kHz (Fig. 5.21(b)) decreased slightly with heating; however, L21/polyester demonstrated higher amplitudes compared to 16K/polyester while at 180-260 kHz, the opposite of this trend was observed. For non-aged composites trends were similar to that of 180-260 kHz.

For 10 vol%, trend of amplitude changes over 180-220 kHz (Fig. 5.21(c)), for aged (and non-aged) composites was very similar to 180-260 kHz. Over 230-260 kHz (Fig. 5.21(d)) despite the lower amplitudes observed in this range, trend of amplitude for aged composites was similar to 180-260 kHz except that changes with heat were much smaller

for neat polyester and 16K/polyester. No significant additional information was obtained by considering smaller frequency bands to describe behavior of material under hydrolytic and thermal aging and thus 180-260 kHz was considered satisfactory for investigating the changes in acoustic signature with moisture aging and subsequent thermal cycling.

5.5. Morphology of Hollow Glass Microsphere/Polyester Composites

Failure modes normally obserevd in particulate composites containing hollow glass microspheres under tensile load include matrix carcking, particle/matrix debonding and glass sphere breakage (Gupta 2004). Composites with higher interfacial strenth are expected to demonstrate less debonding features between the glass spheres and matrix.

Fractured surface of the composites containing glass spheres with different coatings (before heating) were observed by SEM. In all cases, the presence of intact microspheres on the fractured surface were found with minimal amounts of debris being observed due to the high crush strength of the glass spheres used. This was also observed for K46 glass/epoxy composites which have a lower strength compared to 16K series that we used in this work (Gupta & Nagorny 2006). The composites containing 16K hollow glass microspheres demonstrated debonding features in the fractured plane of view which was due to the absence of strong interfacial adhesion (Fig.5.22(a-c)). However, well bonded particles were also observed in the 16K composites to indicate the matrix was not being repelled from the glass (Fig.5.22(d)). Mechanical test results demonstrated decreased stiffness with increased 16K loading though the AE results often found highest amplitudes that were expected for a strong interface, not consistent with the morphological observations. Glass sphere/matrix debonding was also observed for L21 glass spheres; however, fewer cases were seen than with 16K (Fig.5.23(a-b)). Particles with good bonding were observed for this coating too (Fig.5.23(c-d)).

Similar features demonstrating both well bonded and debonded particles were observed for all other composites (Fig.5.24- 5.27) not providing additional information regarding the difference between interfacial strength among different composites. Fewer debonded

particles were observed for these composites compared to 16K and L21 containing composites.

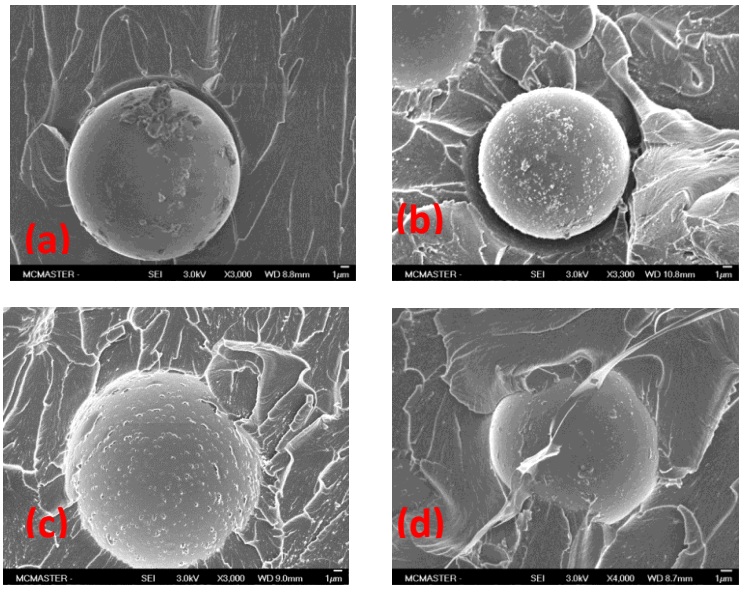

Fig.5.22. Fractured surface for composites containing 16K before heating. (a-b) debonded particles (c) a complete separation of particle from matrix (d) a well bonded particle. Magnification of images are different. Scale bars are provided in each image.

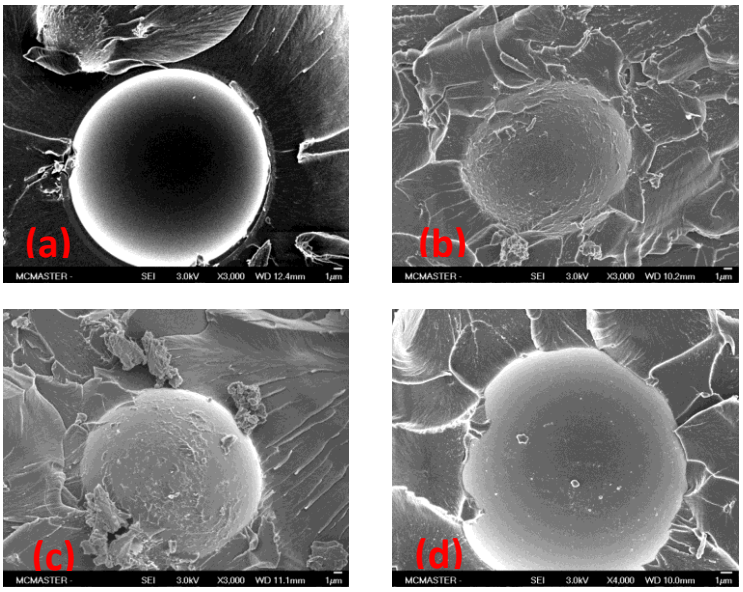

Fig.5.23. Fractured surface for composites containing L21 before heating. (a) a debonded particle, (b) a compelete separation of matrix and particle and (c-d) well bonded particles. Magnification of images are different. Scale bars are provided in each image.

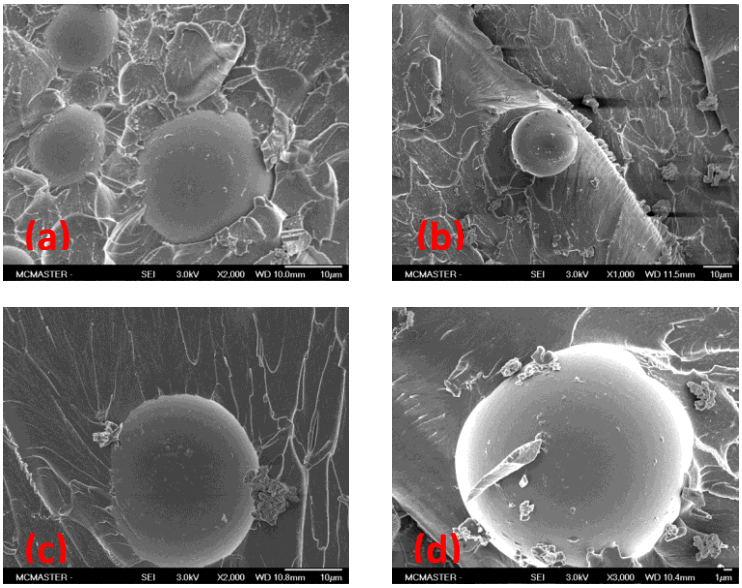

Fig.5.24. Fractured surface for composites containing AS6 before heating. (a-b) debonded particles (c) a compelete separation of matrix and particle (d) a well-bonded particle. Magnification of images are different. Scale bars are provided in each image.

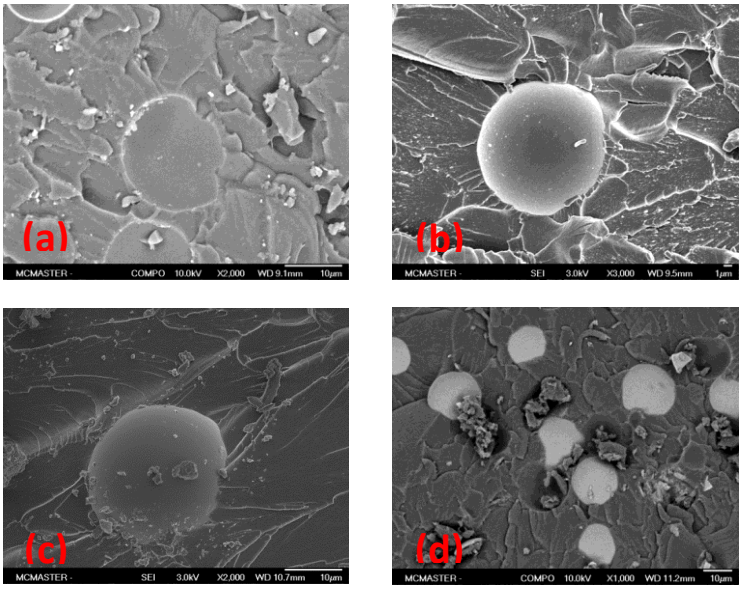

Fig.5.25. Fractured surface for composites containing AS12 before heating. (a) a compelete separation of matrix and particle (b-c) well bonded particle. (d) a lower magnification image showing AS12 glass spheres in matrix. Magnification of images are different. Scale bars are provided in each image.

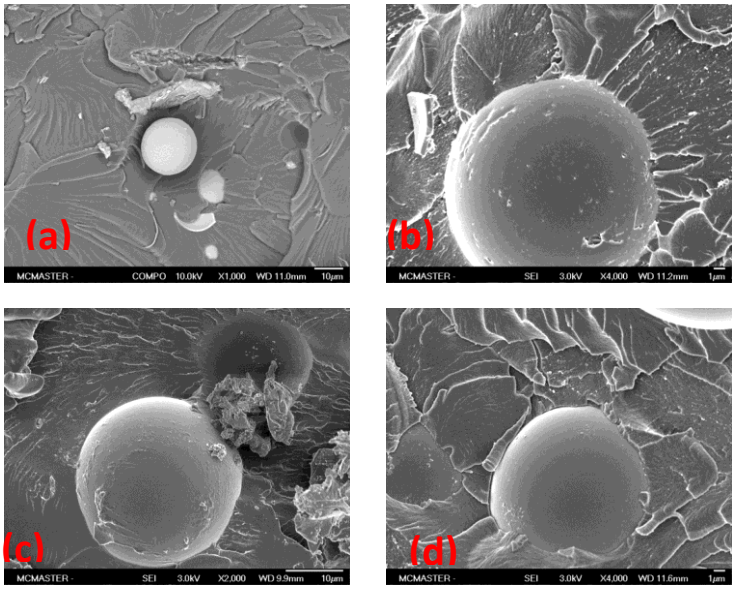

Fig.5.26. Fractured surface for composites containing GS6 before heating. (a) a particle with loose bonding to matrix (b) a complete separation of particle. (c-d) well bonded particles Magnification of images are different. Scale bars are provided in each image.

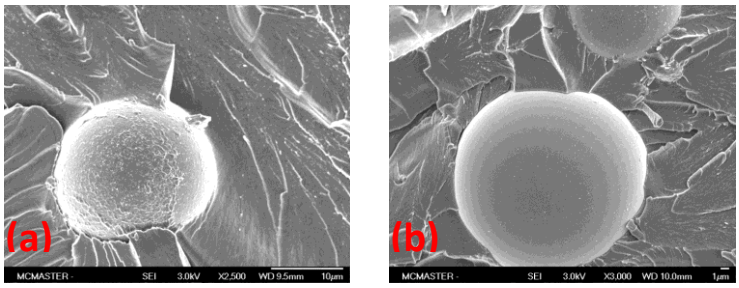

Fig.5.27. Fractured surface for composites containing GS12 before heating. (a) a debonded particle (b) a well bonded particle.Magnification of images are different. Scale bars are provided in each image.

Chapter 6: Conclusion

Active AE assisted in investigating the effect of thermal stresses on the hollow glass microsphere/polyester interface, being used to improve our resolution of how coatings affected the interfacial strength. The apparent sensitivity of elastic waves at a specific frequency range to the rigidity of polymer chains at or near the glass sphere/polyester interface enabled use of attenuation to postulate the state of the glass/polyester interface and its alteration due to thermal cycling and coatings.

6.1. Summary

Evaluation of the interfacial strength in glass/polyester composites and the effect of thermal stresses on the glass/polymer interface were performed using active AE and investigation of its propagation in particulate glass/polyester composites. Differences between mechanical and AE results were observed. AE technique was expected to provide a better tool for investigating the interfacial strength in composites compared to mechanical testing due to its seemingly higher sensitivity to changes in microstructure at meso-scale; however, not a very significant improvement in evaluating the interfacial strength was obtained.

6.1.1. Mechanical Tests

Mechanical tests were performed to investigate the effects of glass loading, glass coating and thermal stresses on a thermoset polyester composite. Comparison of the tensile modulus of composites containing glass spheres with different coatings at 1 and 2 vol% glass loading did not show notable differences. However, by 10 vol% the differences in mechanical properties were notable. A definitive trend showing an increase in modulus with increasing glass loading was taken as a necessary indicator in order to assume interfacial strength improved by a coating. By this criterion, only the AS12, GS6 and GS12 coatings showed improved interfacial strength. Higher coating concentrations demonstrated a better performance.

The negative effect of thermal stresses on stiffness was clearly observed with all polyester composites; however, again differences between different coatings were not very clear. AS6, AS12 and L21 coatings modulus appeared to show increasing trends with increasing glass loading from 1 to 10 vol% and thus were considered better coatings. Lower concentration AS performed better than higher concentration AS, while the opposite was observed for GS coating.

6.1.2. Acoustic Emission

Attenuation behavior of elastic waves is known to increase with materials of lower modulus. Hence, signal amplitudes before and after thermal cycling were compared to evaluate their correlation by multivariate statistics with interfacial strength and damage formation, hypothesizing that lower attenuation corresponded with higher interfacial strength in the case of the polyester composite.

6.1.2.1. Coating Effectiveness: Composites containing 10 vol% glass spheres were the focus since just like with mechanical properties, the lower volume fractions did not show trends as clearly. The coating GS6 demonstrated the highest amplitude in the frequency range of 140-240 kHz, presumably indicating the highest interfacial strength before heating. Other coatings demonstrated similar nominal amplitudes but lower than GS6. A better performance was observed for lower GS thickness. Performance of AS coating was similar at both concentrations. After thermal cycling, AS6 and GS6 demonstrated the highest amplitudes while L21, AS12 and GS12 coatings demonstrated similar values yet lower to the other two types. The polyester with uncoated glass microspheres, 16K, and neat polyester showed the lowest amplitudes. A better performance was observed for lower GS and AS coating thickness.

Looking at the changes in amplitude versus coating type for all glass loading levels to seek consistent trends, 16K showed the weakest interface – as anticipated. AS12 and L21 had slighty higher interface strength, followed by GS6 and GS12. AS6 had the lowest amplitude attenuation in general thus was ranked as having the highest interface strength. The lowest amplitude after heating was observed for 16K, confirming better performance

of surface treated glass spheres under thermal stresses compared to uncoated glass. Changes in the performance of coatings after heating versus before heating could be related to changes in the chemical structure of the coatings at elevated temperatures.

6.1.2.2. Analysis based on Broad versus Narrower Frequency Ranges: The multivariate analysis revealed three distinctive frequency bands, which the analysis above consolidated into a single band where resonances sensitive to differences between the different composites were found. The trend of amplitude versus coating type for the narrower frequency ranges of 130-160 kHz, 180-220 kHz and 230-260 kHz was subsequently considered. Overall, the trend of amplitude for each narrow range was almost identical to that observed over 140-240 kHz; however, some different behaviors were observed. The range of 130-160 kHz revealed changes in amplitudes for the AS12 coating which were more consistent with the mechanical results, thus was chosen as a better frequency range for describing the changes at interface although the behavior of 16K before heating and GS6 after heating over this frequency range could not be explained. At 130-160 kHz range, higher AS thickness and lower GS thickness were more effective before heating while after heating AS coating effectiveness was similar at both concentrations while for GS coating, lower concentration performed better.

6.1.2.3. Effect of Glass Loading: An increase in acoustic amplitude was observed in the glass sphere/polyester composites with increasing glass loading at 140-240 kHz. Acoustic absorption by the viscoelastic matrix was considered to be the dominant attenuation mechanism at the studied wavelength and thus a reduction in matrix volume fraction as well as the increased stiffness that occurred with increased glass loading resulted in increased amplitude. A more definitive increasing trend of amplitude versus glass loading was associated with higher interfacial strength. GS6, AS12 and 16K demonstrated the most clear increasing trends in amplitude with increased glass content compared to L21, AS6 and GS12, which was considered as an indicator of stronger adhesion at their interfaces with the matrix. Trends in amplitude versus glass loading were similarly observed over the three narrower frequency ranges. Over 130-160 kHz a clearer

increasing trend was observed for AS12, GS6 and 16K, both before and after heating, and was chosen as a better descriptive range for the behavior of composites.

6.1.2.4. AE versus Mechanical: Comparison of amplitude over the band of 130-160 kHz versus the modulus of composites containing 10 vol% hollow glass microsphere was expected to illustrate an increasing trend due to decreased attenuation with increased stiffness. For most coatings, consistency was observed between mechanical test results and expected amplitude. 16K demonstrated attenuation lower than what its mechanical test results predicted before heating and GS12 demonstrated a higher attenuation than what was predicted by its mechanical test results. A lower attenuation was observed for GS6 after heating.

Considering the trend in amplitude versus coating type over 130-160 kHz, changes in amplitude with glass loading level and consistency between AE response and mechanical test results, GS6 and AS12 coatings were felt to show higher interfacial strength compared to other coatings before heating while after heating AS12 performed better than other coatings. Performance of AS6 after heating was also better than other coatings however no clear increasing trend was observed for its amplitude versus glass loading. Higher thickness of AS coating demonstrated better interfacial strength.

6.1.2.5. Moisture Aging: using statistical multivariate analysis, the band of 180-260 kHz was observed to respond to changes in the power spectrum with moisture aging and heating. Over this frequency range, aged composites demonstrated lower amplitude compared to non-aged composites due to the plasticizing effect of absorbed water on matrix and also its effect on glass/polyester interface strength by disrupting the interaction between glass to coating or polyester. Composites containing higher glass loadings showed more damage (higher attenuation) with heating due to the higher interfacial area being susceptible to moisture attack. Aged 16K showed amplitudes as low as aged neat polyester, negating the effect of glass spheres in regards to increasing stiffness, possibly due to weaker interfaces. Aged L21 demonstrated more variation perhaps due to disruption of the coating bonds by absorbed water. Aged L21 at lower

concentration showed lower amplitudes than aged 16K; however, after heating it demonstrated a higher amplitude compared to aged 16K. At higher concentration, both aged and non-aged L21 showed higher amplitudes than 16K before and after heating indicating a better resistant against moisture attack and thermal stresses. The trend in amplitude over the narrower frequency ranges of 180-220 kHz and 230-260 kHz were consistent with the broader 180-260 kHz range. Thus 180-260 kHz was considered suitable for investigating the changes at or/and near interface due to aging and heating.

6.1.3. Morphological observation

Morphology of the fractured surfaces of composites containing glass spheres with different coatings was investigated. The presence of more debonded particles was observed for 16K glass spheres compared to any other coated glass sphere. Similar features were observed for the rest of the composites i.e. presence of both well bonded and debonded particles.

6.2. Future work

- Studying the wave propagation in a composite containing glass spheres with a coating that repels the polyester can be compared against attenuation of composites containing 16K and silane treated glass. This will provide more clarity about expected level of interfacial strength between particle and matrix and probably a clearer trend in amplitude versus coating type in active AE.
- Using ultrasonic transducers designed for high temperatures can be considered for generation of active elastic waves. This will provide an AE source with higher reproducibility compared to pencil lead breaks and also allow for generation of wider range of frequencies. Higher frequency elastic waves travelling through composites have lower wavelength which is more comparable to particle size and thus provide a better possibility for investigating the local properties at interface. Acoustic wave velocity measurements can be performed to provide additional information about the stiffness of the material. Composites containing higher glass content will also provide a better chance for observing the changes in wave

propagation with glass content provided the entrapped air amount can be controlled while fabricating the composites.

- The possibility of recording passive AE under thermal stresses through applying a stronger thermal shock (compared to what was done in this study) and use of high temperature sensors can be investigated. Considering other parameters in analyzing the elastic wave propagation besides frequency provide additional information about the debonding processes at interface. An important parameter being calculated from the AE signal related to signal energy is Measured Area of the Rectified Signal Envelop (MARSE) which might be used with passive AE data providing information about the energy of acoustic events at microfailure processes. This parameter can be compared for composites with different coatings in which passive AE (under mechanical load) is recorded before and after heating or for composites in which passive AE recording under thermal stresses has been successfully implemented.
- Finally, elastic wave propagation in a more complex material, which better represents the SMC, can be investigated by adding glass fibers and calcium carbonate to studied composites (or an actual SMC can be considered). Effect of thermal stresses on this material can be investigated. Effect of different heating rates on damage formation can also be studied through both passive and active AE tests. Rapid heating (using an IR oven) is expected to create clearer damage to interface but finding a sensor to survive in such heat will be challenging. Powder priming of these composites might be ultimately performed and compared for different coatings and at different heating rates while observing the ‘paint popping’ to evaluate the agreement between the acoustic results obtained for unpainted composites on coating effectiveness and their endurance under thermal stresses with the actual ‘paint popping’ behavior in painted composites.

References

Amos & Yalcin, 2015. Hollow glass microspheres in sheet molding compounds. In *Hollow glass microspheres for plastics, elastomers and adhesive compounds*. p. 123.

Assarar, M. et al., 2011. Influence of water ageing on mechanical properties and damage events of two reinforced composite materials: Flax-fibres and glass-fibres. *Materials and Design*, 32(2), pp.788–795.

Bardella, L. & Genna, F., 2001. On the elastic behavior of syntactic foams. *International Journal of Solids and Structures*, 38(40-41), pp.7235–7260.

Basu, S.K., Shah, B. & Kia, H.G., 2009. The Effect of Oven-Heat Flux on Powder-Coating Issues of Sheet Molding Compound Panels. *Industrial and engineering chemistry research*, pp.1638–1649.

Beltzer, A.I., Bert, C. & Striz, A., 1983. On wave propagation in random particulate composites. *International Journal of Solids and Structures*, 19(9), pp.785–791.

Beltzer, A.I. & Brauner, N., 1987. The dynamic response of random composites by a casual differential method. *Mechanics of materials*, 6, pp.337–345.

Berg, J. & Jones, F.R., 1998. The role of sizing resins , coupling agents and their blends on the formation of the interphase in glass fibre composites. *Composites Part A: Applied Science and Manufacturing*, pp.1261–1272.

Biwa, S. et al., 2004. Analysis of ultrasonic attenuation in particle-reinforced plastics by a differential scheme. *Ultrasonics*, 43(1), pp.5–12.

Biwa, S., 2001. Independent scattering and wave attenuation in viscoelastic composites. *Mechanics of materials*, 33, pp.635–647.

Biwa, S., Idekoba, S. & Ohno, N., 2002. Wave attenuation in particulate polymer composites : independent scattering / absorption analysis and comparison to measurements. *Mechanics of materials*, 34, pp.671–682.

Bohse, J., 2000. Acoustic emission characteristics of micro-failure processes in polymer blends and composites. *Composites Science and Technology*, 60, pp.1213–1226.

Calabro, A. et al., 1997. A frequency spectral analysis of the fiber failure acoustic emission signal in a single fiber composite. In *IEEE ultrasonics symposium*.

Cardoso, R.J. & Shukla, a, 2002. Effect of particle size and surface treatment on constitutive properties of polyester-cenosphere. *Journal of Materials Science*, 37, pp.603–613.

Dattat, P.K. & Pethrick, R.A., 1980. Ultrasonic studies of glass-filled polymer solids.

Journal of physics D: Applied Physics, 13, pp.153–161.

Dekkers, M.E.J. & Heikens, D., 1983. The effect of interfacial adhesion on the tensile behavior of polystyrene–glass-bead composite. *Journal of Applied Polymer Science Volume 28 issue 12*, 28(12), pp.3809–3815.

Dibenedetto, A.T., 2001. Tailoring of interfaces in glass fiber reinforced polymer composites : a review. *Materials Science and Engineering A*, 302, pp.74–82.

DiBenedetto, A.T. & Wambach, A.D., 1972. The fracture toughness of epoxy-glass bead composites. *International journal of polymeric materials*, 1(2), pp.159–173.

Drury, J.C., 2005. Ultrasonics: Part 7. The ultrasonic beam. *Insight: Non-Destructive Testing and Condition Monitoring*, 47(5), pp.297–299.

Fu, S.-Y. et al., 2008. Effects of particle size, particle/matrix interface adhesion and particle loading on mechanical properties of particulate–polymer composites. *Composites Part B: Engineering*, 39(6), pp.933–961.

Giordano, M. et al., 1998. An acoustic-emission characterization of the failure modes in polymer-composite materials. *Composites Science and Technology*, 58(12), pp.1923–1928.

Giordano, M. et al., 1999. Analysis of Acoustic Emission Signals Resulting From Fiber Breakage in Single Fiber Composites. *Polymer Composites*, 20(6), pp.758–770.

Godin, N. et al., 2004. Clustering of acoustic emission signals collected during tensile tests on unidirectional glass/polyester composite using supervised and unsupervised classifiers. *NDT and E International*, 37(4), pp.253–264.

Godin, N., Huguet, S. & Gaertner, R., 2006. Influence of hydrolytic ageing on the acoustic emission signatures of damage mechanisms occurring during tensile tests on a polyester composite: Application of a Kohonen's map. *Composite Structures*, 72(1), pp.79–85.

Godin, N., Huguet, S. & Gaertner, R., 2005. Integration of the Kohonen's self-organising map and k-means algorithm for the segmentation of the AE data collected during tensile tests on cross-ply composites. *NDT and E International*, 38(4), pp.299–309.

Gomes, F.P.C. et al., 2014. Evaluating the influence of contacting fluids on polyethylene using acoustic emissions analysis. *Polymer Testing*, 39, pp.61–69.

de Groot, P.J., Wijnen, P. a. M. & Janssen, R.B.F., 1995. Real-time frequency determination of acoustic emission for different fracture mechanisms in carbon/epoxy composites. *Composites Science and Technology*, 55(4), pp.405–412.

Groot, P.J. De, Wijnen, P.A.M. & Janssen, R.B.F., 1995. Peter J. de Groot, Peter A. M.

Wijnen & Roger B. F. Janssen. , 55, pp.405–412.

Gupta, N., 2004. Microballoon Wall Thickness Effects on Properties of Syntactic Foams. *Journal of Cellular Plastics*, 40(November 2004), pp.461–480.

Gupta, N. & Nagorny, R., 2006. Tensile properties of glass microballoon-epoxy resin syntactic foams. *Journal of Applied Polymer Science*, 102(2), pp.1254–1261.

Hamarneh, A., Gorzolnik, B. & Horbach, A., 2013. DSM proposes new roads to weight reduction.

Harding, P.H. et al., 1998. Measurment of residual stress effects by means of single-particle composite tests. *Adhesion science and technology*, 12(5), pp.497–506.

Herrera-Franco, P.J. & Drzal, L.T., 1992. Comparison of methods for the measurement of fibre/matrix adhesion in composites. *Composites*, 23(1), pp.2–27.

Huang, J.S. & Gibson, L.J., 1993. Elastic moduli of a composite of hollow spheres in a matrix. *Journal of the Mechanics and Physics of Solids*, 41(1), pp.55–75.

Huguet, S. et al., 2002. Use of acoustic emission to identify damage modes in glass fibre reinforced polyester. *Composites Science and Technology*, 62, pp.1433–1444.

Jayet, Y. et al., 1999. Application of Ultrasonic Spectroscopy for Hydrolytic Damage Detection in GRFC : Correlations with Mechanical. *Journal of Composite Materialsomposite materials*, 34(16), pp.1356–1368.

Jenkins, M.L., Dauskardt, R.H. & Bravman, J.C., 2004. Important factors for silane adhesion promoter efficacy : surface coverage , functionality and chain length. *Journal of Adhesion Science and Technology*, 18(13), pp.1497–1516.

Johnson, M., 2002. Waveform based clustering and classification of AE transients in composite laminates using principal component analysis. *NDT and E International*, 35(6), pp.367–376.

Johnson, M. & Gudmundson, P., 2000. Broad-band transient recording and characterization of acoustic emission events in composite laminates. *Composites Science and Technology*, 60, pp.2803–2818.

Keckl, C., Kuppinger, J.A.N. & Baumgärtner, D., Material and Part Characterization of the Direct SMC Process for Lightweight Class-A Formulations.

Kenyon & Duffey, 1967. Properties of a particulate filled polymer. *Polymer Engineering & Science*, 7(3), pp.189–193.

Kia et al., 2006. Coating development and plant trials for powder priming of SMC. In *Composites*.

Kia, H.., 1993. *Sheet Molding Compounds Science and Technology*, New York: Hanser Publishers.

Kia, H.G., 2009. Development of Low Moisture Absorbing SMC. *Journal of Composite Materials*, 44(1), pp.55–74.

Kia, H.G. et al., 2006a. Powder Priming of SMC. Part I: Assessment of the Current Technologies. *Journal of Composite Materials*, 40(16), pp.1413–1429.

Kia, H.G. et al., 2006b. Powder Priming of SMC. Part II: Failure Mechanism. *Journal of Composite Materials*, 40(16), pp.1431–1447.

Kim, J., Ih, J. & Lee, B., 1995. Dispersion of elastic waves in random particulate composites. *Acoustical society of America*, 97, pp.1380–1388.

Kim, J.Y., 2004. On the generalized self-consistent model for elastic wave propagation in composite materials. *International Journal of Solids and Structures*, 41(16-17), pp.4349–4360.

Kim, J.-Y., 2010. Models for wave propagation in two-dimensional random composites: A comparative study. *The Journal of the Acoustical Society of America*, 127(4), pp.2201–2209.

Kinra, V. et al., 1998. The transmission of a longitudinal wave through a layer of spherical inclusions with a random or periodic arrangemnet. *Journal of mechanics and physics of solids*, 46(I), pp.153–165.

Kinra, V., Petraitis, M. & Datta, S.K., 1980. Ultrasonic wave propagation in a random particulate composite. *Journal of solids and structures*, 16, pp.301–312.

Kinra, V.K., Ker, E. & Datta, S.K., 1982. Influence of particle resonance on wave propagation in a random particulate composite. *Mechanics research communications*, 9(2).

Kishore, Shankar, R. & Sankaran, S., 2005a. Short-beam three-point bend test study in syntactic foam. Part III: Effects of interface modification on strength and fractographic features. *Journal of Applied Polymer Science*, 98(2), pp.687–693.

Kishore, Shankar, R. & Sankaran, S., 2005b. Short-beam three-point bend tests in syntactic foams. Part II: Effect of microballoons content on shear strength. *Journal of Applied Polymer Science*, 98, pp.680–686.

Kotsikos, G. et al., 2000. Environmentally enhanced fatigue damage in glass fibre reinforced composites characterised by acoustic emission. *Composites Part A: Applied Science and Manufacturing*, 31(9), pp.969–977.

Lionetto, F. & Mafezzoli, A., 2008. Polymer characterization by ultrasonic wave

propagation. *Advances in Polymer Technology*, 27(2), pp.63–73.

Liu, X. & Wei, P., 2008. Influences of interfacial damage on the effective wave velocity in composites with reinforced particles. *Science in China Series G: Physics, Mechanics and Astronomy*, 51(8), pp.1126–1133.

Madrer, E. & Pisanova, E., 2000. Characterization and Design of lnterphases in Glass Fiber Reinforced Polypropylene. *Polymer*, 21(3), pp.361–368.

Maharsia, R.R. & Jerro, H.D., 2007. Enhancing tensile strength and toughness in syntactic foams through nanoclay reinforcement. *Materials Science and Engineering: A*, 454-455, pp.416–422.

Manson, G. et al., 2002. Visualisation and Dimension Reduction of Acoustic Emission Data for Damage Detection. *Journal of intelligent materials and structures*, 12(August 2001), pp.529–536.

Mason, L., 2003. Tough sheet molding compound. In *Proceedings of SPE automotive composites conference*.

McConnell, V., 2007. SMC has plenty of road to run in automotive applications. *Reinforced Plastics*, 51(1), pp.20–25.

Minko, S. et al., 2000. Evaluation of the polymer-nonpolymer adhesion in particle- lled polymers with the acoustic emission method. , 14(8), pp.999–1019.

Minko, S. et al., 1998. The strength of the tailored polymer / inclusion interface in polymer composites evaluated in situ by acoustic emission. , 252, pp.247–252.

Mylavarapu, P. & Woldesenbet, E., 2010. A predictive model for ultrasonic attenuation coefficient in particulate composites. *Composites Part B: Engineering*, 41(1), pp.42–47.

Mylavarapu, P. & Woldesenbet, E., 2008. Characterization of Syntactic Foams -- An Ultrasonic Approach. *Journal of Cellular Plastics*, 44(May 2008), pp.203–222.

Netravali, A.N. et al., 1991. Determination of fibre/matrix interfacial shear strength by an acoustic emission technique. *Journal of Materials Science*, 26, pp.6631–6638.

Park, J.M. et al., 2004. Interfacial evaluation of electrodeposited single carbon fiber/epoxy composites by fiber fracture source location using fragmentation test and acoustic emission. *Composites Science and Technology*, 64, pp.983–999.

Park, S. et al., 2000. Effect of Fiber-Polymer Interactions on Fracture Toughness Behavior of Carbon Fiber-Reinforced Epoxy Matrix Composites. *Journal of colloid and interface science*, 228(2), pp.287–291.

Park, S. & Jin, J., 2002. Effect of Silane Coupling Agent on Mechanical Interfacial

Properties of Glass Fiber-Reinforced Unsaturated Polyester. *Journal of Polymer Science Part B: Polymer Physics*, pp.55–62.

Park, S., Jin, J. & Lee, J., 2000. Infuence of silane coupling agents on the surface energetics of glass fibers and mechanical interfacial properties of glass fiber-reinforced composites. *Journal of Adhesion Science and Technology*, 14(13), pp.1677–1689.

Park, S. & Jin, J.S., 2001. Effect of Silane Coupling Agent on Interphase and Performance of Glass Fibers/Unsaturated Polyester Composites. *Journal of Colloid and Interface Science*, 242(1), pp.174–179.

Pavlidou, S. & Papaspyrides, C.D., 2003. The effect of hygrothermal history on water sorption and interlaminar shear strength of glass/polyester composites with different interfacial strength. *Composites Part A: Applied Science and Manufacturing*, 34(11), pp.1117–1124.

Pérez-Pacheco, E. et al., 2013. Effect of moisture absorption on the mechanical behavior of carbon fiber/epoxy matrix composites. *Journal of Materials Science*, 48(5), pp.1873–1882.

Petitcorps, Y. Le, Pailler, R. & Naslain, R., 1989. The Fibre / Matrix lnterfacial Shear Strength in Titanium Alloy Matrix Composites Reinforced by Silicon Carbide or Boron CVD Filaments. *Composite sience and technology*, 35, pp.207–214.

Plueddemann, 1992. *Silane coupling agents* 2nd ed., New York: Plenum.

Potyra, T. et al., 2011. Process, material and part characterization of the innovative direct SMC process. *11th Annual Automotive Composites Conference & Exhibition of the Society of Plastics Engineers 2011, ACCE 2011*, pp.1–9.

Ramirez-Jimenez, C.R. et al., 2004. Identification of failure modes in glass/polypropylene composites by means of the primary frequency content of the acoustic emission event. *Composites Science and Technology*, 64(12), pp.1819–1827.

Sabina, F.J. & Willis, J.R., 1988. A simple self-consistnet analysis of wave propagation in particulate composites. *Wave Motion*, 10, pp.127–142.

Sause, M.G.R. & Horn, S., 2013. Quantification of the Uncertainty of Pattern Recognition Approaches Applied to Acoustic Emission Signals. *Journal of Nondestructive Evaluation*, 32(3), pp.242–255.

Shioya, M. & Takaku, A., 1995. Estimation of fiber and interfacial shear strength by using a single-fiber composite. *Composites Science and Technology*, 55, pp.33–39.

Varga, C. et al., 2010. Improving the mechanical properties of glass-fibre-reinforced

polyester composites by modification of fibre surface. *Materials & Design*, 31(1), pp.185–193.

Wang, X., Zhang, H.-P. & Yan, X., 2011. Classification and identification of damage mechanisms in polyethylene self-reinforced laminates by acoustic emission technique. *Polymers Composites*, p.945.

Wang, Y. et al., 2008. An acoustic emission study on the fracture bahvior of continuous fiber/polyproppylene composite based on commingled yarn. *Polymers and Polymer Composites*, 16(2), pp.101–113.

Waterman, P.C. & Truell, R., 1961. Multiple Scattering of Waves. *Journal of Mathematical Physics*, 2(4), p.512.

Wei, P.J. & Huang, Z.P., 2004. Dynamic effective properties of the particle-reinforced composites with the viscoelastic interphase. *International Journal of Solids and Structures*, 41(24-25), pp.6993–7007.

Wouterson, E.M. et al., 2005. Specific properties and fracture toughness of syntactic foam: Effect of foam microstructures. *Composites Science and Technology*, 65(11-12), pp.1840–1850.

Wu, H.F., Dwight, D.W. & Huff, N.T., 1997. Effects of silane coupling agents on the interphase and performance of glass-fiber reinforced polymer composites. *Composites Science and Technology*, 57, pp.975–983.

Wu, J. et al., 2006. Determine mechanical properties of particulate composite using ultrasound spectroscopy. *Ultrasonics*, 44 Suppl 1, pp.e793–800.

Yang, B.-L. et al., 2009. Damage Mode Identification for the Clustering Analysis of AE Signals in Thermoplastic Composites. *Journal of Nondestructive Evaluation*, 28(3-4), pp.163–168.

Yang, R.-B., 2003. A Dynamic Generalized Self-Consistent Model for Wave Propagation in Particulate Composites. *Journal of Applied Mechanics*, 70(4), p.575.

Yang, R.B. & Mal, a K., 1994. Multiple scattering of elastic waves in a fiber-reinforced composite. *Journal of the Mechanics and Physics of Solids*, 42(12), pp.1945–1968.

Yu, Y.-H. et al., 2006. A study on the failure detection of composite materials using an acoustic emission. *Composite Structures*, 75, pp.163–169.

Yue, C.Y. & Quek, M.Y., 1994. The interfacial properties of fibrous composites Part III Effect of the thickness of the silane coupling agent. *Journal of Materials Science*, 29, pp.2487–2490.

Zhang, L. et al., 2014. Mussel-Inspired Polydopamine Coated Hollow Carbon

Microspheres, a Novel Versatile Filler for Fabrication of High Performance Syntactic Foams. *ACS Applied Materials & Interfaces*, 6(21), pp.18644–18652.

Zhang, W., 1997. *MASc thesis, Curing kinetics of unsaturated polyester resins*. McMaster.